Synthesis and evaluation of hybrid compounds based on antimalarial and anticancer pharmacophores

Shankari Nair

University of Cape Town

December 2012

Synthesis and evaluation of hybrid compounds based on antimalarial and anticancer pharmacophores

A dissertation submitted to the University of Cape Town in fulfilment of

the requirements for the degree

Masters in Chemistry

by

Shankari Nair

Supervisor: Professor Kelly Chibale

Department of Chemistry
University of Cape Town
Rondebosch, 7701
Cape Town
South Africa

December 2012

Declaration

I declare that ***Synthesis and evaluation of hybrid compounds based on antimalarial and anticancer pharmacophores*** is my original work and has not been presented for the award of any degree at any university. I know the meaning of plagiarism and declare that all of the work in the document, save for that which is properly acknowledged, is my own.

_____

Shankari Nair

December 2012

Acknowledgements

I would like to thank my supervisor, Professor Kelly Chibale for his guidance, advice, encouragement and patience throughout this project. I would also like to thank Dr. Aloysius Nchinda for his support and involvement in this project and Ms Elaine Rutherfoord-Jones. To all the Department of Chemistry administrative and technical staff, Ms. Deirdre Brooks, Mr Gianpiero Benincasa, Mr. Noel Hendricks and Mr. Pete Roberts my heartfelt thanks. I would like to thank Prof. Pete Smith and Dr. Carmen Lategan (UCT Pharmacology), Prof. Denver Hendicks and Ms. Hajira Guzgay (UCT/IIDMM) and Dr Digby Warner and Ms Krupa Naran (UCT/IIDMM) for *in vitro* testing of all my compounds.

Many thanks go to the medicinal chemistry research group, especially Dr. Yassir Younis for all his advice and encouragement in the lab (you are a star), Dr. Grace Mugumbate for her help with the *in silico* predictions. To Mr Nicholas Njuguna thanks for your patience and putting up with me and great friendship and random lectures about the world. I would like to thank Dr. Tzu-Shean Feng for her advice and reading my thesis many times and Dr. Sophie Rees-Jones.

To the Chem Lunch group, thanks for all the laughter and chats during lunch these years and to my fantastic friends, thanks especially Shakeela and Verushka. Last and not in the least, to my family, without your support I would be nowhere, thanks ma, mum, dad, Omesan and Joschem.

Conference Contributions

April 2012 – Poster Presentation:

Synthesis and evaluation of hybrid compounds based on antimalarial and anticancer pharmacophores, presented at **12th Frank Warren Conference**, 15 – 18 April 2012, Bloemfontein, South Africa.

October 2012 – Poster Presentation:

Synthesis and evaluation of hybrid compounds based on antimalarial and anticancer pharmacophores, presented at Drug Discovery and Development Centre **"New Paradigms in Drug Discovery, Challenges and Opportunities in Africa"**, 15 – 18 October 2012, Cape Town, South Africa.

Abstract

Malaria stills remains one of the leading causes of death in sub-Saharan Africa, with *P. falciparum* being the most virulent strain of *Plasmodium*. Due to the emergence of drug resistance, new antimalarial agents are needed to circumvent this. Similarly, in the treatment of cancer, there is an urgent need for the design and development of new antineoplastic agents. This work describes the design, synthesis and biological evaluation of chromone-aminoquinoline hybrids as potentially new chemotherapeutic agents. A series of chromone-based hybrid molecules were synthesized using either reductive amination or amide coupling reactions. The compounds were synthesized in order to evaluate their antiplasmodial, antitumour and antimycobacterial activity. Each hybrid was fully characterized using NMR, IR and mass spectrometry techniques. Aminoquinolines were attached with alkyl or amide linkers at position 3 and an amide linker at position 2 of the chromone ring to produce covalently-linked hybrids. Series 1 contained the alkyl-linked hybrids at position 3 of the chromone ring, these compounds generally exhibited potent antiplasmodial activity with **SN24** (*D10*: IC_{50} = 30.7 nM) displaying the greatest potency. Series 2 contained the amide-linked hybrids at position 3 of the chromone ring. The compounds in this series also displayed potent antiplasmodial activity, the most potent compounds being **SN44** (*NF54*: IC_{50} = 38.1 nM), **SN48** (*D10*: IC_{50} = 20.9 nM), **SN54** (*D10*: IC_{50} = 46.8 nM; *NF54*: IC_{50} = 57.5 nM) and **SN57** (*D10*: IC_{50} = 39.7 nM; *NF54*: IC_{50} = 63.3 nM). Additionally, compounds with the aminoquinoline ring at position 2 of the chromone ring displayed enhanced potency as compared to the analogues with attachments at position 3, especially in the *K1* strain of *P. falciparum*. In this group **SN74** (IC_{50} = 82.9 nM), **SN77** (IC_{50} = 37.6 nM) and **SN78** (IC_{50} = 80.9 nM) were the most potent compounds against the *K1* strain of *P. falciparum*. All hybrids were evaluated for their antitumour activity against the oesophageal cancer *WHCO1* cell line, and displayed moderate activity, with **SN78** (IC_{50} = 1.78 µM) being the most active. Poor antimycobacterial activity was observed in these chromone-based hybrids. Physicochemical properties were determined, such as turbidimetric aqueous solubility at pH 7.4 experimentally as well as CLogP, CLogD and Caco-2 were predicted. The hybrids displayed low to moderate solubility (2 – 47 µg/mL). The effect of the aryl substituents on the chromone motif was also investigated in terms of solubility and pharmacological activity. Aryl substituents were attached at various positions of the chromone ring via the Suzuki cross-coupling reaction to produce biaryl chromone ethyl ester analogues. These biaryl chromone esters displayed low solubility (1 – 7 µg/mL), while compounds with aryl substituents at positions 5 and 8 of the chromone ring displayed high solubility (60 µg/mL), due to the possible disruption of planarity of the molecule. These chromone-ethyl esters exhibited moderate to poor antiplasmodial and antimycobacterial activities.

Abbreviations

^{o}C	degree Celsius
δ	chemical shift (NMR)
ACT	Artemisinin-based combination therapy
Ar	aromatic
ATP	adenosine-5'-triphosphate
br	broad
$CDCl_3$	deuterated chloroform
CD_3OD	deuterated methanol
conc.	concentrated
CQ	chloroquine
CQS	chloroquine sensitive
CQR	chloroquine resistant
d	doublet
DCM	dichloromethane
dd	doublet of doublet
DMAP	*N,N*-dimethylaminopyridine
DMF	*N,N*-dimethylformamide
DMSO-d_6	deuterated dimethyl sulfoxide
DNA	deoxyribonucleic acid
EDC.HCl	1-ethyl-3-(3-dimethylaminopropyl) carbodiimide hydrochloride
EI	electron ionization
Et_2O	diethyl ether
Et_3N	triethylamine
EtOAc	ethyl acetate
EtOH	ethanol
eq	equivalent
Fig.	Figure
g	grams
h	hour
Hb	haemoglobin
HCl	hydrochloric acid
Hex	hexane
HOBt	*N*-hydroxybenzotriazole
HPLC	high performance liquid chromatography
Hz	hertz
IC_{50}	half maximal inhibitory concentration
ISP	Rieske iron-sulfur protein
J	coupling constant
m	multiplet
mL	millilitre
m/z	mass/charge ratio
Me	methyl
MeO	methoxy
MeOH	methanol
$MgSO_4$	magnesium sulfate
MIC_{90}/ MIC_{99}	minimum inhibitory concentration required to inhibit the growth of 90 % / 99 % of organisms
min	minute
M.p.	melting point

MHz	megahertz
MTT	3-(4,5-dimethylthiazol-2-yl)-2,5-diphenyltetrazoliumbromide
mV	millivolts
$NaBH(OAc)_3$	sodium triacetoxyborohydride
$NaClO_2$	sodium chlorite
NaOEt	sodium ethoxide
NH_2SO_3H	sulfamic acid
ng	nanogram
nm	nanometer
nM	nanomolar
$PdCl_2(PPh_3)_2$	Bis(triphenylphosphine)palladium(II) dichloride
$POCl_3$	phosphorus oxychloride
P.T.	proton transfer
ppm	parts per million
Qi	ubiquinone reduction site
Qo	ubiquinol oxidation site
R_f	retention factor
RT	room temperature
s	singlet
TLC	thin layer chromatography
t	triplet
td	triplet of doublet
t_r	retention time
µg	microgram
µM	micromolar
WHO	World Health Organization

Table of Contents

Chapter One – Introduction and Background

1.1 Malaria – Background/Introduction

Malaria continues to be one of the greatest threats to mankind, as it is one of the most dangerous infectious diseases.[1] Malaria is endemic in 106 countries as of 2010, and is mainly found in tropical areas such as sub-Saharan Africa, Southeast Asia and Central and South America.[2] With increasing indication of climate change, global warming in particular, there is great concern over the possibility of the spread of malaria to regions that are currently declared malaria-free.[3] Over 216 million malaria-related clinical cases are reported yearly. The World Health Organization (WHO) estimates that malaria kills over 655 000 people annually; most deaths are of pregnant women and children under the age of five, with 91 % of these cases being in sub-Saharan Africa.[4] The African economy is also affected as a consequence as malaria endemic countries tend to have lower rates of economic growth per capita when compared to non-endemic countries.[5] Travellers visiting malaria endemic countries are also at risk.[6] Malaria is said to be a third world country disease and as such, one of the biggest challenges in the management of malaria is to provide cheap and affordable medication.[7]

1.1.1 Life Cycle of the Malaria Parasite

Malaria is caused by a unicellular protozoan parasite of the genus *Plasmodium*. There are four species of *Plasmodium* that infect humans: *P. falciparum, P. malariae*, *P. ovale* and *P. vivax*. *P. falciparum* is the most virulent species in Africa, Asia and South America.[8] *P. knowlesi*, which was known as a primate form of *Plasmodium*, has also been reported to cause human infections.[9] The human malaria parasite has a complex life cycle (Fig. 1.1) that requires a human host for asexual reproduction and a vector host for sexual reproduction. When an infected female *Anopheles* mosquito bites a human, wormlike single-celled parasites called sporozoites are ejected from the salivary glands of the mosquito into the host's bloodstream. The sporozoites begin the exo-erythrocytic cycle by migrating to the liver, where they invade hepatocytes and develop into tissue schizonts. After maturation of the schizonts the hepatocytes rupture, releasing merozoites into the blood stream. Once in the blood, the merozoites invade red blood cells, commencing the erythrocytic cycle. During this cycle, the parasites develop into metabolically-active trophozoites by metabolizing oxygen-carrying haemoglobin (Hb) and proteolysis of haemoglobin to amino acids. The erythrocytic cycle ends when the red blood cell bursts, releasing merozoites and harmful toxins into the bloodstream. This rupture (approximately 48 hours for *P. falciparum*, *P. ovale* and *P. vivax* and 72 hours for *P. malariae*) coincides with the clinical symptoms of malaria, such as high fever, chills, convulsions and anaemia. In the case of severe malaria, symptoms like metabolic acidosis and multi-organ failure are experienced; this may lead to coma or death. The merozoites released are now able to invade other red blood cells and continue the erythrocytic cycle. Some merozoites further

differentiate into gametocytes, which are taken up when the infected human host is bitten again by a female *Anopheles* mosquito. These develop into male and female gametes in the stomach of the mosquito. Upon fertilization, an ookinete is formed, which invades the mosquito gut wall and forms an oocyst. The oocysts mature and rupture to release sporozoites which travel up to the salivary glands of the mosquito to recommence the cycle.[10, 11]

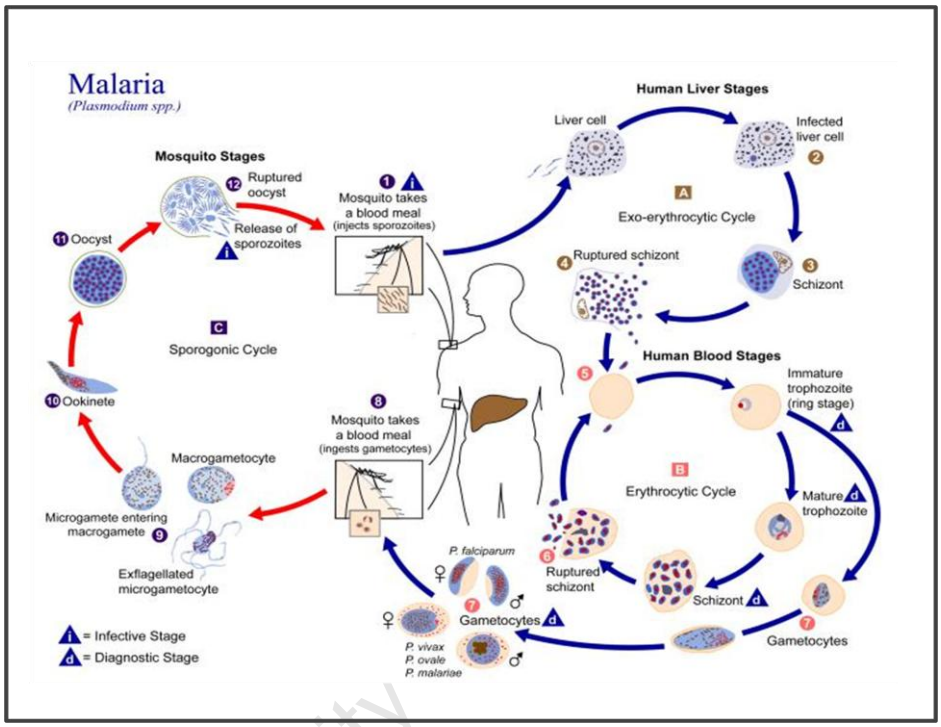

Fig. 1.1: Life cycle of the malaria parasite[10]

1.1.2 Antimalarial Therapy and Classification of Antimalarial Drugs

The complexity of the multiple stages in the malaria lifecycle requires the use of multiple strategies for its control. One way of achieving this is vector control; which is primarily targeted at reducing the number of infectious mosquitoes. The WHO has distributed bed nets and screens to malaria affected areas and have begun spraying insecticides, such as bendiocarb, indoors.[12, 13] This strategy is hampered by the development of resistance to the insecticide by the mosquito.[13] Other strategies include malarial chemotherapy and prophylaxis. The life cycle of the malaria parasite is the target for current antimalarials.[14] The exo-erythrocytic cycle is the ideal target for the development of antimalarials, as this is where the parasite first starts to replicate. However, this is prior to the development of typical malaria-like symptoms and can be very challenging to treat as people are unaware that they are infected.[15] Due to difficulties in studying the liver stage in more detail, most current antimalarials target the erythrocytic cycle or the blood stage of the life cycle.

When designing a drug for *P. falciparum*, the following are necessary criteria:

- Highly efficacious against resistant strains of *P. falciparum*
- Short duration of the medication regimen to ensure patient compliance
- Formulation of an orally-active dosage
- Safety in young children, pregnant women and immuno-compromised individuals
- Stable, with a long shelf-life under tropical conditions
- Ability to be used in combination therapy
- Cheap and affordable[16, 17]

The majority of current antimalarials were not developed through rational design but rather through discovery of the antimalarial activities of natural products, such as quinine and artemisinin or compounds derived from natural products such as artesunate.[16] Advances in technology have effectuated the completion of the *P. falciparum* genome sequence. This has allowed for a better understanding of the parasite's biochemistry, as well as its molecular and cellular biology.[18] The genome project has revealed potentially new parasite-specific targets which are essential for combating the emergence of resistance. Currently available antimalarials can be grouped into two categories: drugs that act on specific stages in the parasite's life cycle and drugs based on their modes of action.[19, 20]

1.1.2.1 Drugs that act on Specific Stages in the Parasite's Life Cycle

Antimalarial therapy can be classified based on which stage in the life cycle it inhibits. Blood schizonticides are active against the asexual erythrocytic cycle, whereas tissue schizonticides target the liver stage and prevent relapse of malaria. The use of gametocytocidal drugs kills non-pathogenic gametocytes and blocks the transmission of gametocytes from the human host to the vector host. Sporontocides, on the other hand, inhibit the development of oocysts and sporozoites in the mosquito, preventing parasite transmission.[21]

1.1.2.2 Drugs Based on Mode of Action

This group consists of drugs based on their modes of action. The majority of antimalarial drugs in clinical use fall under one of the four categories:

- Inhibitors of haemozoin formation
- Inhibitors of nucleic acid synthesis
- Inhibitors of cysteine protease, and
- Activators of oxidative stress[22]

Inhibitors of Haemozoin Formation

The malaria parasite requires a large amount of nutrients for its development, but lacks the capacity to synthesize its own amino acids *de novo* or to scavenge them.[23] Therefore, the malaria parasite takes up the cytoplasm of the erythrocyte, which contains haemoglobin to carry oxygen to the bodily tissues. The encapsulation of the cytoplasmic haemoglobin into vesicles by the parasite is known as endocytosis.[24] These vesicles deliver the ingested haemoglobin to the food vacuole (FV). The food vacuole is a single-membrane organelle with a pH of 4.8 – 5.2, which is host to a variety of biochemical processes.[25] In *P. falciparum* infections, over 70 % of haemoglobin in red blood cells is degraded by the parasite and used as a major source of nutrients.[26] Haemoglobin is digested in the food vacuole by aspartic proteases such as plasmepsin I, II and IV, histo-aspartic proteases, cysteine proteases falcipain 2 and 3 and falcilysin, a zinc metalloprotease.[26–29] Haemoglobin proteolysis produces amino acids and free haeme (ferriprotoporphyrin-IX or Fe(II)PPIX) in the cytosol of the parasite.[30] The iron centre of the free haeme is oxidized from Fe(II) to Fe(III), forming haematin (aqua/hydroxoferriprotoporphyrin IX or H_2O/HO-Fe(III)PPIX), also called the malaria pigment.[31] A build-up of haematin is toxic to the parasite, as this leads to the generation of reactive oxygen species. These highly reactive intermediates disrupt cell structure by reacting with proteins and lipids.[32] The parasite has an internal mechanism to overcome this problem, by converting haematin to haemozoin, an insoluble inert crystal.[33, 25] The crystal structure of haemozoin was elucidated in 1991 by Slater and co-workers and later confirmed by Pagola and co-workers.[34, 35] The current model reveals that haemozoin is a cyclic dimer of haematin, with a bond between the Fe of one haeme to the carboxylate group on another haeme (Fig. 1.2).

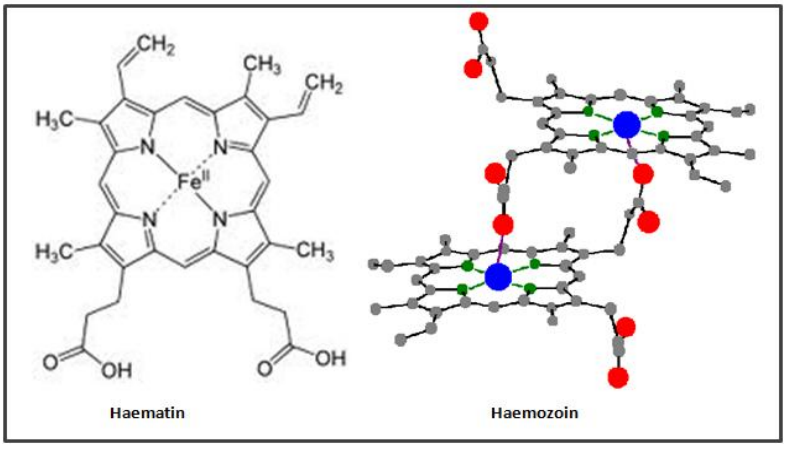

Fig. 1.2: Structure of haematin and haemozoin[36]

Therefore, drugs that belong to this class interrupt haemozoin formation, as these drugs are designed based on β-haematin, a synthetic cyclic dimer of ferriprotoporphyrin IX, which is structurally, spectroscopically and crystallographically identical to haemozoin.[37] The 4-aminoquinolines (chloroquine and amodiaquine), quinoline methanols (quinine and quinidine) and aryl alcohols (mefloquine and halofantrine) form part of this group (Fig. 1.3).[38] These drugs are believed to work by forming complexes with haeme through π-π stacking of their planar aromatic groups, hence blocking the conversion of haeme to haemozoin.[39]

Chloroquine (CQ) is a blood schizonticide which acts on the trophozoite stage in the life cycle and had been the drug of choice in the treatment of malaria for decades.[40] However, the use of chloroquine has been hampered by widespread drug resistance in the parasite.[40] Chloroquine is thought to work in the acidic food vacuole (FV) of the malaria parasite. Chloroquine exists as a neutral species and crosses the vacuolar membrane against a pH-dependent gradient. This is accomplished by the lipophilic nature of the aminoquinoline core, once in the acidic food vacuole the nitrogen atoms become protonated and the resulting species is unable to cross the membrane again, leading to their accumulation within the food vacuole. This process is known as pH-trapping, where a free base diffuses across the membrane and is trapped in the food vacuole as it becomes protonated. Once inside the food vacuole, chloroquine forms a complex with haematin via π-π stacking with the porphyrin ring system on haematin and the quinoline nucleus.[41] This association further enhances drug accumulation within the food vacuole.[42, 43] The conversion of haematin to haemozoin is inhibited, resulting in an increase in toxic haematin and chloroquine-haematin adducts, which in turn leads to the inhibition of enzyme activity, resulting in parasite death and erythrocyte lysis.[44, 45]

Due to the emergence of drug resistance, the WHO facilitated the design and synthesis of new antimalarials such as mefloquine and halofantrine.[11] Mefloquine is a fluorinated quinoline alcohol, which has good antimalarial activity against chloroquine-resistant (CQR) strains of *P. falciparum*.[46] It has been used as a prophylactic due to its long half-life of 14 – 21 days. However, it is believed that this may have contributed to the rapid development of resistance against it.[17] Halofantrine (Fig. 1.3), also an aryl alcohol, is metabolized into its active agent, desbutylhalofantrine.[47] Halofantrine was reported to have excellent activity against CQR strains of *P. falciparum*, however, due to poor toxicity profiles, the use of this drug as an antimalarial has decreased.[48]

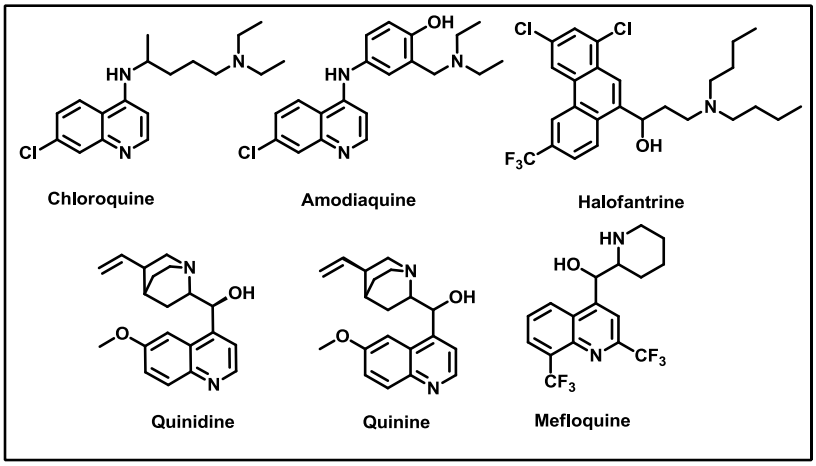

Fig. 1.3: Examples of inhibitors of haemozoin formation

Inhibitors of Nucleic Acid Synthesis

This class consists of the dihydrofolate reductase inhibitors such as pyrimethamine and proguanil. The action of dihydrofolate reductase can be blocked by antifolates, which cause a decrease in tetrahydrofolate, an essential molecule in DNA synthesis (Fig. 1.4).[49, 50] Sulfadoxine, a dihydropteroate synthase inhibitor, also belongs to this class; it acts by mimicking *para*-aminobenzoic acid (PABA) and interacts with the active site through competitive inhibition (Fig. 1.4). This inhibition causes a decrease in the synthesis of essential amino acids such as serine and methionine.[51]

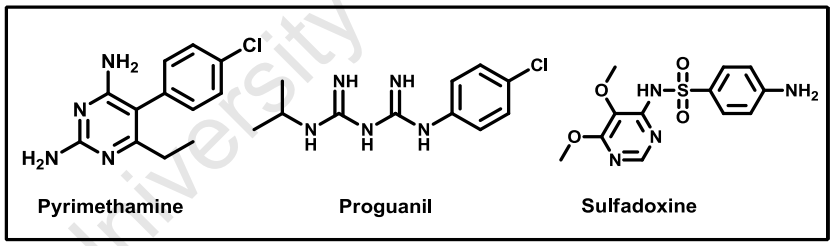

Fig. 1.4: Examples of inhibitors of nucleic acid synthesis: pyrimethamine, proguanil and sulfadoxine

Inhibitors of Cysteine Proteases

Cysteine proteases play an important role in the erythrocytic cycle as they are involved in the haemoglobin degradation process.[52] Recent studies have shown that falcipain cysteine proteases can be inhibited, which results in inhibition of haemoglobin hydrolysis.[53] Cysteine protease inhibitors block the rupture of erythrocytes at the end of the erythrocytic cycle. Peptidyl fluoromethyl ketones and vinyl sulfones have displayed antimalarial activity in the nanomolar range both *in vitro* and *in vivo*.[53–55] Extensive studies on non-peptidyl cysteine proteases inhibitors such as phenothiazines, acyl hydrazines and chalcones have been conducted by various researchgroups.[53, 56, 57]

Activators of Oxidative Stress

Compounds that generate oxidative stress can trigger apoptosis or programmed cell death.[58] Reactive oxygen species (ROS) are produced as by-products of oxygen metabolism, and also produce oxygen radicals that are able to disrupt cell structure by interfering with the lipid bilayer. *Plasmodium* parasites have detoxification mechanisms to deal with these radicals. However, drugs that are able to increase ROS may overcome the cell's internal defence mechanism, resulting in cell damage and eventually lysis.[59] This class contains the artemisinins and the 8-aminoquinolines.[60] Artemisinin and its derivatives dihydroartemisinin, artemether, arteether, artesunate and artelinic acid (Fig. 1.5), are believed to generate oxidative stress via the endoperoxide bridge. Primaquine, an 8-aminoquinoline, (Fig. 1.5) is the only approved drug against the hepatic stages of malaria parasites; it is extensively used in the treatment of *P. vivax* (the species that causes recurrent malaria).

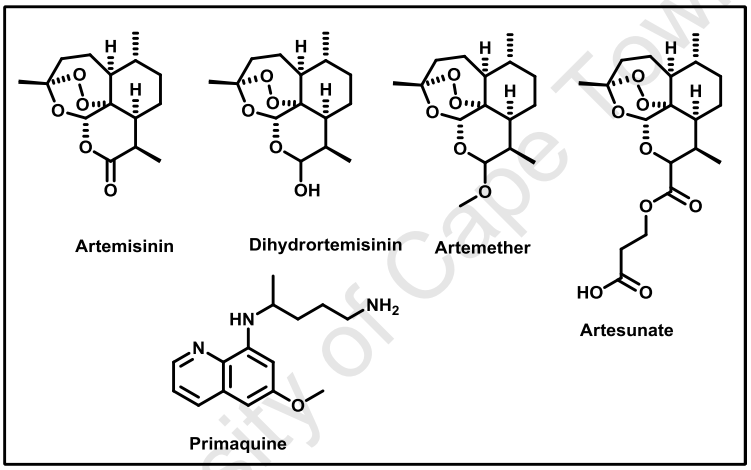

Fig. 1.5: Examples of compounds that generate oxidative stress in the malaria parasite

1.1.3 Resistance

The widespread use of chloroquine worldwide and especially in Africa resulted in the emergence of chloroquine-resistant strains of *P. falciparum* and *P. vivax*. Drug resistance in malaria has been defined as 'the ability of a parasite strain to survive and/or to multiply despite the administration and absorption of a drug given in doses equal to or higher than those usually recommended but within the limits of tolerance of the subject'.[61] However, this definition has now been modified to specify that the drug 'must gain access to the parasite or the infected red blood cell for the duration of the time necessary for its normal action'.[62, 63] Resistance generally occurs through spontaneous mutations; for some drugs, a single mutation is enough to lead to resistance, while in other drugs multiple mutations are needed.[64] In sub-Saharan Africa, the morbidity of the disease, in addition to the development of resistance, is further amplified by the prevalence of malnutrition among children under 5 years of age and the number of individuals living with HIV.[63] There are various

approaches in medicinal chemistry and drug discovery to develop new antimalarials, including combination therapy, the development of natural products, drug rotation, the redesign and repositioning of existing drugs and the use of resistance reversal agents.[65–67]

Combination Therapy

The WHO defines combination therapy in malaria as 'the simultaneous use of two or more blood schizontocidal drugs with independent modes of action and different biochemical targets' and has mandated the use of combination therapy as the most effective way to circumvent resistance, as the combination is often more effective; in the rare event that the parasite is resistant to one of the medicines, the parasite will be killed by the other component of the therapy.[9, 65] The use of combination therapy is validated as reports suggest that if resistance arises from mutations in the target protein, then administrating drugs with different modes of action may reduce the chances of the parasite developing resistance.[68] Artemisinin-based combination therapy (ACT) is recommended by the WHO as the first-line treatment option for malaria, where one of the components is artemisinin or one of its derivatives (artesunate, artemether or dihydroartemisinin). Artemisinins produce quick clearance of parasitaemia but have a short half-life. They are thus given in combination with slowly eliminated antimalarials. Currently, there are five ACT combinations that are recommended for the treatment of uncomplicated malaria. These are:

- Artemether-lumefantrine
- Artesunate-amodiaquine
- Artesunate-mefloquine
- Artesunate-sulfadoxine/pyrimethamine, and
- Dihydroartemisinin-piperaquine[9, 8]

Artemisinins are most effective during the erythrocytic cycle and are also known to reduce the number of gametocytes in the blood. ACTs have been used to successfully treat CQR strains of *P. falciparum* and multidrug-resistant malaria.[69] The use of ACTs in South Africa has brought about a decline in the amount of malaria transmissions and no clinical resistance has been reported for the ACT regimen.[69] However, reports from Western Cambodia suggest that resistance is currently developing.[70] If the first-line treatment plan has failed, artesunate or quinine is given as a combination with tetracycline, doxycyline or clindamycin. The use of chloroquine in combination therapy has proved unsuccessful.[66]

1.2 Cancer – Background/Introduction

Cancer is one of the most common diseases in both developing and developed countries around the world.[71] According to the WHO, at least one in every three people will be affected by some kind of cancer. In South Africa, according to the Cancer Association of South Africa (CANSA), the most prevalent cancer in males is prostate cancer and in females, breast cancer.[72] Cancer is caused when normal cells lose their regulatory mechanisms that control replication and differentiation. In normal cells, the rate at which cells grow is equal to the rate at which they die, whereas in cancerous cells this balance is disrupted.[58] This results in rapid accumulation of cells or a neoplasm, more commonly known as a tumour or cancer. If the rapid growth of cells is localized to a specific area, the tumour is called benign and is easier to treat. However, if cancer cells invade other parts of the body and develop into secondary tumours, they are termed malignant. This is a more serious type of cancer, which is life-threatening and more difficult to treat.[73]

There are over 200 different cancers that affect humans; therefore treatment that controls one form of cancer may not be effective for another. Cancer can be caused by various factors; these include lifestyle factors such as poor diet, smoking and alcohol abuse as well as environmental factors such as exposure to carcinogenic chemicals and genetic factors. (Fig. 1.6).[73]

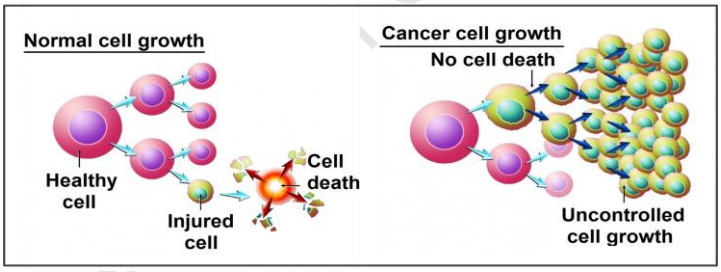

Fig. 1.6: Illustration of normal cell growth versus tumour cell growth[74]

Proto-oncogenes control cell division and differentiation. If mutations occur, this disrupts normal cell function, allowing cells to become cancerous. The proto-oncogene is now called an oncogene, a gene that is able to cause cancer.[75] If DNA is damaged in normal cells, cells have repair mechanisms that can detect damage and block DNA replication. This allows the DNA repair mechanisms to work and repair the damage. If the DNA cannot be repaired, the cell commits suicide, a process known as programmed cell death or apoptosis.[24] Tumour-suppression genes code for the proteins that are involved in the cell's repair mechanisms. If there are defects in these genes, the chances of cells becoming cancerous increases; these defects are also passed from generation to generation. Many genetic defects may lead to cellular defects which increase the risk of developing cancerous cells.

These hallmarks are:

- Evading growth suppressors
- Activating invasion and metastasis
- Enabling replicative immortality
- Inducing angiogenesis
- Resisting apoptosis
- Sustaining proliferation signaling[76]

Cell Cycle

Most anticancer drugs inhibit a particular stage in the cell cycle. The cell cycle in eukaryotes is divided into two phases: the interphase and the mitosis phase (Fig. 1.7). During the interphase the cell grows, accumulates nutrients necessary for mitosis and begins DNA replication. The interphase consists of three phases: the G1 phase or the growth phase, followed by the S phase, the DNA synthesis phase, then followed by the G2 phase, which involves the biosynthesis of microtubules; cells remain in the G2 phase until they enter the mitosis phase. The mitosis phase, or the M phase, is the phase that separates the chromosomes in the nucleus into two identical sets in two separate nuclei; this is immediately followed by cytokinesis, the final stage in the cycle in which cytoplasm is divided and two daughter cells are produced, which are genetically identical to each other and the parent cell. There are mechanisms within the cycle to detect errors in the replication process that bring about programmed cell death. However, if these fail to recognise errors or mutations, cancerous cells may develop.[24, 73]

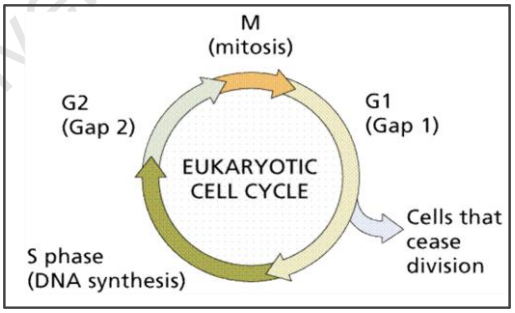

Fig. 1.7: Systematic representation of the cell cycle in eukaryotes[77]

Traditionally, there are three approaches in cancer treatment: surgery, radiotherapy and chemotherapy. However, due to advances in technology and a better understanding of the molecular biology of cancerous cell, hormone and photodynamic therapies are also used. Only the use of chemotherapy will be discussed here; for the other forms of treatment, please refer to the National Cancer Institute (USA) webpage.[78]

1.2.1 Chemotherapy

Chemotherapy is the use of drugs to weaken and destroy cancer cells. This therapy usually affects the whole body. Chemotherapy is normally administered alongside surgery and radiotherapy. Anticancer agents work by accumulating in cancerous cells rather than normal cells. The difficulty with most chemotherapeutic agents is that they are unable to differentiate between normal cells and cancerous cells. These agents target cancer cells, as these cells are fast-growing and need to gather nutrients and synthetic building blocks.[73] In the body, there are other fast growing cells like bone marrow cells and hair cells which are also affected by anticancer agents. This results in bone marrow toxicity and rapid hair loss. Damage to bone marrow cells results in weakening of the immune system, which increases the chances of secondary infections in cancer patients.[73] Anticancer drugs exhibit their action by inhibiting cell differentiation, by interacting either directly or indirectly with DNA. Drugs that block DNA function indirectly act by inhibiting enzymes that are involved in DNA synthesis. Still, cancer therapy is becoming more sophisticated as more information becomes available on the cellular chemistry of cancer cells.

1.2.1.1 Anticancer Drugs that act directly on DNA

This class of drugs interact directly with the nucleic acids on the backbone of DNA. Disruption of DNA function can lead to cell death. These include the intercalating agents, non-intercalating agents and the alkylating agents.

Intercalating Anticancer Agents

These drugs contain a planar or heteroaromatic ring system that wedges itself between the double helix of DNA, causing a distortion in its structure.[79] This change in structure prevents polymerases and other enzymes involved in DNA replication and transcription to function. Several naturally occurring antibiotics fall into this class, including dactinomycin and doxorubicin (Fig. 1.8). Other anthracyclines used are mitoxantrone and amsacrine (Fig. 1.8).

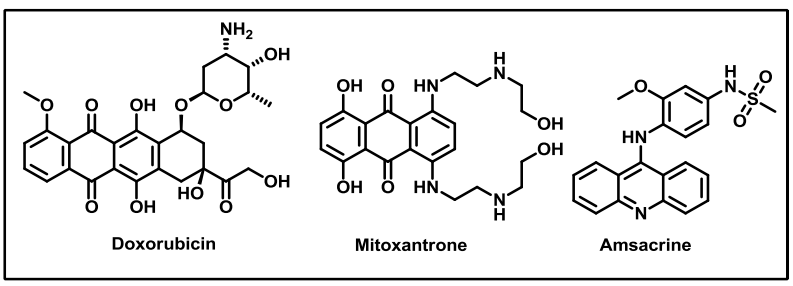

Fig. 1.8 Examples of clinically used intercalating agents

Non-Intercalating Anticancer Agents

These anticancer drugs generally inhibit topoisomerses, which are enzymes that regulate the unwinding and rewinding of DNA during DNA replication. The camptothecins (irinotecan) are a group of naturally occurring cytotoxic alkaloids that target topoisomerase I, while the podophyllotoxins (etoposide and teniposide) target topoisomerase II and prevent the resealing of DNA strands during DNA replication (Fig. 1.9).[73, 80]

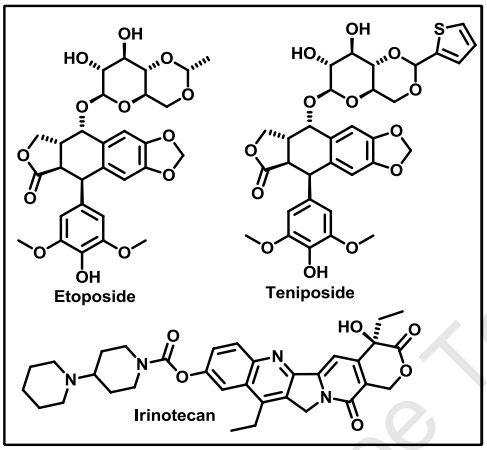

Fig. 1.9: Examples of non-intercalating agents currently available

Alkylating Agents

These are highly electrophilic molecules that form strong covalent bonds with the nucleophilic nitrogenous DNA bases. Some drugs are able to cross-link between the DNA strands if they have two alkylating groups. Alkylating agents are highly carcinogenic compounds due to their ability to damage DNA in both normal and cancerous cells.[81] Cisplatin and its analogues (carboplatin and oxaliplatin) are well-known drugs from this class (Fig. 1.10). Other frequently used alkylating agents are the nitrogen mustards, in particular, uracil mustard.[82] Cyclophosphamide, a prodrug, is another frequently used alkylating agent which is converted to its active form in the liver by cytochrome P450 enzymes.[58]

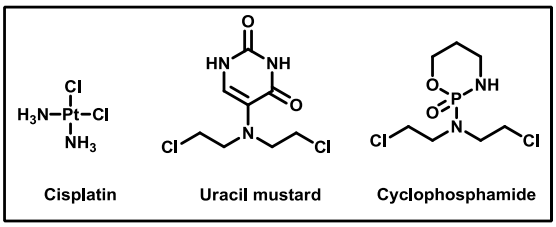

Fig. 1.10: Chemical structures of cisplatin, uracil mustard and cyclophosphamide

1.2.2.2 Anticancer Drugs that indirectly act on DNA

This class of drugs act by targeting the enzymes involved in DNA synthesis and repair mechanisms. These inhibitors are also called antimetabolites and pose as nitrogenous bases that become the new building blocks of DNA. Research done on this class of compounds suggests that these drugs inhibit the S phase of the cell cycle, resulting in programmed cell death.[83] There are several enzymes that are involved in the synthesis of DNA and, in principle, can be potentially inhibited. One of the most commonly used drugs from this class are the dihydrofolate reductase inhibitors such as methotrexate (Fig. 1. 11).[84] The thymidylate synthase is inhibited by 5-fluorouracil; this enzyme is responsible for the biosynthesis of thymidine, a DNA nucleoside (Fig. 1.11).[85] Inhibitors of ribonucleotide reductase, adenosine diaminase and DNA polymerases are clinically used to block DNA synthesis and trigger apoptosis.

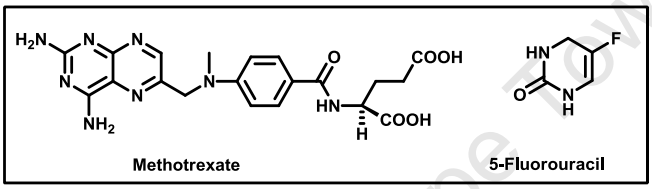

Fig. 1.11: Structure of methotrexate and 5-fluorouracil

1.2.2.3 Drugs that act on Signalling Pathways

Traditional cancer therapies involve administering drugs that are often cytotoxic to both normal and cancerous cells. As such, selectivity is dependent on the preferential accumulation and increase in concentration of the drugs within cancerous cells as opposed to normal cells. The protein kinase inhibitors are a broad range of inhibitors that prevent phosphorylation of specific amino acids, which blocks signal transduction, leading to inactivation of transcription factors. PTK787 (vatalanib) and SU5416 (semaxanib) are examples of kinase inhibitors while flavopiridol and (*R)*-reoscovitine are examples of cyclin-dependent inhibitors (Fig. 1.12).[73]

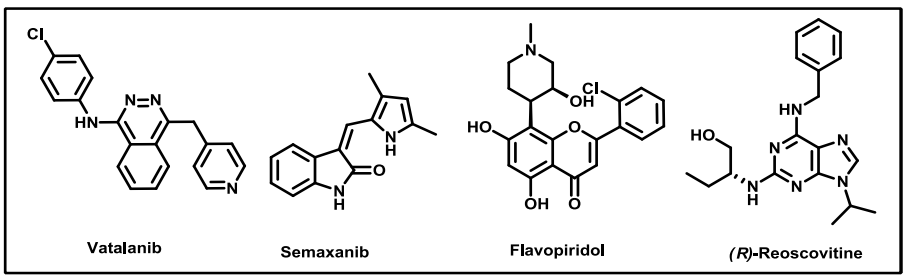

Fig. 1.12: Chemical structures of vatalanib, semaxanib, flavopiridol and (*R)*-reoscovitine

1.3 Chromones – Introduction and Antitumour Activity

Introduction

Chromones, derived from the Greek word '*chroma*' meaning colour, are a group of naturally occurring compounds that are widely distributed in nature, especially in the plant kingdom. The chromone ring system, or 1-benzopyran-4-one (Fig. 1.13), is a core fragment in many flavonoids. Flavonoids are a major class of secondary metabolites found in vascular and in some nonvascular plants.[86] Many flavonoids have been reported to possess medicinal properties, including anti-HIV, antibacterial, anti-inflammatory and anticancer activities.[87–95]

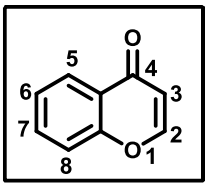

Fig. 1.13: Structure of the chromone scaffold

The rigid bicyclic chromone fragment has been classified as a privileged substructure in drug design and discovery.[96] Privileged substructures are components of a compound or a molecular framework that are able to provide ligands for diverse receptors in biological systems.[96, 97] The collective term 'chromones' will be used in this discussion as a reference to chromone derivatives. Although a variety of chromone derivatives possess biological activity, only a few are presently used as therapeutic agents. The first chromone used in its pure form clinically was khellin (Fig. 1.14). This compound was originally extracted from the seeds of the *Ammi visnaga* plant and used as a diuretic to relieve renal colic in Ancient Egypt, but is now more commonly used for the management of vitiligo, a pigmentation disorder.[98–100] Other clinically used drugs containing the chromone moiety include sodium cromoglycate (Lomudal®, Sanofi-Aventis), used as a mast cell stabilizer in treating and managing allergic and exercise-induced asthma; and diosmin, marketed as Daflon®, a phlebotropic drug in the treatment of venous diseases and haemorrhoids.[101–104]

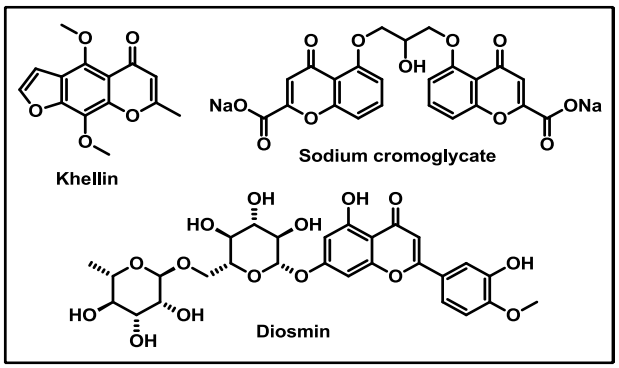

Fig. 1.14: Examples of chromone-based compounds previously or currently used as pharmaceutical agents

Several naturally occurring benzopyran derivatives are potentially useful antitumour agents due to their ability to inhibit protein kinase-dependent signal transduction pathways, specifically tyrosine kinases.[105] Tyrosine kinase receptors are membrane-bound proteins that allow transfer of a phosphate group from ATP to a tyrosine residue, which in turn triggers a signalling cascade that results in activation of transcription factors and cell proliferation.[73] These enzymes act like 'on/off' switches in cells, controlling the activation of transcription factors. A faulty tyrosine kinase that is continuously switched 'on' results in continuous activation of transcription factors which may lead to the initiation and/or progression of cancer.[75]

Some naturally occurring chromones such as genistein, quercetin, apigenin and myricetin, are known to inhibit tyrosine kinases (Fig. 1.15).[106–109] Genistein, a 5,7-dihydroxy-3-(4-hydroxyphenyl)-4*H*-chromen-4-one, is a highly specific tyrosine kinase inhibitor. Reports suggest that genistein inhibits epidermal growth factor (EGF) response in cultured A431 (human epidermoidal) cancer cells.[107] EGF is responsible for stimulation of cell growth, proliferation and cell differentiation; therefore interruption of its activity results in inhibition of the cell cycle.[110] Studies conducted by Papazisis and co-workers demonstrated that genistein has a role in triggering apoptosis and promotes cell cycle arrest in γ-irradiated K562 leukaemia cell lines.[111] This further suggests that the chromone pharmacophore could be an attractive template for the development of potential antitumour and antiplasmodial agents.

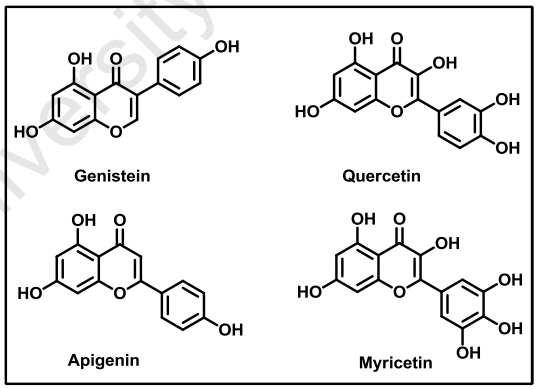

Fig. 1.15: Examples of chromone-based compounds that have exhibited kinase inhibition activity

Antitumour Activity of Chromones

There are many reports of compounds that contain the chromone substructure possessing antitumour activity.[112–117] Recently, Dyrager and co-workers described the synthesis and antitumour activity of chromone-based kinase inhibitors that target the p38α MAP kinase enzyme.[113] They conducted docking studies and indicated that the chromone substructure binds to the ATP binding

site of the p38α MAP kinase enzyme. Fig. 1.16 depicts the suggested interactions between the substituents on the chromone ring and the ATP binding pocket.

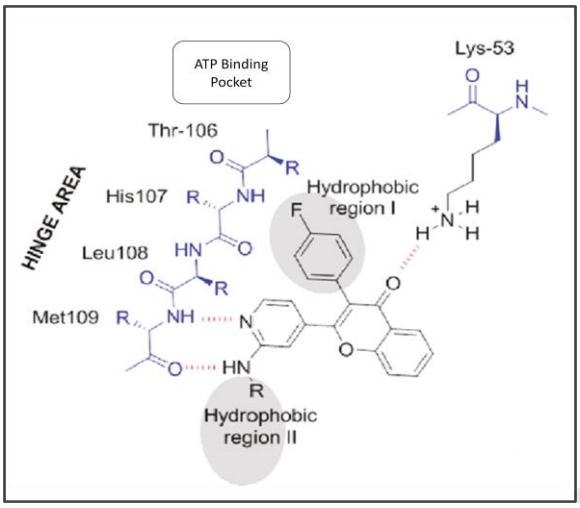

Fig. 1.16: Suggested interactions of the chromone derivative synthesized by Dyrager et al[113]

As stated in section 1.2, compounds that inhibit the signal transduction cascade lead to programmed cell death, resulting in the inhibition of growth of cancerous cells. This led to Forghieri and co-workers using a chromone substructure as a low molecular weight tyrosine phosphatase inhibitor.[118] Another example of the chromone substructure in antitumour research is a formylchromone derivative (6-(biphenyl-4-yl)-4-*oxo*-4H-chromene-3-carbaldehyde) designed by Shim and colleagues as a potential tyrosine phosphatase inhibitor (Fig. 1.17).[112] There are numerous reports on the chromone substructure being involved in antitumour activity; however, only selected examples were highlighted here. Reports on the chromone substructure having antiplasmodial activity are, however, limited.[119] Kunert *et al* reports the moderate antiplasmodial activity of a bischromone extract isolated from *Selaginella bryopteris*.[120]

These privileged structures have displayed favourable antitumour activity; therefore their incorporation in hybrid molecules could be useful in the design and development of potential new chemotherapeutics.

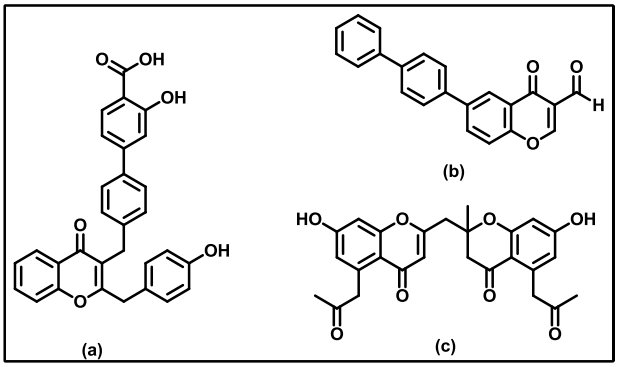

Fig. 1.17: (a) Most potent chromone described in Forghieri *et al*[118], (b) most active compound by Shim *et al*[112], and (c) bischromone structure by Kunert *et al*[120]

1.4 Hybrids – Background/Introduction

Hybrid molecules are comprised of two or more molecular components, referred to as pharmacophoric units, which are covalently linked together.[121] Hybrids differ from prodrugs; which are compounds that are administered as pharmacologically inactive agents that are converted to their active forms by bio-activation or metabolic processes.[122] In the light of increasing emphasis on combination therapy in treating diseases, especially in the treatment of malaria, one can argue that it may be advantageous to combine two drugs into a single molecular entity (Fig. 1.18). Among the numerous benefits of hybrids include their potentially lower cost of synthesis and lower risk of adverse drug-drug interactions compared to multi-component drugs.[123] This type of design is sometimes referred to as 'covalent bitherapy'.[121] When designing a hybrid molecule, the following should be taken into account: issues of the individual component's association with drug resistance, potency, solubility, mode of administration, pharmacokinetics, metabolism and toxicity.[121, 124]

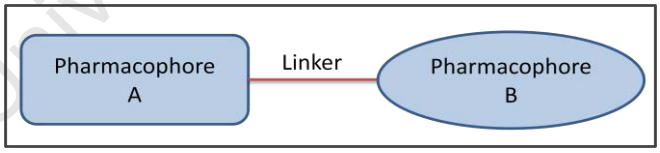

Fig. 1.18: Illustration of a hybrid drug: molecular components A and B being linked by a Linker

There are numerous forms in which a hybrid molecule can be presented:

- Both components A and B in the active form
- Either component A or B in the active form while the other is in a prodrug form
- Both components A and B in the prodrug form[125]

Another key consideration in hybrid drug design is the choice of linker, as the nature of the linker and the distance between the pharmacophores can play an essential role in the pharmacokinetics of the molecule. The choice of linker depends on the hybrid drug's intended properties, such as

dissociation upon administration or to remain intact until being cleaved at the target. These molecules can be linked in various ways, and depending on the rationale behind the design, hybrid molecules can be classified into the following categories:

- Directly Linked – the pharmacophores are connected via a functional group of each molecule, which produces a highly enzymatically hydrolyzable functional group, such as an ester, carbamate or amide.[126] An example of this is estramustine (below), a hybrid between estradiol and mechlorethamine linked via an ester bond.[127]

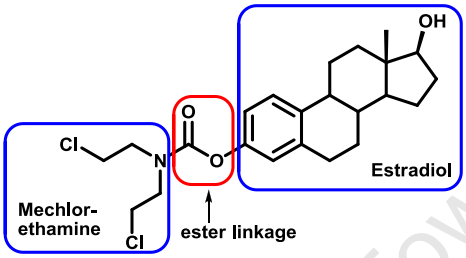

Estramustine

- Spacer Linked – the pharmacophores are connected via either a cleavable or non-cleavable linker. A non-cleavable linker is generally a non-hydrolyzable chemical bond; this is exemplified by the trifluoromethylartemisinin-mefloquine hybrid.[121, 128] In contrast, the cleavable linker is generally a hydrolyzable bond that can be hydrolyzed by plasma enzymes, as seen in NO-Aspirin. [126]

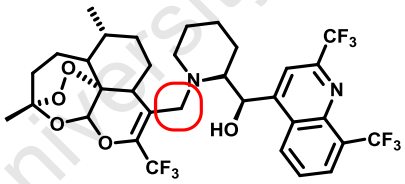

non-cleavable linkage

trifluoromethylartemisinin-mefloquine hybrid

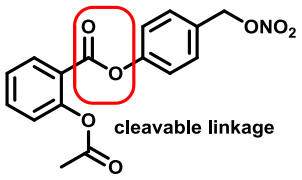

NO-Aspirin

- Fused – the pharmacophores are connected via a very short linker that allows the two molecules to fuse into one. The fentanyl-agmatine hybrid is an example of fused hybrids.[123, 129]

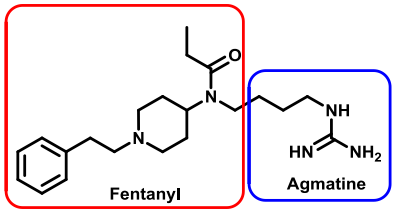

fentanyl-agmatine hybrid

- Merged – the pharmacophores have merged using common functional groups on the two molecules to produce a smaller compound; this can be seen in the anti-inflammatory symbiotic prototype LASSBio-468.[129, 124]

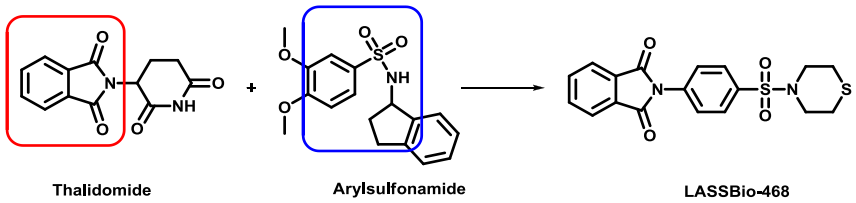

1.4.1 Examples of Hybrid Drugs in Malaria

4-Aminoquinoline-1,2,4-Trioxane-Based Hybrids

Cosledan *et al* reported the synthesis and development of trioxaquine as a potential antimalarial drug candidate.[130] Trioxaquines are hybrid compounds comprising of a 4-aminoquinoline and 1,2,4-trioxane linked to a cyclohexyl moiety by a spiro carbon atom. These molecules were created to have dual modes of action, as the trioxane pharmacophore can be involved in haeme alkylation while the 4-aminoquinoline nucleus can be used in haeme stacking.[131] Compound PA1103/SAR116242 (Fig. 1.19) was selected for preclinical development as it exhibited high potency against several chloroquine-sensitive and -resistant strains of *P. falciparum*. The hybrid was found to be effective in humanized mice infected with *P. falciparum* and displayed a good drug profile (absorption, metabolism and safety parameters).[130]

Endoperoxide-Quinoline-Based Hybrids

Walsh and co-workers designed and prepared an artemisinin-quinine hybrid in which dihydroartemisinin was directly linked to a carboxylic acid derivative of quinine via an ester linkage (Fig. 1.19).[132] The hybrid was found to have potent activity against the drug susceptible *3D7* and drug resistant *FcB1 P. falciparum* strains. To determine if the covalent linker between the two pharmacophores is required, the two pharmacophores (dihydroartemisinin and quinine) were tested individually and as a 1:1 molar ratio mixture. It was observed that the chemically-linked hybrid had superior activity. The mode of action of this drug is unknown, but it was postulated that the hybrid is cleaved *in vitro*. However, this has raised concerns over the comparison of the activities of the hybrids with their individual components as the individual components are not identical to the pharmacophore that each represents due to the chemical alterations that were done in order to form the covalent bond.[121]

4-Aminoquinoline-Pyrimidine-Based Hybrids

Recently, a series of 4-aminoquinoline-pyrimidine based hybrids were synthesized by Manohar and colleagues as potential antimalarials.[133] The 4-aminoquinoline and pyrimidine scaffolds were connected via a flexible linear diaminoalkane linker. The compounds were evaluated for their antiplasmodial activities against both CQ-sensitive *D6* and CQ-resistant *W2* strains of *P. falciparum*, with some hybrids possessing good *in vitro* potency. The hybrid with *N*-ethyl piperazine as a substituent on the pyrimidine scaffold had the greatest *in vivo* potency in the *P. berghei* malaria mouse model (Fig. 1.19). The results indicate that a synergistic effect is seen in the covalent binding of the 4-aminoquinoline to the pyrimidine substructure.[133]

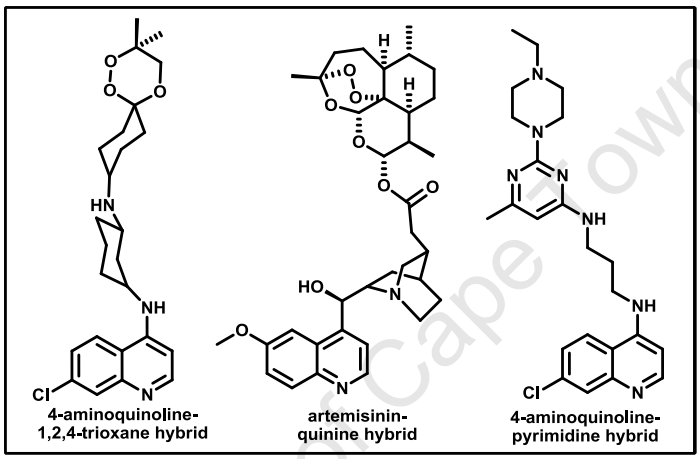

Fig. 1.19: Structure of hybrid molecules designed as potential antimalarial agents

1.4.2 Examples of Hybrid Drugs in Cancer

Estramustine

Estramustine (Emcyt®, manufactured by Pfizer) is the only hybrid drug used clinically for the treatment of prostate cancer (Fig. 1.20) and is administered as a phosphate salt to enhance water solubility.[126, 134, 135] The steroid, estradiol, is connected to a nitrogen mustard-carbamate via an ester linkage. The hybrid interacts with cellular microtubules and inhibits the G2 phase in the cell cycle and thus inhibits DNA replication. To circumvent the emergence of resistance to this drug studies are in progress to optimize the use of estramustine in combination therapy.[126, 136]

Artemisinin-Acridine-Based Hybrids

Jones and co-workers reported the synthesis of artemisinin-acridine hybrids in which an artemisinin substructure was covalently linked to 9-diaminoalkyl-6-chloro-2-methoxyacridines (Fig. 1.20).[137] The hybrids exhibited appreciable antitumour activity against *HL60* (human leukemia cells), *MDA-MB-231* (metastatic human breast cells) and *MCF-7* (human breast cells) cancer cell lines. It was observed that the chemically-linked hybrid had superior activity compared to the acridine

pharmacophore in the antitumour assays using flow cytometry, it was reported that the most potent hybrids appeared to induce apoptosis in *HL60* cancer cells, which indicated that cell arrest occurred during the G1 phase of the cell cycle.[137]

2-Phenylbenzofuran-Imidazole-Based Hybrids

Yang *et al.* reported the synthesis of directly-linked hybrids that contain the 2-phenylbenzofuran and imidazole moieties.[138] Both the pharmacophores (benzofuran and imidazole) have potent cytotoxic activities and thus covalently linking them into a single entity was thought to enhance the potency. A small library of compounds was synthesized to determine the structure-activity relationship of these hybrids, and it was evident from the antitumour testing that one hybrid displayed potent activity in human tumour cell lines (Fig. 1.20).[138]

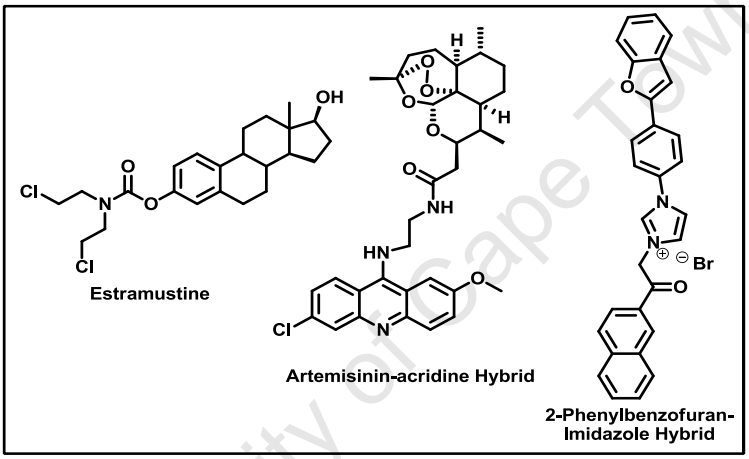

Fig. 1.20: Examples of hybrid molecules designed as antitumour agents

There are numerous reviews available discussing, in detail, the design and development of hybrid molecules as potential therapeutics for other diseases. However, only a few were discussed here in particular to malaria and cancer.[121, 123, 126, 139, 140]

1.5 Aims and Objectives

Overall Aim:

The general objective of this research is to identify novel chromone-based hybrid molecules with *in vitro* activity against the malaria parasite in the chloroquine-sensitive (CQS) *D10* and *NF54* strains and the chloroquine-resistant (CQR) *K1* strain of *P. falciparum* and the oesophageal *WHCO1* cancer cell line.

Objectives:

- To synthesize chromone-based hybrids and investigate their structure-activity relationship (SAR) as antiplasmodial and antitumour agents
- Determination of the contribution of pharmacophoric units to the pharmacological activity of hybrids by screening appropriate intermediates, i.e. screening the respective individual pharmacophores and 1:1 molar ratio mixtures
- *In-silico* and *in vitro* profiling of synthesized compounds for solubility

1.6 References

1. S. N. Cohen, K. O. Phifer and K.L. Yeilding, *Nature*, **1964**, *202*, 1543.
2. E. Ashley, R. McGready, S. Proux and F. Nosten, *Travel Med. Infect. Dis.*, **2006**, *4*, 159.
3. S. W. Lindsay and W. J. Martens, *Bull. W.H.O.*, **1998**, *76*, 33.
4. World Health Organization, *World Malaria Report 2011 Fact Sheet*, World Health Organization, Geneva, 2011.
5. J. Sachs and P. Malaney, *Nature*, **2002**, *415*, 680.
6. A. Dassonville-Klimpt, A. Jonet, M. Pillon, C. Mullie and P. Sonnet, in *Science against Microbial Pathogens: Communicating Current Research and Technological Advances*, Formatex, Spain, **2011**, *1*, 23.
7. A. Björkman and A. Bhattarai, *Acta Tropica*, **2005**, *94*, 163.
8. World Health Organization, *World Malaria Report 2011*, World Health Organization, Geneva, 2011.
9. World Health Organization, *Guidelines for the Treatment of Malaria*, World Health Organization, Geneva, 2010.
10. Centre for Disease Control and Prevention, [Cited: 24.10.2012] http://www.cdc.gov/MALARIA/.
11. A. Kumar, S. B. Katiyar, A. Agarwal and P. M. S. Chauhan, *Curr. Med. Chem.*, **2003**, *10*, 1137.
12. R. Kigozi, S. M. Baxi, A. Gasasira, A. Sserwanga, S. Kakeeto, S. Nasr, D. Rubahika, G. Dissanayake, M. R. Kamya, S. Filler and G. Dorsey, *PloS One*, 2012, **7**, 42857.
13. Malaria Foundation International, *Background Information on Malaria*, 1998.
14. V. V. Demidov, *Drug Discov. Today*, **2003**, *8*, 913.
15. S. Hoffman, *Bull. W.H.O.*, **2001**, *79*, 174.
16. D. A. Fidock, P. J. Rosenthal, S. L. Croft, R. Brun and S. Nwaka, *Nature Rev. Drug Discov.*, **2004**, *3*, 509.
17. R. G. Ridley, *Nature*, **2002**, *415*, 686.
18. M. J. Gardner, N. Hall, E. Fung, O. White, M. Berriman, R. W. Hyman, J. M. Carlton, A. Pain, K. E. Nelson, S. Bowman, I. T. Paulsen, K. James, J. A. Eisen, K. Rutherford, S. L. Salzberg, A. Craig, S. Kyes, M. Chan, V. Nene, S. J. Shallom, B. Suh, J. Peterson, S. Angiuoli, M. Pertea, J. Allen, J. Selengut, D. Haft, M. W. Mather, A. B. Vaidya, D. M. A. Martin, A. H. Fairlamb, M. J. Fraunholz, D.

S. Roos, S. A. Ralph, G. I. McFadden, L. M. Cummings, G. M. Subramanian, C. Mungall, J. C. Venter, D. J. Carucci, S. L. Hoffman, C. Newbold, R. W. Davis, C. M. Fraser and B. Barrell, *Nature*, **2002**, *419*, 498.

19. M. Delves, D. Plouffe, C. Scheurer, S. Meister, S. Wittlin, E. A. Winzeler, R. E. Sinden and D. Leroy, *PLoS Medicine*, **2012**, *9*, 1001169.
20. S. K. Chauhan and P. M. S. Srivastava, *Curr. Med. Chem*, **2001**, *8*, 1535.
21. P. A. Winstanley, *Parasitol. Today,* **2000**, *16*, 146.
22. S. Dey, S. Bindu, M. Goyal, C. Pal, A. Alam, M. S. Iqbal, R. Kumar, S. Sarkar and U. Bandyopadhyay, *J. Biol. Chem.,* **2012**, *287*, 26630.
23. K. L. Olszewski, J. M. Morrisey, D. Wilinski, J. M. Burns, A. B. Vaidya, J. D. Rabinowitz and M. Llinás, *Cell Host Microbe*, **2009**, *5*, 191.
24. R. H. Garrett and C. M. Grisham, *Biochemistry*, Thomson Brooks Cole, California, 3rd Ed., 2005.
25. B. L. Tekwani and L. A. Walker, *Comb. Chem. High T. Scr.*, **2005**, *8*, 63.
26. T. Egan, *Targets*, **2003**, *2*, 115.
27. R. Banerjee, J. Liu, W. Beatty, L. Pelosof, M. Klemba and D. E. Goldberg, *Proc. Natl. Acad. Sci. USA*, **2002**, *99*, 990.
28. P. J. Rosenthal, P. S. Sijwali and B. R. Shenai, *Curr. Pharm. Des.*, **2002**, *8*, 1659
29. K. K. Eggleson, K. L. Duffin and D. E. Goldberg, *J. Biol. Chem.*, **1999**, *274*, 32411.
30. D. Kuter, K. Chibale and T. J. Egan, *J. Inorg. Biochem.*, **2011**, *105*, 684.
31. T. J. Egan, *Parasitology*, **2008**, *157*, 127.
32. V. Shulaev, D. J. Oliver and V. S. Virginia, *Plant Physiol*., **2006**, *141*, 367.
33. T. J. Egan, *Mini Rev. Med. Chem*., **2001**, *1*, 113.
34. A F. Slater, W. J. Swiggard, B. R. Orton, W. D. Flitter, D. E. Goldberg, A Cerami and G. B. Henderson, *Proc. Natl. Acad. Sci. USA,* **1991**, *88*, 325.
35. S. Hackett, J. Hamzah, T. M. E. Davis and T. G. St Pierre, *Biochim. Biophys. Acta*, **2009**, *1792*, 93.
36. Biochemistry of *Plasmodium*, [Cited: 16.10.2012] www.tulane.edu/~wiser/malaria/fv.html.
37. S. Pagola, P. W. Stephens, D. S. Bohle, A. D. Kosar and S. K. Madsen, *Nature*, **2000**, *404*, 307.
38. P. Newton and N. White, *Annu. Rev. Med.*, **1999**, *50*, 179.
39. M. Mungthin, P. G. Bray, R. G. Ridley and S. A. Ward, *Antimicrob. Agents Ch.*, **1998**, *42*, 2973.
40. P. M. O'Neill, P. G. Bray, S. R. Hawley, S. A. Ward and B. K. Park, *Pharmacol. Ther.*, **1998**, *77*, 29.
41. S. R. Vippagunta, A. Dorn, H. Matile, A. K. Bhattacharjee, J. M. Karle, W. Y. Ellis, R. G. Ridley and J. L. Vennerstrom, *J. Med. Chem.*, **1999**, *42*, 4630.
42. P. G. Bray, O. Janneh, K. J. Raynes, M. Mungthin, H. Ginsburg and S. A. Ward, *J. Cell Biol.,* **1999**, *145*, 363.
43. P. G. Bray, M. Mungthin, R. G. Ridley and S. A. Ward, *Mol. Pharm.*, **1998**, *54*, 170.
44. M. Y. Rose, R. A. Thompson, W. R. Light and J. S. Olson, *J. Biol. Chem.*, **1985**, *260*, 6632.
45. J. M. Combrinck, T. E. Mabotha, K. K. Ncokazi, A. Melvin, D. Taylor, P. J. Smith, H. C. Hoppe and T. J. Egan, *ACS Chem. Biol.*, **2012**, doi: org/10.1021/cb300454t (In Press)
46. N. J. White, *Drug Resist. Update*, **1998**, *1*, 3.
47. T. J. Egan, E. Hempelmann and W. W. Mavuso, *J. Inorg. Biochem.*, **1999**, *73*, 101.
48. S. Krishna, F. ter Kuile, W. Supanaranond, S. Pukrittayakamee, P. Teja-Isavadharm, D. Kyle and N. J. White, *Br. J. Clin. Pharm.*, **1993**, *36*, 585.
49. A. F. Cowman, M. J. Morry, B. A. Biggs, G. A. Cross and S. J. Foote, *Proc. Natl. Acad. Sci. USA,* **1988**, *85*, 9109.
50. A. Gregson and C. V. Plowe, *Pharmacol. Rev.*, **2005**, *57*, 117.
51. P. Olliaro, *Pharmacol. Therapeut.*, **2001**, *89*, 207.
52. P. J. Rosenthal, *Int. J. Parasitol.*, **2004**, *34*, 1489.
53. P. J. Rosenthal, in *Cysteine Proteases of Pathogenic Organisms*, Springer Science+Business Media, U.S.A, **2011**, *712*, 30.
54. P. J. Rosenthal, W. S. Wollish, J. T. Palmer and D. Rasnick, *J. Clin. Invest.*, **1991**, *88*, 1467.

55. J. E. Olson, G. K. Lee, A. Semenov and P. J. Rosenthal, *Bioorg. Med. Chem*., **1999**, *7*, 633.
56. R. Li, G. L. Kenyon, F. E. Cohen, X. Chen, B. Gong, J. N. Dominguez, E. Davidson, G. Kurzban, E. M. Edwin, P. J. Rosenthal and J. H. McKerrow, *J. Med. Chem.*, **1995**, *38*, 5031.

57. P. V. Desai, A. Patny, J. Gut, P. J. Rosenthal, B. Tekwani, A. Srivastava and M. Avery, *J. Med. Chem.*, **2006**, *49*, 1576.
58. J. S. Bertram, *Mol. Aspects Med.*, **2000**, *21*, 167.
59. J. Nordberg and E. S. J. Arner, *Free Radical Bio. Med*., **2001**, *31*, 1287.
60. J. N. Burrows, K. Chibale and T. N. C. Wells, *Curr. Top. Med. Chem.*, **2011**, *11*, 1226.
61. A. O. Talisuna, P. Bloland and U. D'Alessandro, *Clin. Microbiol. Rev*., **2004**, *17*, 235.
62. I. Naidoo and C. Roper, *Trends Parasitol*., **2010**, *26*, 447.
63. P. B. Bloland, *Drug Resistance in Malaria*, Department of Communicable Disease Surveillance and Response, World Health Organization, Geneva, 2001.
64. S. Thaithong, *Bull. W.H.O.,* **1983**, *61*, 709.
65. World Health Organization, *Antimalarial drug combination Therapy. Report of a Technical Consultation*, World Health Organization, Geneva, 2001.
66. T. J. Egan and C. H. Kaschula, *Curr. Opin. Infect. Dis.*, **2007**, *20*, 598.
67. A. Nzila, Z. Ma and K. Chibale, *Future Med. Chem*., **2011**, *3***,** 1413.
68. World Health Organization, *World Malaria Report 2010*, World Health Organization, Geneva, 2010.
69. T. K. Mutabingwa, *Acta Tropica*, **2005**, *95*, 305.
70. H. Noedl, Y. Se, K. Schaecher, B. L. Smith, D. Socheat and M. M. Fukuda, *New Engl. J. Med.*, **2008**, *359*, 2619.
71. World Health Organization, *World Cancer Fact Sheet 2012*, World Health Organization, Geneva, 2012.
72. Cancer Association of South Africa, *Summary Statistics of Cancer Diagnosed*, Cancer Association of South Africa, Johannesburg, 2004.
73. G. L. Patrick, *An Introduction to Medicinal Chemistry*, Oxford University Press, Oxford, 3rd Ed., 2005.
74. National Comprehensive Cancer Network, [Cited: 25.10.2012] http://www.nccn.com.
75. S. Pelengaris and M. Khan, *Molecular Biology of Cancer*, Blackwell Publishing, Oxford, 5th Ed., 2003
76. D. Hanahan and R. A. Weinberg, *Cell*, **2011**, *144*, 646.
77. Cell Division: Binary Fission and Mitosis, [Cited: 16.10.2012] www.emc.maricopa.edu/faculty/farabee/biobk/biobookmito.html.
78. National Cancer Institute, *Cancer Fact Sheet*, [Cited: 10.10.2012] http://www.cancer.gov/cancertopics/factsheet/Therapy/radiation.
79. R. Palchaudhuri and P. J. Hergenrother, *Curr. Opin. Biotech.,* **2007**, *18*, 497.
80. R. D. Snyder and M. R. Arnone, *Mutat. Res.,* **2002**, *503*, 21.
81. G. Lamoureux and C. Agüero, *ARKIVOC*., **2009**, *1*, 251.
82. P. G. Baraldi, N. Zaid, D. Preti, F. Fruttarolo, M. A. Tabrizi, A. Iaconinoto, G. Pavani, M. D. Carrion, L. Cara and R. Romagnoli, *ARKIVOC*., **2006**, *7*, 20.
83. S. Hatse, E. De Clercq and J. Balzarini, *Biochem. Pharmacol.,* **1999**, *58*, 539.
84. A. Jordan, J. A. Hadfield, N. J. Lawrence and A. T. McGown, *Med. Res. Rev.*, **1998**, *18*, 25.
85. K. Sasaki, N. H. Tsuno, E. Sunami, G. Tsurita, K. Kawai, Y. Okaji, T. Nishikawa, Y. Shuno, K. Hongo, M. Hiyoshi, M. Kaneko, J. Kitayama, K. Takahashi and H. Nagawa, *BMC Cancer*, **2010**, *10*, 370.
86. M. F. Cohen, Y. Sakihama and H. Yamasaki, *Recent Res. Devel. Plant Physiol*., **2001**, *2*, 157.
87. B. Q. Li, T. Fu, Y. Dongyan, J. A Mikovits, F. W. Ruscetti and J. M. Wang, *Biochem. Bioph. Res. Co.*, **2000**, *276*, 534.
88. T. P. T. Cushnie and A. J. Lamb, *Int. J. Antimicrob. Ag.*, **2005**, *26*, 343.6.
89. M. Serafini, I. Peluso and A. Raguzzini, *Proc. Nutr. Soc.*, **2010**, *69*, 273.

90. K. Brusselmans, R. Vrolix, G. Verhoeven and J. V. Swinnen, *J. Biol. Chem.*, **2005**, *280*, 5636.
91. D. F. Birt, S. Hendrich and W. Wang, *Pharmacol. Therapeut.*, **2001**, *90*, 157.
92. O. Prakash, R. Kumar and V. Parkash, *Eur. J. Med. Chem.*, **2008**, *43*, 435.
93. Y. Sun, G. Liu, H. Huang and P. Yu, *Phytochemistry*, **2012**, *75*, 169.
94. M. Mazzei, E. Sottofattori, R. Dondero, M. Ibrahim, E. Melloni and M. Michetti, *Il Farmaco*, **1999**, *54*, 452.
95. S. Khadem and R. J. Marles, *Molecules*, **2012**, *17*, 191.
96. D. A. Horton, G. T. Bourne and M. L. Smythe, *Chem. Rev.*, **2003**, *103*, 893.
97. L. Costantino and D. Barlocco, *Curr. Med. Chem.*, ***2006***, *13*, 65.
98. A. M. Edwards and J. B. Howell, *Clin. Exp. Allergy,* **2000**, *30*, 756
99. Khellin Wellness Times, [Online: 26.01.2012], [Cited: 15.07.2012] http://www.wellnesstimes.com/health-resources/articles/khellin.
100. N. S. Patel, K. V. Paghdal and G. F. Cohen, *Dermatol. Surg.,* **2012**, *38*, 381.
101. M. Plit, *Fam. Pract*., **1982**, *3*, 9.
102. P. Gloviczki, A. J. Comerota, M. C. Dalsing, B. G. Eklof, D. L. Gillespie, M. L. Gloviczki, J. M. Lohr, R. B. McLafferty, M. H. Meissner, M. H. Murad, F. T. Padberg, P. J. Pappas, M. A. Passman, J. D. Raffetto, M. A. Vasquez and T. W. Wakefield, *J. Vasc. Surg.*, **2011**, *53*, 2.
103. R. W. Frick, *J. Vasc. Dis*., 2000, *51*, 197.
104. W. Thanapongsathorn and T. Vajrabukka, *Dis. Colon Rectum,* **1992**, *35*, 1085.
105. D. S. Lawrence and J. Niu, *Pharmacol. Ther*., **1998**, *77*, 81.
106. J. M. Berg, J. L. Tymoczko and L. Stryer, *Biochemistry*, W.H. Freeman and Company, New York, 6th Ed., 2006.
107. T. Akiyama, J. Ishida, S. Nakagawa, H. Ogawara, S. Watanabe, N. Itoh, M. Shibuya and Y. Fukami, *J. Biol. Chem.,* **1987**, *262*, 5592.
108. C. Kanadaswami, L. Lee, P. H. Lee, J. Hwang, F. Ke, Y. Huang and M. Lee, *In vivo,* **2005**, *19*, 895.
109. K. Michalak, O. Wesolowska, N. Motohashi and A. B. Hendrich, *Top. Heterocycl. Chem*., **2007**, *8*, 223.
110. P. P. Roger, S. Reuse, P. Servais, B. Van Heuverswyn and J. E. Dumont, *Cancer Res*., **1986**, *46*, 898.
111. K. Papazisis, D. Zambouli, O. T. Kimoundri, E. S. Papadakis, V. Vala, G. D. Geromichalos, S. Voyatzi, D. Markala, E. Destouni, L. Boutis and A. H. Kortsaris, *Cancer Letts.*, **2000**, *160*, 107.
112. Y. S. Shim, K. C. Kim, D. Y. Chi, K. Lee and H. Cho, *Bioorg. Med. Chem. Lett.*, **2003**, *13*, 2561.
113. C. Dyrager, L. N. Mollers, L. K. Kjall, J. P. Alao, P. Diner, F. K. Wallner, P. Sunnerhagen and M. Grøtli, *J. Med. Chem.*, **2011**, ***54***, 7427.
114. A. Boumendjel, E. Nicolle, T. Moraux, B. Gerby, M. Blanc, X. Ronot and J. Boutonnat, *J. Med. Chem*., **2005**, *48*, 7275.
115. J. Quintin, C. Roullier, S. Thoret and G. Lewin, *Tetrahedron*, **2006**, *62*, 4038.
116. M. Isaka, M. Sappan, P. Auncharoen and P. Srikitikulchai, *Phytochem. Lett.*, **2010**, *3*, 152.
117. W. Huang, M. Liu, Y. Li, Y. Tan and G. Yang, *Bioorg. Med. Chem*., **2007**, *15*, 5191.
118. M. Forghieri, C. Laggner, P. Paoli, T. Langer, G. Manao, G. Camici, L. Bondioli, F. Prati and L. Costantino, *Bioorg. Med. Chem.,* **2009**, *17*, 2658.
119. R. Batista, A. D. Jesus, S. Júnior, and A. B. D. Oliveira, *Molecules*, **2009**, *14*, 3037.
120. O. Kunert, R. C. Swamy, M. Kaiser, A. Presser, S. Buzzi, A. V. N. Appa Rao and W. Schühly, *Phytochem. Lett.*, **2008**, *1*, 171.
121. J. J. Walsh and A. Bell, *Curr. Pharm. Design*, **2009**, *15*, 2970.
122. C. R. Craig and R. E. Stitzel, *Modern Pharmacology with Clinical Applications*, Lippincott Williams and Wilkins, Philadelphia, 5th Ed., 1997.
123. F. W. Muregi and A. Ishih, *Drug Develop. Res.*, **2010**, *32*, 20.
124. C. Alberto and M. Fraga, *Expert Opin. Drug Discov.*, **2009**, *4*, 60.
125. B. Meunier, *Accounts Chem. Res.*, **2008**, *41*, 69.
126. L. K. Gediya and V. C. O. Njar, *Expert Opin. Drug Discov.*, **2009**, *4*, 1099

127. D. T. Trafalis, *Cancer Lett.*, **2006**, *243*, 202.
128. F. Grellepois, P. Grellier, D. Bonnet-Delpon and J. P. Begue, *Chem. Bio. Chem.*, 2006, **6**, 648.
129. R. Morphy and Z. Rankovic, *J. Med. Chem.*, **2005**, *48*, 6523.

130. F. Cosledan, L. Fraisse, A. Pellet, F. Guillou, B. Mordmuller, P. G. Kremsner, A. Moreno, D. Mazier, J. Maffrand and B. Meunier, *Proc. Natl. Acad. Sci. USA*, **2008**, *105*, 17579.
131. S. A. Laurent , C. Loup, S. Mourgues, A. Robert and B. Meunier, *Chem. Bio. Chem*., **2005**, *6*, 653.
132. J. J. Walsh, D. Coughlan, N. Heneghan and A. Bell, *Bioorg. Med. Chem. Lett.*, **2007**, *17*, 3599.
133. S. Manohar, U. C. Rajesh, S. I. Khan, B. L. Tekwani and D. S. Rawat, *ACS Med. Chem. Lett.*, **2012**, *3*, 6.
134. Y. Qurishi, A. Hamid, R. Majeed, A. Hussain, A. K. Qazi, M. Ahmed, M. A. Zargar, *Future Oncol.*, **2011**, *7*, 1007.
135. P. O. Anderson, J. E. Knoben and W. G. Troutman, Handbook of *Clinical Drug Data*, McGraw-Hill Medical Publishing Division, United States of America, 10th Ed., 2002.
136. D. P. Petrylak, C. M. Tangen, M. H. A. Hussain, P. N. Lara, J. A. Jones, M. E. Taplin, P. A. Burch, D. Berry, C. Moinpour, M. Kohli, M. C. Benson, E. J. Small, D. Raghavan and E. D. Crawford, *New Engl. J. Med.,* **2004**, *351*, 1513.
137. M. Jones, A. E. Mercer, P. A. Stocks, L. J. I. La Pensee, R. Cosstick, B. K. Park, M. E. Kennedy, I. Piantanida, S. A. Ward, J. Davies, P. G. Bray, S. L. Rawe, J. Baird, T. Charidza, O. Janneh and P. M. O' Neill, *Bioorg. Med. Chem. Lett.*, **2009**, *19*, 2033.
138. X. Yang, W. Wan, X. Deng, Y. Li, L. Yang and L. Li, *Bioorg. Med. Chem. Lett.*, **2012**, *22*, 2726.
139. V. V. Kouznetsov and A. Gómez-Barrio, *Eur. J. Med. Chem.*, **2009**, *44*, 3091.
140. R. Capela, G. G. Cabal, P. J. Rosenthal, J. Gut, M. M. Mota, R. Moreira, F. Lopes and M. Prudêncio, *Antimicrob. Agents Ch.*, **2011**, *55*, 4698.

Chapter Two – Design, Synthesis and Biological Evaluation of Chromone-Aminoquinoline Hybrids

2.1 Introduction

This chapter describes the design, synthesis and characterization of an exploratory series of novel compounds obtained by the hybridization of an antimalarial and an anticancer pharmacophore. The pharmacophores of choice are the 4-aminoquinoline and chromone motifs. The synthetic procedures used were based on standard chemistry protocols. The resultant structurally related molecules formed the basis of a more focused structure-activity relationship (SAR) study. All analogues synthesized were evaluated for their *in vitro* antiplasmodial and antitumour activities. Furthermore, testing for antimycobacterial activity was also carried out in addition to various physicochemical property profiling.

2.2 Rationale for the Synthesis of Chromone-Aminoquinoline Hybrids

A pharmacophore is described as 'a molecular framework that carries the essential features responsible for a drug's biological activity'.[1] The use of pharmacophore hybridization is thought to be analogous to conventional combination therapy, with the exception that the two drugs are now covalently-linked and are available as a single entity.[2] This approach offers a large SAR study which precludes the need for large libraries, drastically shortening the time needed to identify potential leads.[3] Covalently linking two distinct chemical moieties with different modes of action to produce a hybrid is now a commonly used strategy in the discovery and development of antimalarial drugs.[4]

In this work, hybrids were developed using cleavable amide and non-cleavable alkyl linkers. Additionally, the concept of a compound having superior activity to its individual components through a synergistic or additive effect was investigated by evaluating the activity of hybrids and their precursors. In principle, the biological activities are envisaged to be maximized by the incorporation of the chromone core, an anticancer pharmacophore, to the 4-aminoquinoline moiety, an antimalarial pharmacophore, via a covalent linker at positions 2 and 3 of the chromone ring. Some key structural and chemical features targeted for investigation through SAR studies are summarized in Fig. 2.1. One of the objectives of this project was to evaluate the linker between the pharmacophores. For this, two types of linkers were chosen; an alkyl (non-cleavable) linker and an amide (cleavable) linker; where the latter has the potential to be hydrolyzed *in vivo* to produce the individual pharmacophores. Various electron-withdrawing groups such as bromo, chloro, and fluoro groups, and electron-donating groups and electron-releasing groups such as methoxy and methyl groups, were added at position 6 of the chromone ring to study the electronic properties of the chromone ring and its effect on antiplasmodial and antitumour activity. In the synthesis of alkyl- and amide-linked hybrids, the relevant primary amine, aldehydes and carboxylic acids were prepared

first. The reactivity, synthesis and characterization are described below, followed by the synthesis and characterization of the target hybrid compounds.

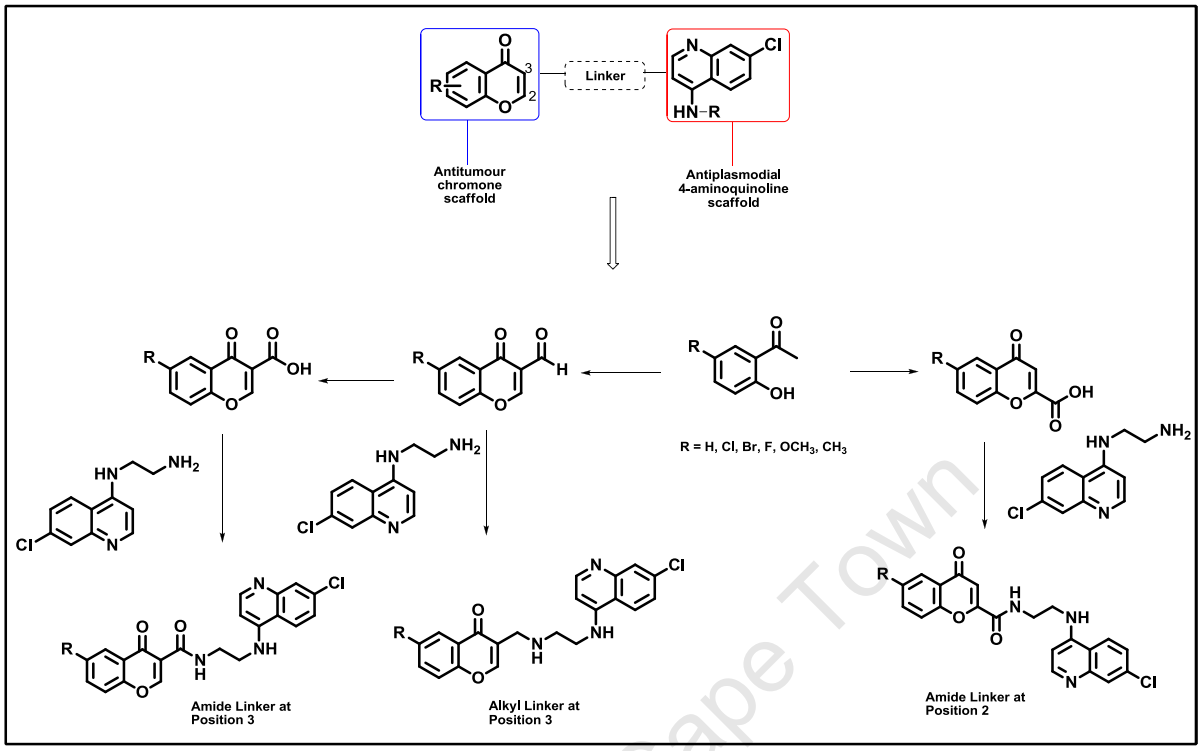

Fig. 2.1: Outline of target compounds

2.3 Aminoquinolines – Introduction, Reactivity, Synthesis and Characterization

Introduction

Aminoquinolines consist of a quinoline scaffold, which is prevalent in a variety of pharmacologically active antimalarials (Fig. 2.2).[5] Chloroquine (CQ) is perhaps one of the most recognizable drugs from this group, along with other antimalarials including amodiaquine, piperaquine, primaquine, quinine and mefloquine. The quinoline nucleus has been found to inhibit haeme polymerization and haemozoin formation.[6] This in turn leads to the intraparasitic accumulation of free haeme, which is highly toxic to the malaria parasite as highlighted in chapter one.

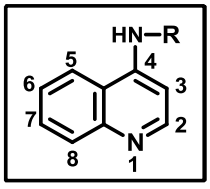

Fig. 2.2: 4-Aminoquinoline nucleus

Previous SAR studies conducted on chloroquine and closely related 4-aminoquinoline antiplasmodial compounds report that for optimal antiplasmodial activity in CQ-sensitive (CQS) and CQ-resistant (CQR) strains of *P. falciparum*, the following structural features must be present:

- a quinoline ring, with no alkyl substitutions attached;
- a halogen at position 7 of the quinoline ring, except for fluorine;
- a nitrogen atom at position 1 of the quinoline ring that is able to undergo protonation; and
- a protonatable nitrogen atom at the end of the side chain attached to the quinoline ring at position 4.[7, 8]

Egan and co-workers established that the aminoquinoline ring is essential for antiplasmodial activity, as the motif associates with haematin.[7] They also reported that having a chloro, bromo or iodo group at position 7 of the aminoquinoline ring improves antiplasmodial activity.[7] β-haematin inhibition studies conducted by Egan and co-workers have found that aminoquinolines that have an electron-donating group at C_7 of the ring have the highest inhibition rates.[8] Research has suggested that if a compound can inhibit β-haematin formation, it has the potential to display excellent antiplasmodial activity. Further studies have suggested that the length of the alkyl group between the two nitrogen atoms on the 4-amino side chain must be between 2 and 4 carbon atoms, or between 10 and 12 carbon atoms to maintain activity against CQR strains of *P. falciparum*.[9] The inclusion of protonatable nitrogen atoms at position 1 of the aminoquinoline ring and at the end of the side chain attached at position 4 is required for vacuolar accumulation (Fig. 2.3). These points validate the use of the aminoquinoline scaffold in the search of new antimalarials, as compounds having this moiety have had high levels of success in the treatment and prophylaxis of malaria. Another key characteristic of these compounds is that they have relatively easy and cheap synthetic routes; additionally, drug resistance occurs due to the inability of the drug to access the target site and not from structural changes to the target.[6, 10]

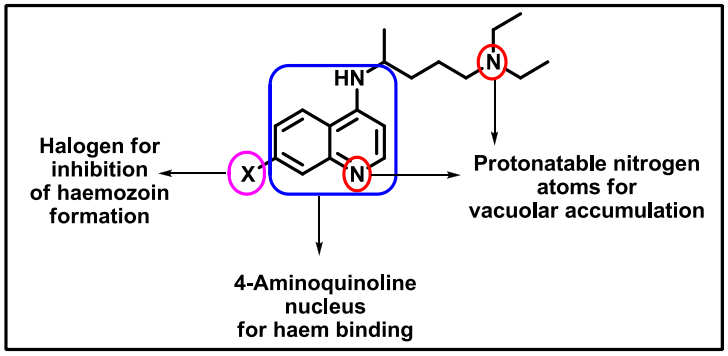

Fig.2.3: Structure-Activity Relationship of chloroquine reported by Egan *et al.*[7]

Reactivity

Quinolines are heterocyclic rings produced by the fusion of benzene and pyridine rings. Quinoline chemistry is similar to that of benzene and pyridine wherein the benzene ring favours electrophilic substitution and the pyridine ring favours nucleophilic substitution.[11] These compounds are generally more π-deficient due to their mesomeric and inductive effects which are attributed to the nitrogen atom within the ring (Fig. 2.4). This effect is most evident at C_2 and C_4 due to the close proximity of the nitrogen atom. The reactivity at these positions can be further increased by the introduction of electron-withdrawing groups, such as halogens, on the ring.

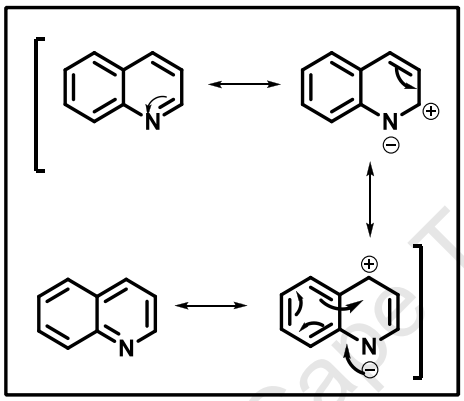

Fig. 2.4: Illustration of the mesomeric and inductive effects of the nitrogen atom on the quinoline ring

Synthesis of N^1-(7-chloroquinolin-4-yl)ethane-1,2-diamine, ***SN08***

The primary amine, **SN08**, was prepared by stirring 4,7-dichloroquinoline in ethylene diamine for 1 hour at 100 °C and then increasing the temperature to 140 °C for a further 4 hours (Scheme 2.1). **SN08** was isolated as a pale-yellow solid with a satisfactory yield.

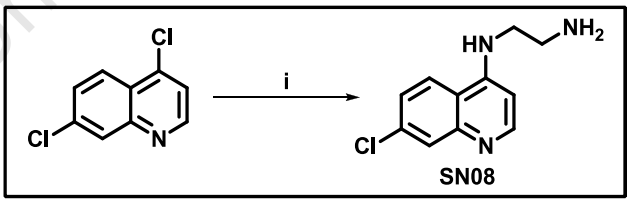

Scheme 2.1: Reagents and conditions: i. Ethylene diamine (6.0 eq), 100 – 140 °C, 5 h

The reaction follows a nucleophilic aromatic substitution route (S_NAr) where the addition of a nucleophile is followed by the elimination of the leaving group (Fig. 2.5). Ethylene diamine acts as the nucleophile, attacking the carbon atom at position 4 of the heteroaromatic ring. The carbanion is resonance-stabilized by the delocalization of the negative charge within the ring. Subsequent elimination of the chloro group and release of HCl produces the amine.[11]

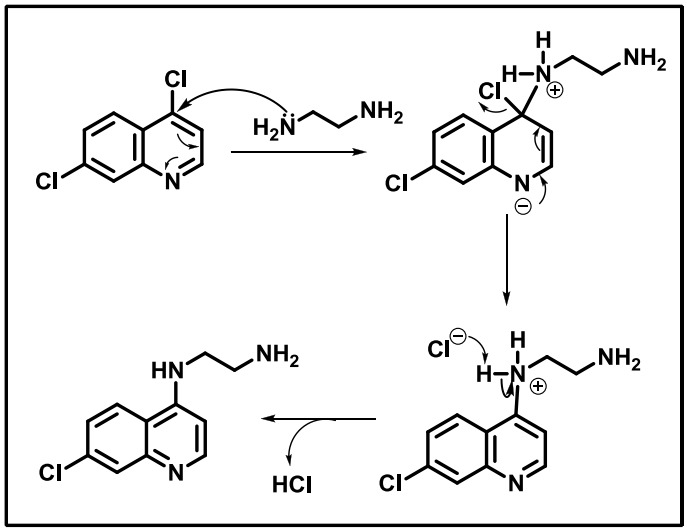

Fig. 2.5: Proposed mechanism of formation of N^1-(7-chloroquinolin-4-yl)ethane-1,2-diamine, **SN08**

Spectroscopic Analysis of 4-aminoquinoline derivative

The synthesized quinolines exhibit a unique pattern in their ^{1}H and ^{13}C NMR spectra, with the methylene protons resonating upfield between 2.98 and 3.44 ppm in the ^{1}H NMR spectrum (Fig. 2.6). Analysis of the ^{1}H NMR spectrum depicts the vicinal coupling of H_1 to H_2 and H_3 to H_4 with *J* values of 5.7 and 9.0 Hz respectively; these are consistent with those reported in the literature.[12] H_4 was seen as a doublet of doublet (dd) due to its coupling to H_3 and its additional long-range coupling to H_5. In the ^{13}C NMR spectrum of **SN08**, eleven signals were observed corresponding to the total number of carbon atoms in the molecule, with the carbon *para* to the nitrogen atom within the heterocyclic ring, resonating at 152.8 ppm as the most downfield signal. In the infrared spectrum, which was recorded in KBr, there is a distinct band at 1578 cm^{-1}, corresponding to the imine stretching frequency. The uncorrected melting point of **SN08** was found to be in the range of 128 – 131 ^{o}C, which is similar to the value reported in literature of 131 – 132 ^{o}C.[12]

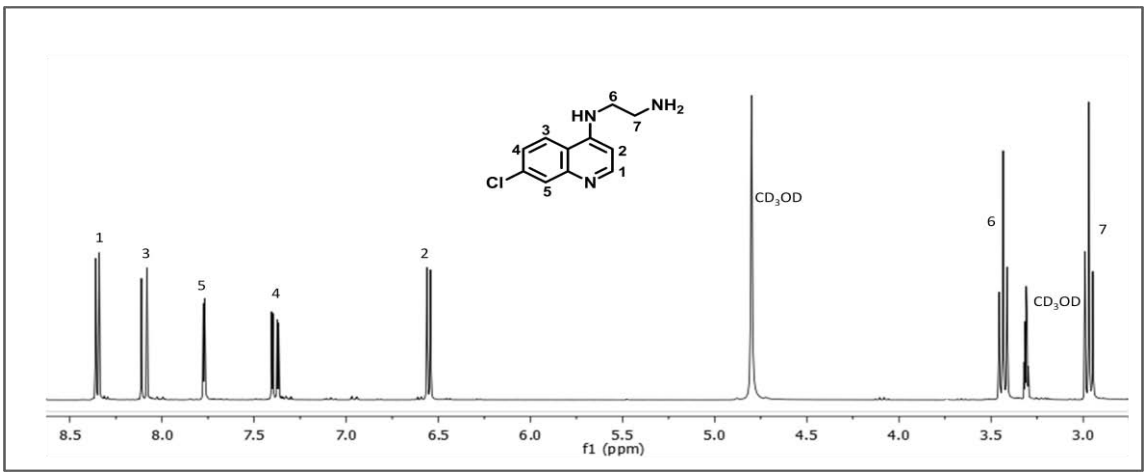

Fig. 2.6: ^{1}H NMR spectrum of **SN08** in CD_3OD at 300 MHz

2.4 Chromone-Aminoquinoline Hybrids

The synthesis of the chromone-aminoquinoline hybrids was accomplished by the coupling of a chromone derivative to the aminoquinoline nucleus. Described below is the reactivity of chromones, followed by the synthesis and characterization of the target compounds.

Chromones – Introduction and Reactivity

The chromone substructure is a privileged motif in drug discovery and thus can be used in the search of potentially useful chemotherapeutic agents.[13] Chromones are heterocyclic molecules that are derivatives of benzopyran with a substituted keto group on a γ-pyrone ring. They are able to undergo a wide range of chemical reactions with nucleophiles and electrophiles. Typically, nucleophiles attack at positions 2 and 4 of the heterocyclic ring; however, attacks at position 2 lead to the opening of the pyrone ring resulting in the loss of the C_2-C_3 π bond. Opening of the chromone ring can also be achieved by treatment with aqueous alkali.[14] Electrophilic reactions normally occur at O_1, C_3 or the carbonyl oxygen, due to the accumulation of electron density of the heteroatoms (Fig. 2.7).[11] The pyrone ring, on the other hand, is relatively unreactive towards electrophiles as electrophilic reagents such as strong acids tend to protonate the pyrone ring thereby inactivating it.[15] The presence of a halogen or triflate allows chromones to be used as substrates in various coupling reactions to introduce alkyl or aryl substituents.

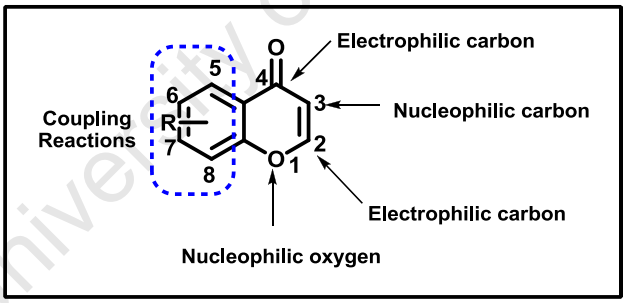

Fig. 2.7: Illustration of the reactivity of chromones

2.4.1 Chromone-Aminoquinoline Alkyl-Linked Hybrids, Series 1

The aminoquinoline nucleus was linked via an alkyl chain to position 3 of the chromone moiety to produce Series 1. This was prepared using the primary amine, **SN08**, and an aldehyde in a reductive amination reaction step. To achieve this, chromone-3-carbaldehydes were synthesized; the synthesis and characterization of these aldehydes is described below.

2.4.1.1 Synthesis and Characterization of Chromone-3-Carbaldehydes

A series of substituted chromone-3-carbaldehydes, **SN18 – SN23** and **SN83-1 – SN95-1**, were prepared using the synthetic methodology developed by Nohara, utilizing the Vilsmeier-Haack

reaction.[16] Substituted 2-hydroxyacetophenones were treated with phosphorus oxychloride ($POCl_3$) in anhydrous *N,N*-dimethylformamide (DMF) at low temperature (Scheme 2.2). The crude compounds were recrystallized from acetone to afford the pure aldehydes (Table 2.1).

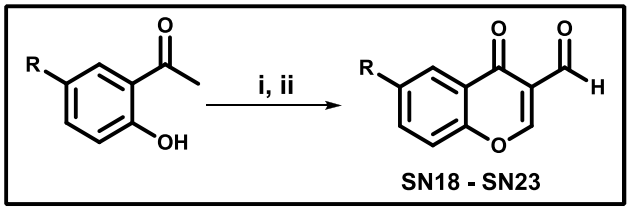

Scheme 2.2: Reagents and conditions: i. $POCl_3$ (6 eq), DMF, N_2, 12 h; ii. H_2O, 0 ^oC

Table 2.1: Isolated yields, molecular ion peaks and melting points of chromone-3-carbaldehydes

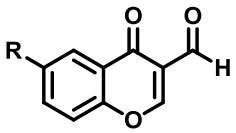

Code	R	Yield (%)	$[M]^+$		Melting Point (^oC)
			Expected	Found	
SN18	H	61	174.0	174.0	144 – 146
SN19	Cl	89	207.9	207.9	166 – 167
SN20	Br	90	251.9	251.8	158 – 160
SN21	F	66	192.0	192.1	146 – 149
SN22	OCH_3	56	204.1	203.9	145 – 148
SN23	CH_3	67	188.1	187.9	156 – 159

In a Vilsmeier-Haack reaction, *N,N*-dimethylformamide and phosphorus oxychloride are used in conjunction to produce a chloroiminium ion, a carbon electrophile. The amide functional group in DMF reacts with $POCl_3$, which removes the amide oxygen and replaces it with a chlorine atom; this step is unfavourable except for the formation of the strong phosphorus-oxygen bond. The iminium cation then reacts with the acetophenone enolate, which is generated by the protonation of the carbonyl oxygen. This produces a chromen-4-one, which attacks another iminium cation to produce a cationic intermediate. Subsequent hydrolysis and proton transfer (P.T.) adds a formyl group on position 3 of the chromone ring to produce the chromone-3-carbaldehydes (Fig. 2.8).[11]

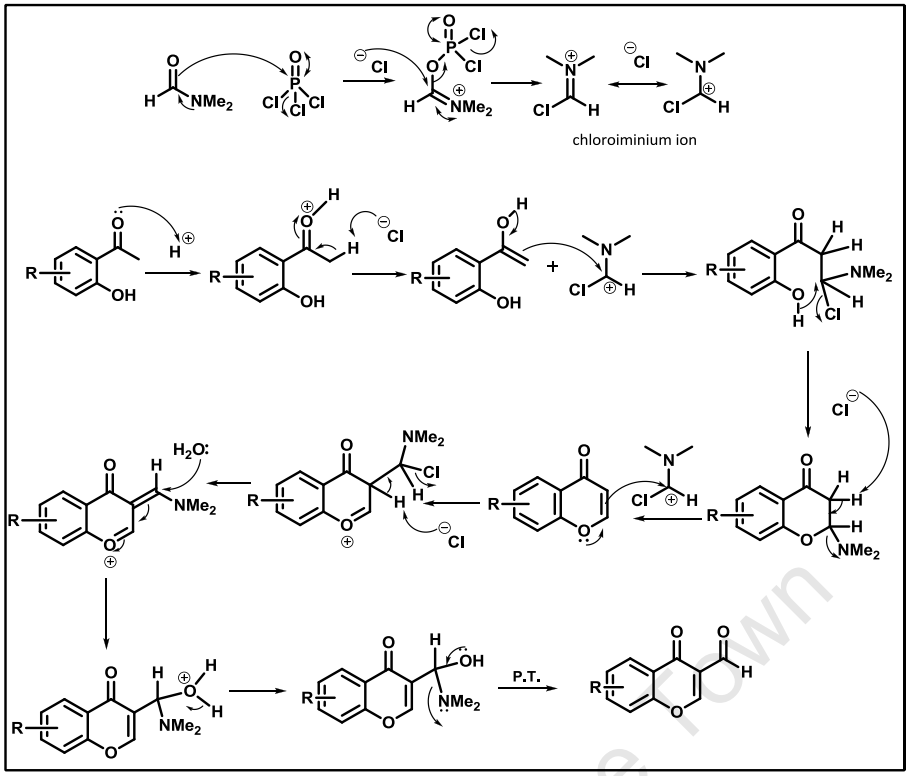

Fig. 2.8: Proposed mechanistic route for the formation of chromone-3-carbaldehydes

Spectroscopic Analyses of Chromone-3-carbaldehydes

In the ^{1}H NMR spectra of these compounds, the distinctive signal above 10 ppm confirms the presence of the aldehyde proton. The proton adjacent to the oxygen in the chromone ring resonates at 8.5 ppm due to the heteroatom and the neighbouring double bond. The remaining protons on the chromone ring (for further details, please see chapter five) correspond to values reported in the literature.[16] Further indication of the presence of the formyl group was seen in the infrared spectrum recorded in KBr, which showed two separate absorption bands at 1600 cm^{-1} due to the two carbonyl functional groups within the molecule. Mass spectra analyses indicated the presence of the molecular ion peaks of the aldehydes. Once the aldehydes were synthesized, the next step was the synthesis of the covalently-linked chromone-aminoquinoline hybrids.

2.4.1.2 Synthesis and Characterization of Alkyl-Linked Hybrids, Series 1

These target compounds were prepared by reductive amination of the chromone-3-carbaldehydes with **SN08**. The amine and aldehydes were stirred in anhydrous dichloromethane and methanol at room temperature to generate the imines *in situ*.[17] The formation of the imine was detected by the disappearance of the aldehyde spot on TLC. Once the disappearance of the starting material was observed, sodium triacetoxyborohydride [$NaBH(OAc)_3$] was added to reduce the imine and produce the secondary amines, **SN24** – **SN28** and **SN31** (Scheme 2.3).

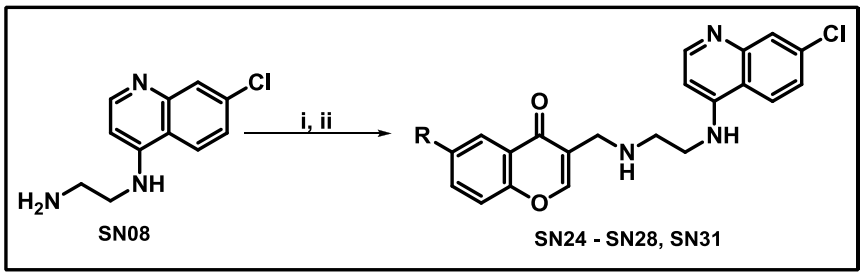

Scheme 2.3: Reagents and conditions: i. **SN18** – **SN23** (1.0 eq), DCM, CH_3OH, N_2, RT; ii. $NaBH(OAc)_3$ (3.0 eq), RT, 16 h

Spectroscopic Analyses of Alkyl-Linked Hybrids

The ^1H NMR spectrum of **SN25** is presented in Fig. 2.9, illustrating the general pattern of the covalently-linked hybrids. The disappearance of the aldehyde proton signal of the chromone-3-carbaldehyde was a clear indication that the reductive amination had been successful. In addition, the appearance of a singlet at 3.18 ppm was assigned to the newly-formed methylene group, H_5. The protons on the aminoquinoline nucleus remain at relatively similar chemical shifts as observed previously, with the exception of the signals for H_6 and H_7, which have moved further downfield from 2.98 and 3.44 ppm to 3.52 and 3.62 ppm, respectively, due to the attachment to the chromone scaffold. The COSY spectrum confirmed the correlation and coupling between the aromatic protons. The ^{13}C NMR spectra indicated twenty-one carbons for the alkyl-linked hybrids except for **SN27** and **SN28**, which had twenty-two carbons due to the methoxy and methyl groups on their chromone structures. Analyses of the spectroscopic data indicated the successful syntheses of the chromone alkyl-linked aminoquinoline hybrids.

Table 2.2: Isolated yields, molecular ion peaks and melting points of Alkyl-Linked Hybrids

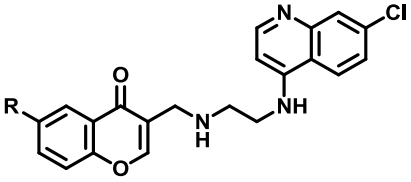

Code	R	Yield (%)	$[M]^+$		Melting Point (°C)
			Expected	Found	
SN31	H	50	379.1	379.0	81 – 83
SN24	Cl	65	413.1	412.8	96 –100
SN25	Br	75	457.0	458.5	122 – 125
SN26	F	60	397.1	395.1	117 – 119
SN27	OCH_3	41	409.1	409.1	94 – 98
SN28	CH_3	52	393.1	393.0	118 – 120

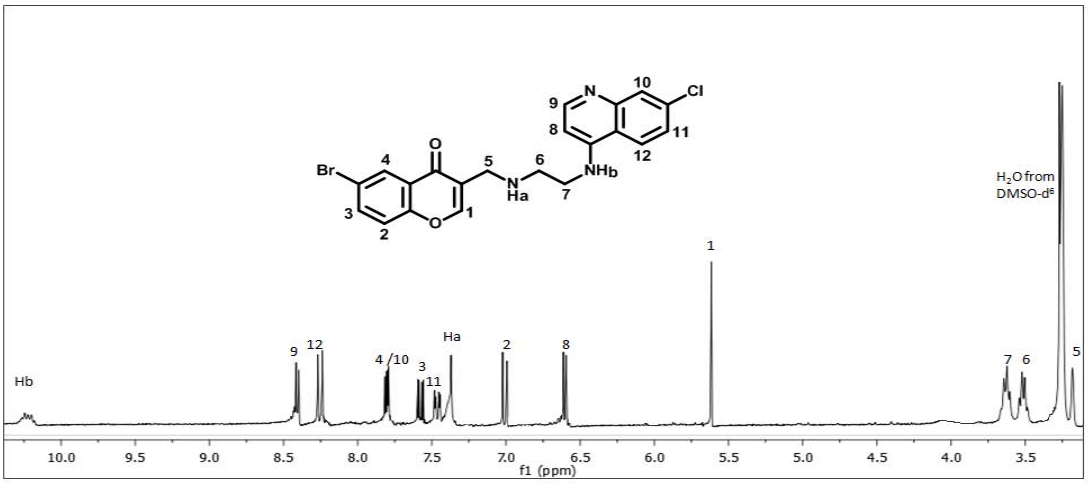

Fig. 2.9: ^{1}H NMR of **SN25** in DMSO-d_6 at 400 MHz

2.4.2 Chromone-Aminoquinoline Amide-Linked Hybrids, Series 2 and Series 3

Series 2 and 3 contain the amide-linked chromone-aminoquinoline hybrid compounds; these were synthesized via amide coupling procedures involving a coupling agent, EDC (1-ethyl-3-(3-dimethylaminopropyl) carbodiimide), with **SN08** and the chromone carboxylic acids. The carboxylic acids in these cases were the chromone-3-carboxylic acids and chromone-2-carboxylic acids. The synthesis and characterization of these acids are described below followed by the synthesis and characterization of the hybrids.

2.4.2.1 Synthesis and Characterization of Chromone-3-Carboxylic Acids

A series of chromone-3-carboxylic acids, **SN11**, **SN29**, **SN38**, **SN40** – **SN42** and **SN83-2** – **SN95-2**, were prepared using the Lindgren oxidation route (Scheme 2.4). Lindgren oxidation involves the selective oxidation of aldehydes to carboxylic acids using a mixture of water and a polar solvent.[18] Sodium chlorite was used as the oxidizing agent with sulfamic acid as the scavenger to remove any by-product, specifically the hypochlorite generated in the reaction. This procedure works efficiently when the chromone-3-carbaldehydes were vigorously stirred in a mixture of dichloromethane and distilled water for 4 – 6 hours. Recrystallization of the crude material from methanol produced the pure acids in high yields. A summary of the carboxylic acids can be seen in Table 2.3, with the exception of compounds **SN83-2** to **SN95-2** as these will be discussed in chapter three.

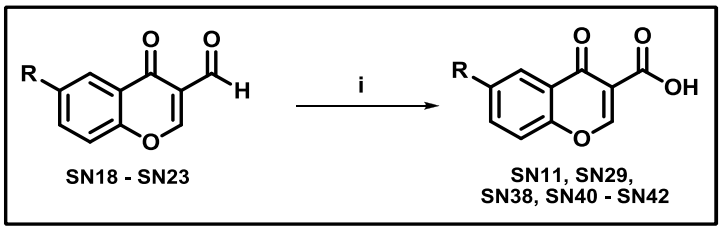

Scheme 2.4: Reagents and conditions: i. $NaClO_2$ (6.0 eq), NH_2SO_3H (8.0 eq), DCM, H_2O, RT, 4 – 6 h

Table 2.3: Isolated yields, molecular ion peaks and melting points of chromone-3-carboxylic acids

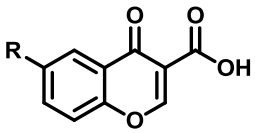

Code	R	Yield (%)	$[M]^+$		Melting Point (°C)
			Expected	Found	
SN11	H	78	190.0	190.0	147 – 150
SN29	Cl	77	223.9	223.9	212 – 215
SN38	Br	56	267.9	267.9	175 – 178
SN40	F	85	208.0	208.0	222 – 224
SN41	OCH_3	81	220.0	220.0	155 – 157
SN42	CH_3	77	204.2	204.0	225 – 228

Spectroscopic Analyses of Chromone-3-carboxylic acids

Distinctive features of carboxylic acids are the broad downfield singlets in the ^1H NMR spectra, generally seen at 13 ppm. It was also observed that there was a downfield shift of the chromone proton due to the acidic group. The remaining protons on the ring resonate in similar chemical environments as their corresponding aldehydes. In comparing the ^{13}C NMR spectra of the chromone-3-carbaldehydes and chromone-3-carboxylic acids, the signal for C_4 shifted upfield, whereas the carboxylic acid carbon resonated downfield when compared to the aldehyde carbon. Analysis of the infrared spectrum of **SN29**, 6-chloro-4-*oxo*-4*H*-chromene-3-carboxylic acid, indicated two carbonyl stretches at 1625 and 1739 cm^{-1} and a broad band at 3443 cm^{-1} corresponding to the O-H stretch. These analyses and the mass spectrometry data confirm the successful oxidation of the aldehydes into chromone-3-carboxylic acids.

2.4.2.2 Synthesis and Characterization of Chromone-2-Carboxylic Acids

The synthesis of the chromone-2-carboxylic acids, **SN68 – SN72**, was accomplished by the Baker-Venkataraman rearrangement using diethyl oxalate and sodium ethoxide followed by an acid promoted cyclization (Scheme 2.5).[19, 20]

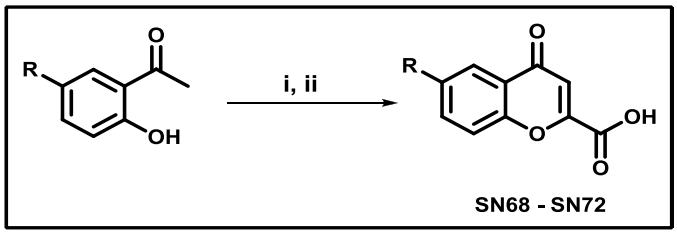

Scheme 2.5: Reagents and conditions: i. Diethyl oxalate (1.1 eq), NaOEt, N_2, 95 ^{o}C, 2h;
ii. Glacial acetic acid, HCl (conc.), 95 ^{o}C, 2h

This rearrangement proceeds via an enolate intermediate formed between the 2-hydroxyacetophenone and diethyl oxalate (Fig. 2.10). This is followed by an acyl transfer in sodium ethoxide, which was generated *in situ* to generate the 1,3-diketone, which was not isolated but used as a crude mixture. Ring closure occurred when the crude mixture was treated with concentrated hydrochloric acid and glacial acetic acid. Recrystallization from glacial acetic acid afforded the chromone-2-carboxylic acids as pure off-white/grey solids with moderate yields. These acids had poor solubility in chlorinated and alcoholic solvents as opposed to their chromone-3-carboxylic acid counterparts.

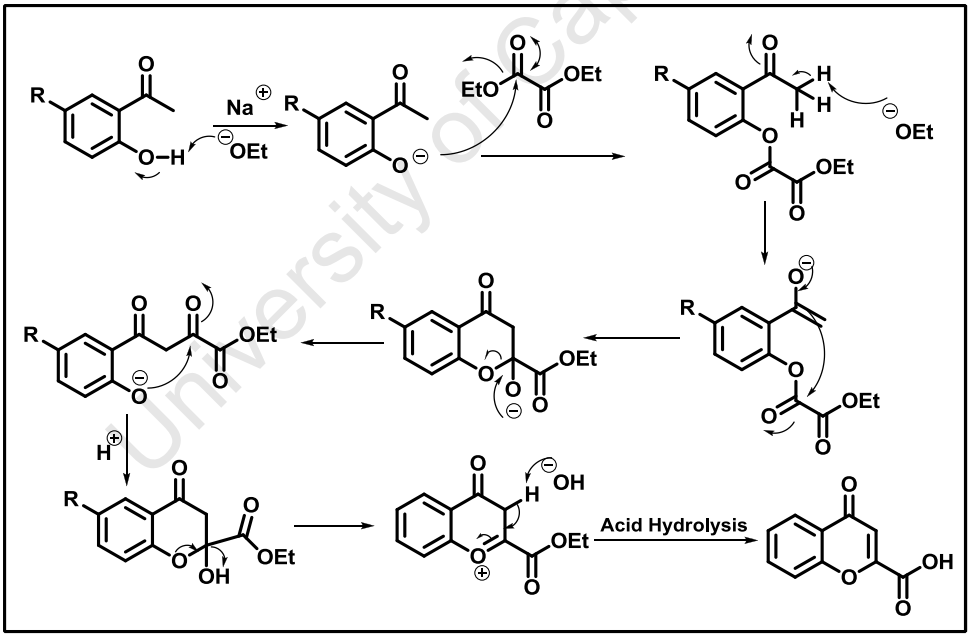

Fig. 2.10: Proposed mechanistic route for the formation of chromone-2-carboxylic acids, **SN68** – **SN72**

Spectroscopic Analyses of chromone-2-carboxylic acids

Due to the poor solubility of the acids in chloroform, ^{1}H NMR spectra were recorded in deuterated dimethyl sulfoxide. As a result, the carboxylic acid proton was not observed presumably due to the rapid exchange with water present in DMSO-d_6. The other signals represent the remaining protons on the ring with chemical shifts corresponding to those reported in the literature.[21, 22] The ^{13}C NMR

spectra confirmed ten carbons for the carboxylic acids except for **SN72**, which had eleven carbons due to the methoxy group on the chromone motif. Additionally, two downfield signals at 164 and 178 ppm in the spectra corresponding to the two carbonyl carbon atoms were observed. Further confirmation of the successful synthesis of the chromone-2-carboxylic acids was the identification of the molecular ion peaks in the mass spectrometry analyses (Table 2.4). It was observed that the melting points of the chromone-2-carboxylic acids were generally much higher than those of the chromone-3-carboxylic acids as reported in literature.[23]

Table 2.4: Isolated yields, molecular ion peaks and melting points of chromone-2-carboxylic acids

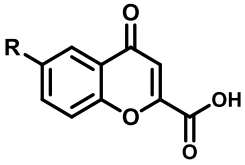

Code	R	Yield (%)	$[M]^+$		Melting Point (^oC)
			Expected	Found	
SN68	H	72	190.0	190.0	252 – 255
SN69	Cl	60	223.9	223.9	242 – 245
SN70	Br	60	267.9	267.7	263 – 265
SN71	F	28	208.0	207.8	243 – 245
SN72	OCH_3	62	220.0	219.9	279 – 281

2.4.2.3 Synthesis and Characterization of Amide-Linked Hybrids, Series 2 and 3

The 4-aminoquinoline derivative was attached via an amide linker to position 3 (Series 2) and position 2 (Series 3) on the chromone ring (Scheme 2.6).

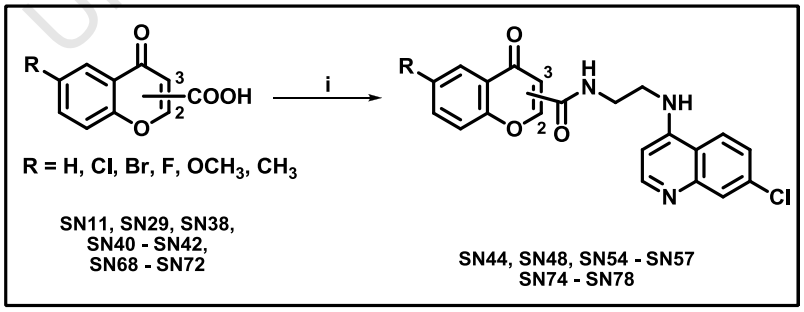

Scheme 2.6: Reagents and conditions: i. EDC (1.3 eq), HOBt (1.3 eq), **SN08** (1.5 eq), DMAP (0.5 eq), DCM, DMF, N_2, 16h

The amide bond was formed by the condensation of the primary amine, **SN08**, with the carboxylic acids in the presence of EDC. EDC was used here as the hydrochloride salt and therefore required the addition of Et_3N (triethylamine) to neutralize the HCl. DMAP (*N,N*-Dimethylaminopyridine) was

used as a catalyst. The mechanism involves the deprotonation of the carboxylic acid by EDC, followed by nucleophilic attack by the carboxylate onto the carbodiimide. This allows for the formation of an isourea intermediate. HOBt (*N*-hydroxybenzotriazole) intercepts the activated ester intermediate to displace a highly water soluble urea group (1-(2-(dimethylamino)ethyl)-3-ethylurea) and suppresses any racemization that may take place. The production of urea as a by-product accelerates the forward reaction, allowing the terminal amine group on **SN08** to attack the HOBt ester and produce the amide product.[11] A detailed mechanism is shown in Fig. 2.11.

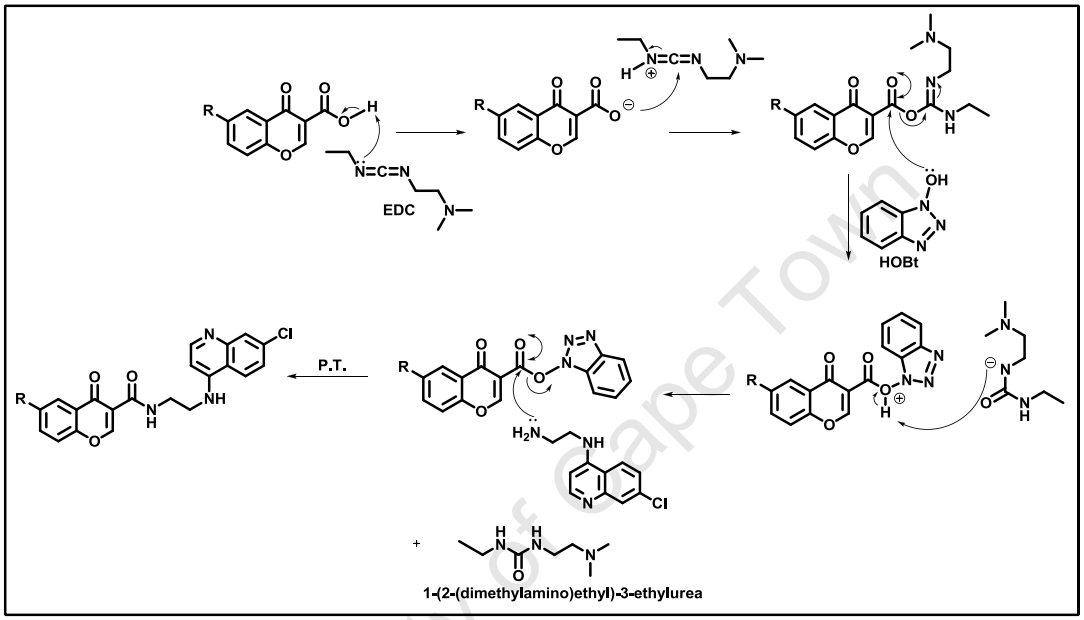

Fig. 2.11: Mechanism of formation of amide-linked hybrid compounds

These coupling reactions were conducted in either DMF or a mixture of DCM/DMF as solvents, depending on the solubility of the acid used. The purification was accomplished using a gradient of DCM:MeOH as the eluent on silica gel to obtain the target compounds in varying yields (Table 2.5).

Spectroscopic Analyses of Series 2 and Series 3

SN74 will be used as a representative of the amide-linked hybrid compounds and will thus be analysed in detail. The ^{1}H NMR spectrum of **SN74** (Fig. 2.12) confirmed the formation of the amide hybrid as there was a downfield shift of the aliphatic protons (H_6 and H_7) from 2.98 and 3.44 ppm in **SN08** to 3.67 and 3.74 ppm in the hybrid. The aromatic signals remain in relatively similar chemical shift environments and produced similar coupling constants as in their precursors, except for H_1, which shifted downfield as it is now adjacent to the amide bond and not the electron-withdrawing carboxylic acid. Analysis of the COSY spectrum indicated the position of the signals produced by the protons attached to the nitrogens; H_a was found to have vicinal coupling with H_6 and H_b with H_7, both signals were seen as multiplets. In the ^{13}C NMR spectrum of **SN74**, the signals for the aliphatic

carbons shifted significantly upfield, from 40.8 and 46.1 ppm in **SN08** to 38.4 and 41.9 ppm, due to the amide bond formation. The carbon atoms on the aminoquinoline and chromone nucleus were found to resonate in similar chemical shift environments as those in their respective starting compounds. An additional indication of successful synthesis was that the total number of signals was equal to the number of carbon atoms in the structure. The other amide-linked hybrids follow a similar trend in their spectra. Mass spectrometry analyses further indicated successful synthesis of the amide-linked hybrid series.

Table 2.5: Isolated yields and molecular ion peaks of amide-linked hybrid molecules

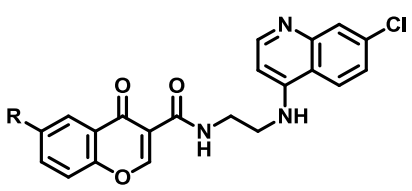

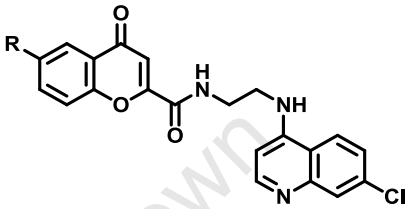

Series 2					Series 3				
Code	R	Yield (%)	$[M]^+$		Code	R	Yield (%)	$[M]^+$	
			Expected	Found				Expected	Found
SN44	H	49	393.1	393.0	**SN74**	H	46	393.1	393.0
SN48	Cl	46	427.1	428.0	**SN75**	Cl	70	427.1	427.0
SN54	Br	36	470.9	472.1	**SN76**	Br	72	470.9	472.8
SN55	F	62	411.1	410.8	**SN77**	F	65	411.1	410.9
SN56	OCH_3	46	423.1	422.8	**SN78**	OCH_3	55	423.1	422.8
SN57	CH_3	52	407.1	404.9					

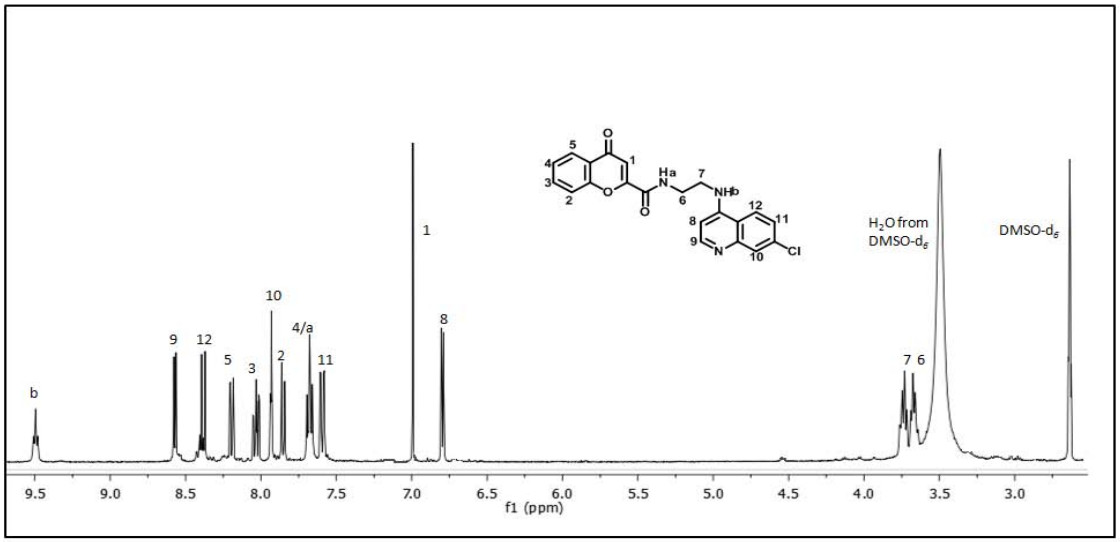

Fig. 2.12: ^{1}H NMR of **SN74** in DMSO-d_6 at 400 MHz

2.5. Physicochemical Properties and Biological Evaluation

2.5.1 Physicochemical Properties

For a compound to be an effective and efficient drug, it should have a good ADME profile. ADME is the acronym for the Absorption, Distribution, Metabolism and Excretion of a drug within an organism.[24] Therefore, in the design and development of potential therapeutic agents, these physicochemical parameters are essential. A few of these properties were determined through a combination of *in silico* and experimental tools. Kerns and Di report that if a compound has a solubility of:

- <10 µg/mL, low solubility
- 10 – 60 µg/mL, moderate solubility
- >60 µg/mL, high solubility[24]

In general, solubility and permeability tend to be complementary to each other up to a point. However, if the solubility is too high then the permeability maybe too low; therefore a balance is needed to give the best possible absorption. The incorporation of halogens onto the structure of the hybrids was envisaged to increase lipophilicity, which may improve penetration through membranes. However, this may also lead to a decrease in solubility.

From the results, it was observed that the hybrids had intermediate turbidimetric aqueous solubility with most compounds having moderate solubility. In Table 2.6, it was observed that hybrids with halogens as substituents had low to moderate solubility due to their lipophilic nature. The distribution coefficient (CLogD) was calculated, which is the measure of the distribution of a compound between two solvents of different polarities such as octanol and an aqueous buffer solution and is thus pH dependent. CLogD values were calculated at the physiological pH of 7.4. The lower the CLogD, the greater the aqueous solubility; this was the general trend observed for the aminoquinoline-chromone hybrids with the notable exceptions of **SN75** and **SN76**. Also reported are the predicted Caco-2 values, which can be used as an indication of permeability. There are several different models to determine permeability. However, due to the high cost and technical complexities associated with these experiments, the values may be predicted using *in silico* prediction tools. This was the approach used in this study, where the Caco-2 values were predicted using Volsurf+. The program reports the Caco-2 values between -1 and +1, with -1 indicating low permeability and +1 indicating high permeability.

Hybrids with moderate to low solubility displayed high permeability as they are more hydrophobic, except for **SN77** and **SN78**, which did not seem to follow the trend. It was evident that overall,

Series 3 had high ClogD and low Caco-2 values suggesting that the amide linker attached at position 2 of the chromone imparted greater permeability and poorer solubility compared to the other series. Series 2 displayed similar but lower CLogD values as series 3, however, the general trend is the same.

Table 2.6: Physicochemical Properties of Hybrid Compounds

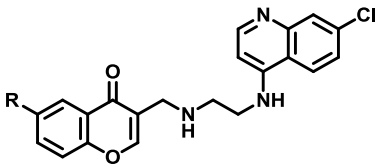

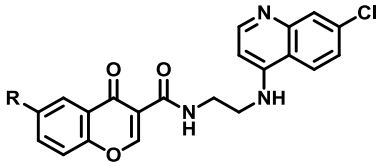

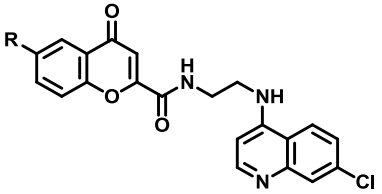

Series 1						Series 2					Series 3				
R	Code	[a]Solubility (µg/mL)	[b]CLogD	[c]CLogP	[c]Caco-2	Code	[a]Solubility (µg/mL)	[b]CLogD	[c]CLogP	[c]Caco-2	Code	[a]Solubility (µg/mL)	[b]CLogD	[c]CLogP	[c]Caco-2
H	**SN31**	30	1.99	3.76	0.78	**SN44**	16	2.47	3.96	0.73	**SN74**	8	2.51	3.97	0.57
Cl	**SN24**	17	2.61	4.52	0.83	**SN48**	9	3.08	4.71	0.76	**SN75**	34	3.12	4.73	0.65
Br	**SN25**	18	2.77	4.73	0.83	**SN54**	9	3.24	4.93	0.76	**SN76**	47	3.28	4.94	0.66
F	**SN26**	16	2.16	3.97	0.65	**SN55**	41	2.61	4.18	0.56	**SN77**	4	2.65	4.18	0.43
OCH_3	**SN27**	4	2.51	3.84	0.73	**SN56**	8	2.31	4.03	0.65	**SN78**	2	2.35	4.05	0.50
CH_3	**SN28**	32	1.99	4.22	0.85	**SN57**	16	2.47	4.42	0.76					

[a] Experimental determined solubility at pH 7.4, 0.01M phosphate buffered saline containing 1 % DMSO

[b] CLogD values were estimated at pH 7.4 using Marvin Sketch, Version 5.5.10[25]

[c] CLogP and Caco-2 values were estimated using Volsurf +, MDL[26]

2.5.2 Biological Evaluation

In vitro Antiplasmodial Activity

The *in vitro* antiplasmodial activities of the synthesized compounds were determined against chloroquine-sensitive (CQS) *D10* and *NF54* strains and the chloroquine-resistant (CQR) *K1* strain of *P. falciparum*. Results are summarized in Table 2.7. Chloroquine was used as a control for all antiplasmodial assays, where the IC_{50} (the half maximal inhibitory concentration) of the synthesized compounds were determined.

From the results, it was noted that the alkyl-linked hybrids, Series 1, had low potency against the *D10* strain relative to chloroquine (IC_{50} = 38.1 nM), with the exception of **SN24** (IC_{50} = 30.7 nM) and **SN08** (IC_{50} = 39.8 nM), which were comparable to chloroquine. **SN24**, the most active hybrid of this series, displayed moderate solubility (17 µg/mL) with a high predicted Caco-2 value of 0.83, indicating good permeability. Against the *NF54* strain, all compounds displayed comparable activity. In the *K1* strain, the hybrid compounds showed weaker activity relative to their activity in the *D10* and *NF54* strains. This suggests some degree of potential cross-resistance with chloroquine. Interestingly, the 1:1 molar ratio mixture of the starting materials (*D10*: IC_{50} = 32.9 nM; *NF54*: IC_{50} = 29.3 nM) showed comparable potency to chloroquine (IC_{50} = 38.1 nM) against the CQS strains of *P. falciparum*.

The compounds in Series 2 displayed good potency against the *D10* strain when compared to chloroquine (IC_{50} = 38.1 nM), in particular **SN48** (IC_{50} = 20.9 nM), **SN54** (IC_{50} = 46.8 nM) and **SN57** (IC_{50} = 39.7 nM). Activities against the *NF54* strain were also good when compared to chloroquine (IC_{50} = 29.3 nM); hybrids **SN44** (IC_{50} = 38.1 nM), **SN54** (IC_{50} = 57.5 nM) and **SN57** (IC_{50} = 63.3 nM) displayed the most potent activity. In the *K1* strain, hybrid **SN44** (IC_{50} = 160.0 nM) exhibited the highest activity, while the others were less active (IC_{50} = 160 – 564 nM).

Series 3 contains the hybrids with the aminoquinoline motif attached at position 2 of the chromone ring; these compounds showed activity poorer than chloroquine against the *D10* and *NF54* strains. However, in the *K1* strain, these compounds displayed better activity than chloroquine (IC_{50} = 190.7 nM). **SN77** (IC_{50} = 37.6 nM) displayed the most potent activity, while **SN74** (IC_{50} = 82.9 nM) and **SN78** (IC_{50} = 80.9 nM) were slightly less active, but still better than chloroquine. These hybrids exhibited low solubility (2 - 47 µg/mL) in general, but relatively moderate predicted Caco-2 permeability (0.43 – 0.66). It was observed that the 1:1 molar ratio mixtures of the precursors for each series had greater potency than the covalently-linked hybrids, suggesting that

there may be no added benefit in covalently joining them together. Furthermore, the parent compound **SN08** (*D10*: IC_{50} = 39.8 nM; *NF54*: IC_{50} = 33.1 nM), which contains the 4-aminoquinoline motif, displayed comparable activity to chloroquine; whereas the chromone precursors displayed IC_{50} values in the micromolar range (6 – 28 μM). This suggests that all the activity is primarily derived from the 4-aminoquinoline scaffold of **SN08** and not from the chromone substructure. This may explain the greater activity observed for the 1:1 molar ratio mixtures. From the data obtained so far, it is evident that there are no synergistic effects for the 1:1 molar ratio mixtures. Similarly, hybridization of **SN08** did not have an antagonistic effect on the antiplasmodial activity.

From the antiplasmodial data obtained, there did not appear to be a significant difference in activity between the hybrids with alkyl and amide linkers at position 3 of the chromone ring. Alternatively, attachment of the amide linker at position 2 of the chromone ring appeared to significantly improve the antiplasmodial activity of the hybrids against the *K1* strain of *P. falciparum*. Additionally, it was noted that compounds possessing the highest potency also displayed the lowest solubility.

Table 2.7: *In vitro* Antiplasmodial IC_{50} values against CQS *D10* and *NF54* strains and CQR, *K1* strain of *P. falciparum* of hybrid compounds

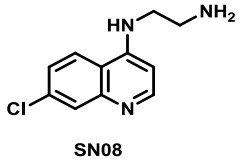
SN08

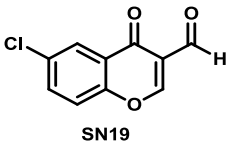
SN19

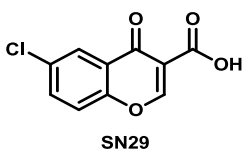
SN29

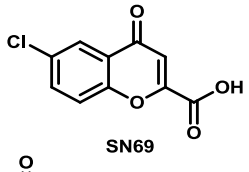
SN69

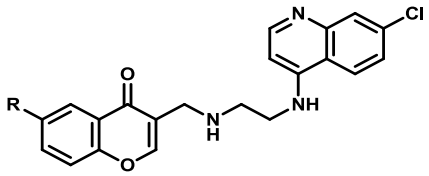

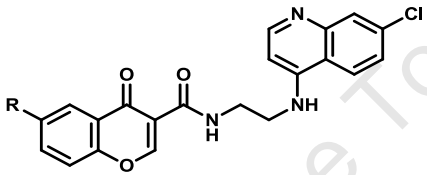

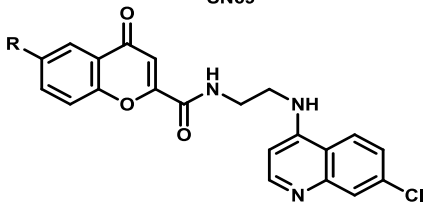

R	Code	Series 1						Code	Series 2						Code	Series 3					
		D10		*NF54*		*K1*			*D10*		*NF54*		*K1*			*D10*		*NF54*		*K1*	
		ng/mL	nM	ng/mL	nM	ng/mL	nM		ng/mL	nM	ng/mL	nM	ng/mL	nM		ng/mL	nM	ng/mL	nM	ng/mL	nM
H	SN31	31.9	84.0	25.2	66.3	75.8	199.6	SN44	27.8	70.6	15.0	38.1	62.9	160.0	SN74	28.6	72.6	35.4	90.0	32.6	82.9
Cl	SN24	12.7	30.7	24.5	59.1	86.0	207.6	SN48	8.95	20.9	28.5	66.5	79.6	185.9	SN75	64.5	150.6	124	289.5		-
Br	SN25	32.4	70.6	36.6	79.8	-	-	SN54	22.1	46.8	27.2	57.5	-	-	SN76	143.1	302.7	250	528.9		-
F	SN26	21.8	54.8	21.7	54.5	53.4	134.2	SN55	37.9	92	34.5	83.8	-	-	SN77	23.2	56.3	37.7	91.5	15.5	37.6
OCH_3	SN27	38.3	-	28.9	70.5	114	278.1	SN56	33.2	78.3	20.2	47.7	239	563.9	SN78	22.39	52.8	36.4	85.9	34.3	80.9
CH_3	SN28	41.0	104	23.7	60.2	69.5	176.5	SN57	16.2	39.7	25.8	63.3	112	274.6							
	SN19	12610	6045	-	-	-	-	SN29	29420	13098	-	-		-	SN69	63810	28410		-	-	-
	SN08	8.82	39.8	12.3	55.5	-	-	SN08	8.82	39.8	12.3	55.5	-	-	SN08	8.82	39.8	12.3	55.5	-	-
	SN08 : SN19	14.2	32.9	12.6	29.3	-	-	SN08 : SN29	61.2	137.1	14.6	32.7	-	-	SN08 : SN69	10.3	23.1	14.3	32.0	-	-
	CQ	12.2	38.1	10.6	33.1	61	190.7														

(-) indicates not determined

In vitro Antitumour Activity

The *in vitro* antitumour activities of the synthesized compounds were determined against the oesophageal cancer *WHCO1* cell line. The IC_{50} values are reported in Table 2.8, where doxorubicin was used as a positive control. The results indicate that all compounds in Series 1 had moderate antitumour activity, with much higher IC_{50} values ranging from 13.6 – 23.9 µM, compared to the control doxorubicin (IC_{50} = 0.5 µM). A similar activity trend was observed in the amide-linked hybrids (Series 2), except for **SN56** (IC_{50} = 7.6 µM) which displayed moderate antitumour activity. In Series 3, all compounds exhibited weaker potency, with the noticeable exception of **SN78** (IC_{50} = 1.78 µM).

Also noted is the low turbidimetric solubility, moderate CLogD values and intermediate Caco-2 permeability. Unlike the case in the antiplasmodial activity data, the 1:1 molar ratio mixtures did not display superior activity relative to the hybrid compounds. Additionally, the individual monomeric precursor compounds also possessed weak antitumour activity. However, it appears that **SN08**, one of the parent compounds, was more potent than its chromone partner in each of the series. This could be a reason for the greater activity of the 1:1 molar ratio mixtures.

Table 2.8: *In vitro* Antitumour IC_{50} values of target hybrid compounds against *WHCO1* cancer cell line

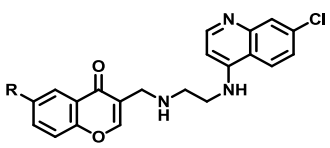
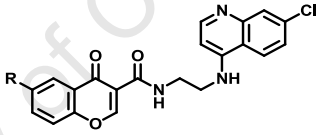
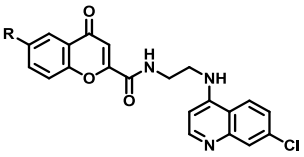

R	Series 1		Series 2		Series 3	
	Code	IC_{50} (µM)	Code	IC_{50} (µM)	Code	IC_{50} (µM)
H	**SN31**	16.7	**SN44**	11.2	**SN74**	17.6
Cl	**SN24**	14.6	**SN48**	13.0	**SN75**	14.3
Br	**SN25**	17.9	**SN54**	15.4	**SN76**	52.5
F	**SN26**	15.4	**SN55**	18.8	**SN77**	17.3
OCH_3	**SN27**	23.9	**SN56**	7.6	**SN78**	1.78
CH_3	**SN28**	13.6	**SN57**	10.4		
	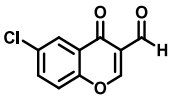 **SN19**	26.2	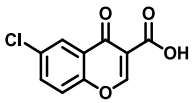 **SN29**	73.2	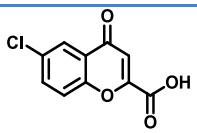 **SN69**	80.79
	SN08:SN19	14.5	**SN08:SN29**	15.8	**SN08:SN69**	13.09
	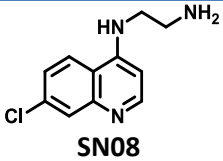 **SN08**	12.6	**Doxorubicin**	0.5		

In vitro Antimycobacterial Activity

The target hybrids were also evaluated for their antimycobacterial activity *in vitro* against the *H37Rv* strain of *Mycobacterium tuberculosis* using kanamycin as the control. These results are summarized in Table 2.9. The alkyl- and amide-linked hybrid molecules, their monomeric parent constituents and their 1:1 molar ratio mixtures all displayed very poor antimycobacterial activity with MIC_{90} at Day 14 of the assay exceeding 160 µM. MIC_{90} values are the concentration effecting a 90 %reduction in growth at the end of the incubation period relative to untreated controls.[27] Only one hybrid, **SN78** (MIC_{90} = 40 µM), showed moderate antimycobacterial activity.

Table 2.9: *In vitro* Antimycobacterial MIC_{90} values of target hybrid compounds against the *H37Rv* strain of *Mycobacterium tuberculosis*

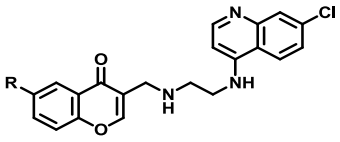
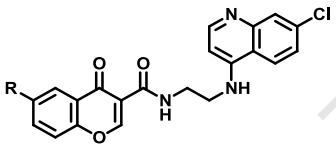
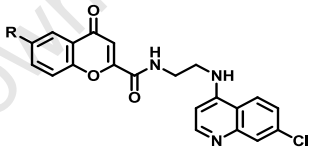

R	Series 1 Code	Series 1 MIC_{90} (µM)	Series 2 Code	Series 2 MIC_{90} (µM)	Series 3 Code	Series 3 MIC_{90} (µM)
H	**SN31**	> 160	**SN44**	> 160	**SN74**	> 160
Cl	**SN24**	> 160	**SN48**	> 160	**SN75**	> 160
Br	**SN25**	> 160	**SN54**	> 160	**SN76**	> 160
F	**SN26**	> 160	**SN55**	> 160	**SN77**	> 160
OCH_3	**SN27**	> 160	**SN56**	> 160	**SN78**	40
CH_3	**SN28**	> 160	**SN57**	> 160		
	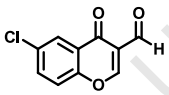 **SN19**	>160	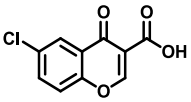 **SN29**	> 160	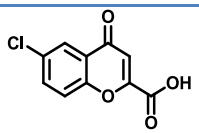 **SN69**	> 160
	SN08:SN19	80	**SN08:SN29**	> 160	**SN08:SN69**	> 160
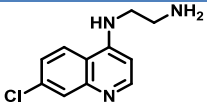 **SN08**		>160	**Kanamycin**	3.13		

2.6 Conclusion

A series of novel chromone-based hybrids were synthesized and characterized using various spectroscopic and analytical techniques, including ^{1}H, ^{13}C NMR, IR spectroscopy and mass spectrometry. Some physicochemical properties were determined for the hybrids to help interpret their biological activity. The antiplasmodial, antitumour and antimycobacterial activities of the hybrids were evaluated *in vitro*. These compounds exhibited good to excellent antiplasmodial activity in both CQS and CQR strains of *P. falciparum*, and moderate antitumour activity, except **SN78** (IC_{50} = 1.78 µM) which demonstrated the most promising activity. From these results it can be concluded that the type of linker did not appear to affect pharmacological activity, whereas attachment of the amide linker at position 2 of the chromone ring appeared to significantly improve the antiplasmodial activity of the hybrids in the CQR *K1* strain of *P. falciparum*. From their poor antimycobacterial activity, it was evident that the hybrids do not merit further investigation as antimycobacterial agents.

2.7 References

1. P. Ehrlich, *Dtsch. Chem. Ges.*, **1909**, *42*, 17.
2. B. T. Grimberg and R. K. Mehlotra, *Pharmaceuticals*, **2011**, *4*, 681.
3. C. Biot and K. Chibale, *Infect. Disord. Drug Targets*, **2006**, *6*, 173.
4. S. S. Chauhan, M. Sharma and P. M. S. Chauhan, *Drug News Perspect.*, **2010**, *23*, 632.
5. S. K. Chauhan and P. M. S, Srivastava, *Curr. Med. Chem.*, **2001**, *8*, 1535.
6. P. M. O' Neill, P. G. Bray, S. R. Hawley S. A. Ward and B. K. Park, *Pharmacol. Ther.,* **1998**, *77*, 29.
7. T. J. Egan, R. Hunter, C. H. Kaschula, H. M. Marques, A. Misplon and J. Walden, *J. Med. Chem.,* **2000**, *43*, 283.
8. C. H. Kaschula, T. J. Egan, R. Hunter, N. Basilico, S. Parapini, D. Taramelli, E. Pasin and D. Monti, *J. Med. Chem.*, **2002**, *45*,3531.
9. D. De, F. M. Krogstad, L. D. Byers and D. J. Krogstad, *J. Med. Chem.*, **1998**, *41*, 4918.
10. F. W. Muregi, P. G. Kirira and A Ishih, *Curr. Med. Chem.*, **2011**, *18*, 113.
11. J. Clayden, N. Greeves, S. Warren and P. Wothers, *Organic Chemistry*, Oxford University Press, Oxford, 1st Ed., 2001.
12. N. Sunduru, M. Sharma, K. Srivastava, S. Rajakumar, S. K. Puri, J. K. Saxena and P. M. S. Chauhan, *Bioorg. Med. Chem.*, **2009**, *17*, 6451.
13. D. A. Horton, G. T. Bourne and M. L. Smythe, *Chem. Rev.*, **2003**, *103*, 893.
14. G. Singh, R. Singh, N. K. Girdhar and M. P. S. Ishar, *Tetrahedron*, **2002**, *58*, 2471.
15. J. A. Joule and K. Mills, *Heterocyclic Chemistry*, John Wiley and Sons, Chichester, 5th Ed., 2010.
16. A. Nohara, T. Umetani, K. Ukawa and Y. Sanno, *Chem. Pharm. Bull.*, **1974**, *22*, 2959.
17. W. Friebolin, B. Jannack, N. Wenzel, J. Furrer, T. Oeser, C. P. Sanchez, M. Lanzer, V. Yardley, K. Becker and E. Davioud-charvet, *J. Med. Chem.*, **2008**, *51*, 1260.
18. B. O. Lindgren and T. Nilsson, *Acta Chem. Scand*., **1973**, *27*, 888.
19. W. Baker, *J. Chem. Soc*., **1933**, 1381.
20. H. S. Mahal and K. Venkataraman, *J. Chem. Soc*., **1934**, 1767.
21. S. Choi, A. Pradhan, N. L. Hammond, A. G. Chittiboyina, B. L. Tekwani and M. A. Avery, *J. Med. Chem.*, **2007**, *50*, 3841.
22. G. Liu, J. Xu, M. Geng, R. Xu, R. Hui, J. Zhao, Q. Xu, H. Xu and J. Li, *Bioorg. Med. Chem.*, **2010**, *18*, 2864.
23. Sigma-Aldrich. [Cited: 13.08.2012] http://www.sigmaaldrich.co.za.

24. E. H. Kerns and L. Di, *Drug-like Properties: Concepts, Structure Design and Methods from ADME to Toxicity Optimization*, Elsevier Academic Press, California, 1st Ed., 2008.
25. *Marvin Sketch*, Version 5.5.1.0, ChemAxon Kft, Budapest, 2011.
26. *Volsurf +*, Version 1.0.4, Molecular Discovery, Middlesex, 2009.
27. S. G. Franzblau, M. A. Degroote, S. H. Cho, K. Andries, E. Nuermberger, I. M. Orme, K. Mdluli, I. Angulo-Barturen, T. Dick, V. Dartois and A. J. Lenaerts, *Tuberculosis*, **2012**, *92*, 453.

Chapter Three – Design, Synthesis and Biological Evaluation of Chromone Analogues

3.1 Introduction

This chapter focuses on the design, synthesis and characterization of a series of chromone ester derivatives. All target compounds herein discussed were evaluated for their antiplasmodial activities against CQS strains of *P. falciparum* as well as their antimycobacterial activity. The antimalarial activity of the 4-aminoquinoline nucleus has been well documented and thus will not be reviewed again.[1, 2] There is very little known about the antiplasmodial activity of chromones; these small molecules have the potential to be developed into drug leads due to their privileged substructure classification. In this chapter, chromones will be examined in two ways: a) evaluation of antiplasmodial activity by investigation of the structural attributes of the chromone ring and b) evaluation of aqueous solubility.

3.2 Mitochondrial Cytochrome bc_1 Complex

Due to the emergence of resistance to CQ-based therapies, which target the acidic food vacuole in the parasite, new antimalarial agents that have different sites and mechanisms of action are needed. One such target is the respiratory chain of *P. falciparum*, which differs from the analogous mammalian system.[3–5] The *Plasmodium* cytochrome bc_1 complex (ubiquinol:ferricytochrome *c* oxidoreductase) or Complex III in the oxidative phosphorylation chain is the central enzyme in the mitochondrial electron transfer chain. Therefore interference of its function results in loss of mitochondrial function.[6] It is comprised of three catalytic subunits: cytochrome *b*, which carries a low and high potential haeme group, cytochrome c_1, which has one covalently bound haeme moiety and a high potential Rieske iron-sulfur protein (ISP) containing a $[Fe_2S_2]$ cluster.

The general function of the complex is to transfer electrons from ubiquinol to cytochrome *c* coupled with the translocation of protons across the inner mitochondrial membrane. This movement of electrons creates a proton-motive force (PMF) in the form of an electrochemical proton potential that is used in the synthesis of ATP.[7, 8] The main feature of this model is the presence of two separate ubiquinol:ubiquinone binding sites. The ubiquinol oxidation site (Qo) is located near the inner mitochondrial membrane, with the ubiquinone reduction site (Qi) situated at the mitochondrial matrix; both the quinol oxidase and quinine reductase are positioned in the cytochrome *b* subunit of the complex.[9] The PMF is generated in a bifurcated redox reaction when it uses one of the protons released during the oxidation of ubiquinol to reduce the iron-sulfur cluster of the Rieske protein. The reduced ISP then undergoes conformational change, bringing the cytoplasmic domain of ISP and the haeme of cytochrome *c* in contact, thus facilitating electron transfer.[6] Inhibitors of the cytochrome bc_1 complex block the transfer of electrons, thereby

collapsing the trans-membrane electron potential.[10, 11] This inhibits dihydroorotate dehydrogenase (DHODH), an enzyme used in the biosynthesis of pyrimidine.[5] The malaria parasite is unable to salvage pyrimidines, which are a class of heterocycles used in DNA and RNA synthesis, and thus the enzyme is essential for its development.[12]

The Qo and Qi sites in the bc_1 subunit have natural inhibitors such as antimycin, myxothiazol and stigmatellin (Fig. 3.1).[6, 13] Stigmatellin contains a 5,7-dimethoxy-8-hydroxychromone system with a hydrophobic alkenyl chain at position 2 and is a potent inhibitor of the Qo site.[9] Evidence from crystallography, spectroscopy and kinetic studies suggests that stigmatellin binds to the Qo site in a distal position and associates with ISP via a hydrogen bond to a histidine residue. This association raises the potential of the iron-sulfur cluster and restricts movement of the cytoplasmic domain of the ISP and thus inhibits electron transfer, by increasing the redox midpoint of the ISP from 290 mV to 540 mV.[9, 14] This indicates that the binding of stigmatellin does inhibit the cytochrome bc_1 complex and thus reduces the function of the mitochrondrion. Stigmatellin was found to be highly toxic in humans and is therefore not recommended for medicinal use.[6]

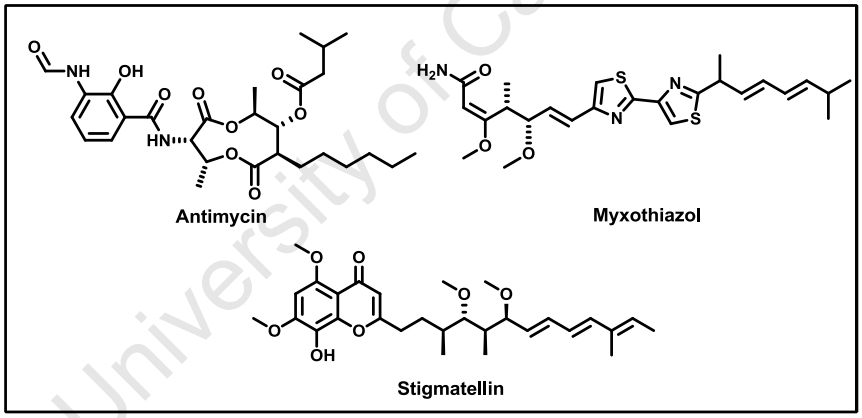

Fig. 3.1: Chemical structures of selected natural inhibitors of the cytochrome bc_1 complex

3.3 Rationale for the Synthesis of Chromone Ethyl Ester Derivatives

The Qo site can be blocked by inhibitors binding to the quinol active site; various crystallographic and spectroscopic analyses indicate that inhibitors of the Qo site can either fix the hydrophilic domain of the Rieske iron-sulfur protein or promote movement of the cytoplasmic domain.[15] Molecules that contain a chromone or quinone substructure are postulated to fix the position of the hydrophilic domain of the Rieske iron-sulfur protein.[16] Currently, atovaquone, a quinone-containing structure, is an ubiquinone competitive inhibitor, which inhibits the cytochromone bc_1 complex by blocking the translocation of electrons. Atovaquone is used in combination with proguanil for the treatment and prevention of multidrug-resistant malaria; this is marketed as Malarone® by

GlaxoSmithKline (Fig. 3.2).[17] This is an expensive treatment regimen as the drug has to be taken every day for prophylaxis, and since malaria mainly affects the poorer regions of the world, alternative cheaper antimalarial agents are needed.

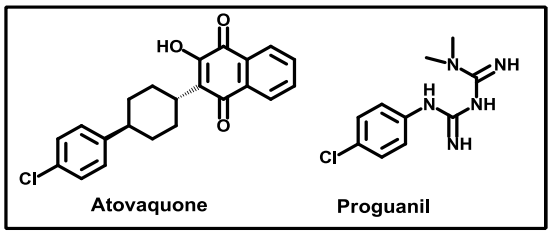

Fig. 3.2: Chemical structures of atovaquone and proguanil, the active agents of the antimalarial drug Malarone®

In the design of potential cytochrome bc_1 complex inhibitors, the inclusion of a polar group may allow for a hydrogen bond between it and a histidine residue in the Qo active site; these must be linked to an alkyl or aryl chain that lies along the cylindrical hydrophobic domain. The investigation of an inhibitor with a chromone moiety is justified as it will provide a polar head group with its carbonyl at positions C_3 and C_4 of the chromone ring. Since the chromone substructure is classified as a privileged structure, these inhibitors may have the ability to produce compounds with drug-like properties.[18] Studies on the quinolone template indicate that the incorporation of an aromatic group and an ethyl ester chain has the potential to provide drug hits.[16] A broad range of aryl groups were chosen based on the nature of the groups attached to the ring, i.e. electron-withdrawing groups or electron-donating groups. Fig. 3.3 summarizes this concept and illustrating an assortment of aryl groups that were used.

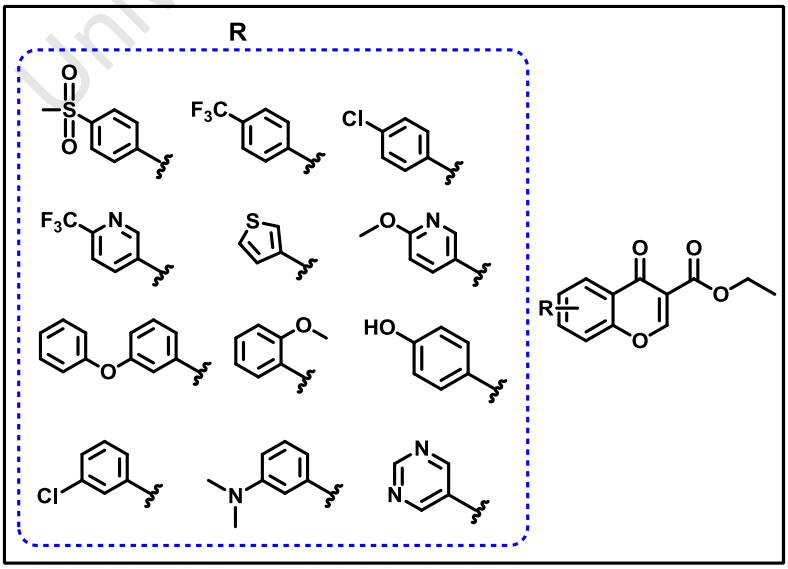

Fig. 3.3: Rationale for the design of target compounds

3.4 Introduction of Aryl Groups onto the Chromone Ring

In the design of this series, the Suzuki-Miyaura coupling reaction was chosen as the desired route to introduce various aryl groups onto position 6 of the chromone ring. This methodology provides easy access to diverse chromone derivatives by the introduction of various substituents using palladium-mediated C-C coupling reactions.

Overview of Palladium Catalyzed Reactions

Palladium is the most frequently used transition metal in organic chemistry reactions. There are several well-known palladium catalyzed coupling reactions, such as the Buchwald-Hartwig, Heck, Negishi, Sonogashira, Stille and Suzuki cross coupling reactions.[19] The Nobel Prize in chemistry in 2010 was awarded to Richard. F. Heck, Ei-ichi Negishi and Akira Suzuki for the development of these reactions.[20-22] The general mechanism of these types of reactions consist of three steps; oxidative addition, transmetallation and reductive elimination (Fig. 3.4). These catalytic cycles generally require a zerovalent palladium catalyst. However, Pd(II) complexes are more frequently used as pre-catalysts as they are more air-stable than the Pd(0) counterparts. If these are used as the pre-catalysts, they need to be reduced *in situ* before the cycle can commence. The first step in the reaction is oxidative addition, where the Pd(0) inserts between the sp^2 carbon and the leaving group (LG), like a halogen or triflate, resulting in cleavage of the bond with an increase in oxidation state and coordination number of the metal. In terms of reactivity, the reaction is dependent on the nature of the LG, such that LG = I>Br≈OTf>>Cl>>F. Transmetallation with a nucleophilic organometallic reagent like a boronic acid transfers the R group to the metal and displaces the leaving group under basic conditions. Subsequent reductive elimination creates a new carbon-carbon bond and reduces the oxidation state and coordination number of the metal, thereby regenerating the catalyst.[23–25]

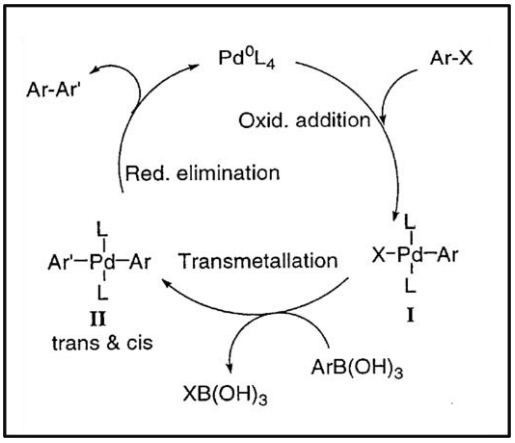

Fig. 3.4: General catalytic cycle for the palladium-mediated cross coupling reactions, where Ar = aromatic group, L = ligand and X = leaving group

Synthesis of Chromone Ester Derivatives

Various boronic acids with aryl substituents were chosen based on their ring activating and ring deactivating properties. 6-Bromo-4-*oxo*-4*H*-chromene-3-carbaldehyde, **SN20**, and 4-chlorophenyl-boronic acid were used in a pilot reaction, in the determination of viable reaction conditions for the introduction of aryl groups at position 6 of the chromone ring. $Pd(PPh_3)_2Cl_2$ was used as the catalyst, 1M K_2CO_3 as the base and DMF as the solvent. This combination previously produced successful results within our research group. However, the reaction did not generate the desired product after heating at 95 ^oC overnight (Table 3.1). The reaction was repeated with another high boiling point solvent such as 1,4-dioxane with no noticeable effect. Other Suzuki protocols were employed, such as changing the base to 1M Na_2CO_3 and increasing the reaction time; all of these proved futile as the desired product was not obtained. It was reasoned that the chromone-3-carbaldehyde was too reactive causing the chromone ring to open. To counteract this, the reaction temperature was reduced to 60 ^oC with no improvement. Using standard esterification conditions, **SN65** was prepared from oxalyl chloride and methanol in anhydrous DCM under anhydrous conditions. Further attempts at Suzuki coupling were made using the methyl ester at 60 and 95 ^oC; this also failed to give the desired result. Another strategy employed was to use the base in its solid form to eliminate the possibility of water acting as a nucleophile to open the chromone ring; this strategy, too, did not yield the desired result.

Table 3.1: Summary of unsuccessful Suzuki cross coupling conditions for the introduction of aryl groups at position 6 of the chromone ring

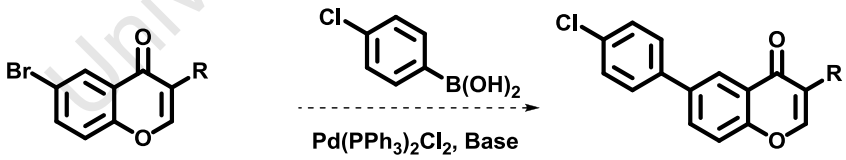

R	Base	Solvent	Temp (^oC)	Time
CHO	K_2CO_3 (1M)	DMF	95	12 h
CHO	K_2CO_3 (1M)	Dioxane	95	12 h
CHO	Na_2CO_3 (1M)	DMF	95	12 h
CHO	K_2CO_3 (1M)	DMF	RT - 60	3 days
$COOCH_3$	K_2CO_3 (1M)	DMF	95	12 h
$COOCH_3$	K_2CO_3 (1M)	DMF	RT - 60	12 h
CHO	K_2CO_3 (s)	DMF	95	12 h
$COOCH_3$	K_2CO_3 (s)	DMF	95	12 h

Finally, the product was obtained by using the methodology reported in Shim *et al*.,[26] in which the palladium-mediated cross coupling was conducted on 1-(5-bromo-2-hydroxyphenyl)ethanone first using standard Suzuki cross coupling reaction conditions to give position 6-substituted aryl acetophenones, **SN83** – **SN92**. This was followed by ring closure using a Vilsmeier-Haack reaction as described in 2.4.1.1, to give the desired C_6-aryl substituted chromone-3-carbaldehyde (Scheme 3.1).

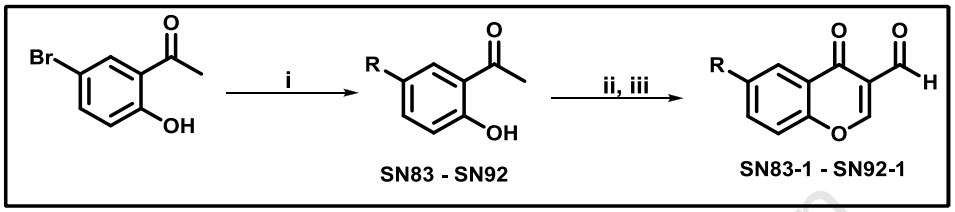

Scheme 3.1: Reagents and conditions: i. R-B(OH)$_2$ (1.2 eq), Pd(PPh$_3$)$_2$Cl$_2$ (0.05 eq), 1M K$_2$CO$_3$ (1.05 eq), DMF, 95^{o}C, 12 h; ii. POCl$_3$ (6 eq), DMF, N$_2$, 12 h; iii. H$_2$O, 0 ^{o}C

Evidence of an example of a successful Suzuki reaction can be seen in the ^{1}H NMR of **SN90** (Fig. 3.5), as the protons on the newly introduced ring appear as a multiplet between 7.33 – 7.36 ppm, with H_4 resonating as a doublet with a coupling constant of 2.3 Hz, indicative of long range coupling to H_3. H_3 exists as a doublet of doublet due to its coupling with H_2 and H_4. Another key feature was the singlet upfield in the spectrum, belonging to the methyl protons adjacent to the ketone functional group and the presence of the hydroxyl group signal. Evidence for the synthesis of the chromone aldehyde was observed in the ^{1}H NMR spectrum of **SN90-1**. The splitting pattern was similar to that observed in the chromone derivatives described in chapter two. Additionally, the hydroxyl signal as well as the methyl protons at 2.64 ppm in (a) have disappeared, indicating ring closure. In spectrum (b), there is a signal in the aldehyde region, suggesting that the Vilsmeier-Haack reaction proceeded successfully. The appearance of the new signal at 8.56 ppm in (b) integrating for one proton was assigned to the newly formed chromone proton H_1. The signal for H_2 has shifted downfield due to the pyrone system.

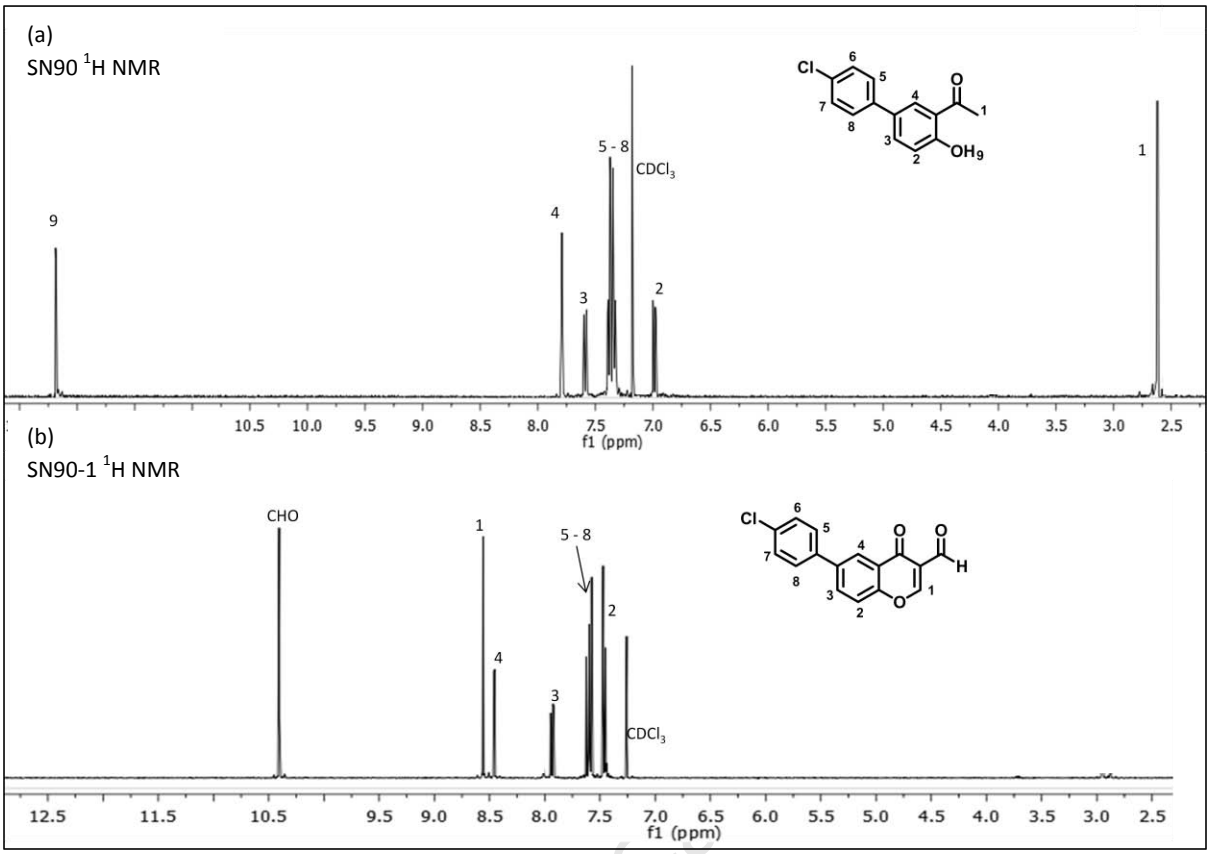

Fig. 3.5: ^{1}H NMR spectra of (a) **SN90** and (b) **SN90-1** in $CDCl_3$ at 400 MHz

This synthetic procedure was used for the introduction of other functionalized aryl groups to produce the chromone aldehydes, **SN83-1** – **SN92-1**. The aldehydes were subjected to a Lindgren oxidation using sodium chlorite and sulfamic acid to produce the chromone-3-carboxylic acids, **SN83-2** – **SN95-2**, with aryl groups at C_6 of the ring. The chemistry of a Lindgren oxidation was extensively discussed in section 2.4.2.1 and will not be repeated here. In the preparation of the ethyl chromone esters, it was thought that similar reagents and reaction conditions could be utilized as for the synthesis of the methyl esters. A pilot experiment was carried out using **SN38** as the source of the acid, oxalyl chloride as the chlorinating agent and ethanol as both the reagent and the solvent. This reaction was unsuccessful as no conversion to the product was observed; this was deduced by TLC analysis of the reaction. Thionyl chloride was then used as an alternative reagent for the generation of the acid chloride. The chromone-3-carboxylic acids underwent esterification using thionyl chloride and an excess of absolute ethanol under anhydrous conditions at 40 ^oC overnight (Scheme 3.2), to produce the ethyl esters **SN38-3** and **SN83-3** – **SN95-3**. Compound **SN70-3**, a chromone ethyl ester with the ester group attached at position 2, was synthesized for comparison purposes. A saturated solution of sodium carbonate was used in the work-up to remove any excess

thionyl chloride from the reaction. The pure target compounds either precipitated out of solution or were obtained using preparative TLC.

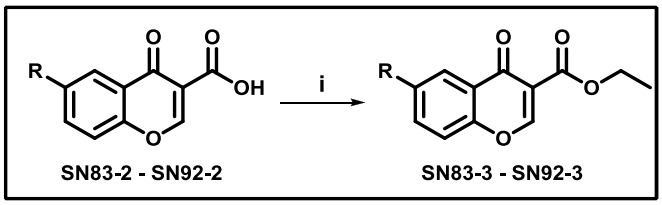

Scheme 3.2: Reagents and conditions: i. $SOCl_2$ (1.5 eq), EtOH, 40 ^{o}C, 18 h

The mechanism (Fig. 3.6) involves an *in situ* generated acyl chloride reacting with ethanol in a nucleophilic substitution reaction. Thionyl chloride ($SOCl_2$) is used to convert the OH group, a poor leaving group, into a good one, by protonating the OH group. $SOCl_2$ contains an electrophilic sulfur in its structure and is thus attacked by the nucleophilic oxygen in the carboxylic acid to produce an unstable electrophilic intermediate. The Cl^- generated reacts with the thio-intermediate to produce the acyl chloride releasing HCl and SO_2 as gases. The acyl chloride subsequently reacts with the alcohol to form an unstable alkoxide intermediate, eliminating the chloride and thus generating the ester.[24] A summary of the analytical properties of these compounds is presented in Table 3.2.

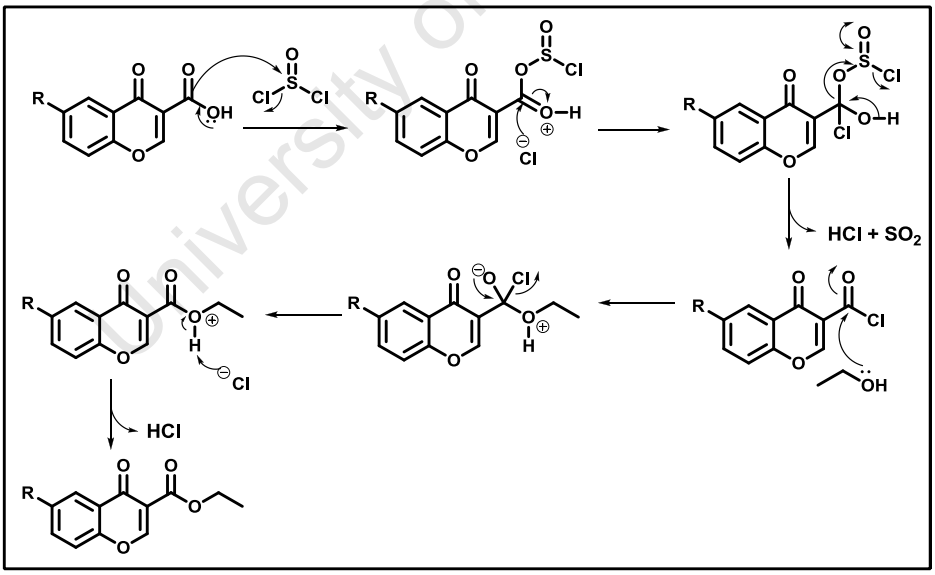

Fig. 3.6: Proposed mechanistic route for the formation of chromone ethyl esters

Table 3.2: A summary of the analytical properties of chromone-ethyl ester derivatives, with aryl groups at position 6 of the chromone ring

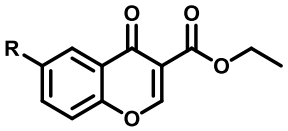

Code	R	Yield (%)	$[M]^+$		Melting Point (°C)
			Expected	Found	
SN38-3	Br	38	295.9	295.8	85 – 89
SN83-3	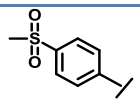	49	372.1	371.8	158 – 162
SN84-3	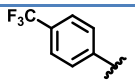	83	362.1	362.1	109 – 111
SN85-3	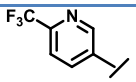	24	363.1	363.0	141 – 143
SN87-3		85	300.1	300.0	54 – 56
SN90-3	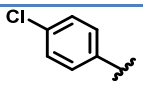	78	328.1	328.0	128 – 131
SN91-3	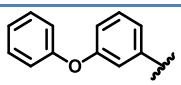	48	386.2	385.9	31 – 34
SN92-3	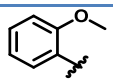	69	324.1	323.9	42 – 45

Characterization of Chromone Ester Derivatives

The ^{1}H and ^{13}C NMR spectra of **SN83-3** are presented in Fig. 3.7, illustrating the general pattern of the chromone ethyl ester series. The ethyl protons are easily distinguished in the ^{1}H NMR spectrum as a triplet and quartet upfield in the spectrum for H_{11} and H_{10}, respectively. The protons on the chromone ring resonate in similar chemical shift regions as those in its precursor, **SN83-2** (6-(4-(methylsulfonyl)phenyl)-4-*oxo*-4*H*-chromene-3-carboxylic acid), with the exception of H_1, which has moved upfield in the spectrum due to the less electron-withdrawing ethyl ester group. Two sets of doublet of doublets were observed for the aromatic protons on the side chain (H_5 – H_8), which is characteristic of a *para*-substituted aromatic ring. Analysis of the ^{13}C NMR of the same compound further indicated successful synthesis of target compounds as there are two new signals upfield in the spectrum, which were assigned as the ethyl chain carbons. The signal at 173.2 ppm was produced by the carbon of the carbonyl group within the chromone ring, with the ester carbonyl appearing at 165.9 ppm and C_1 at 163.1 ppm. Mass spectrometry analyses also

indicated that these ethyl esters with aryl groups at position 6 of the heterocyclic ring were successfully synthesized.

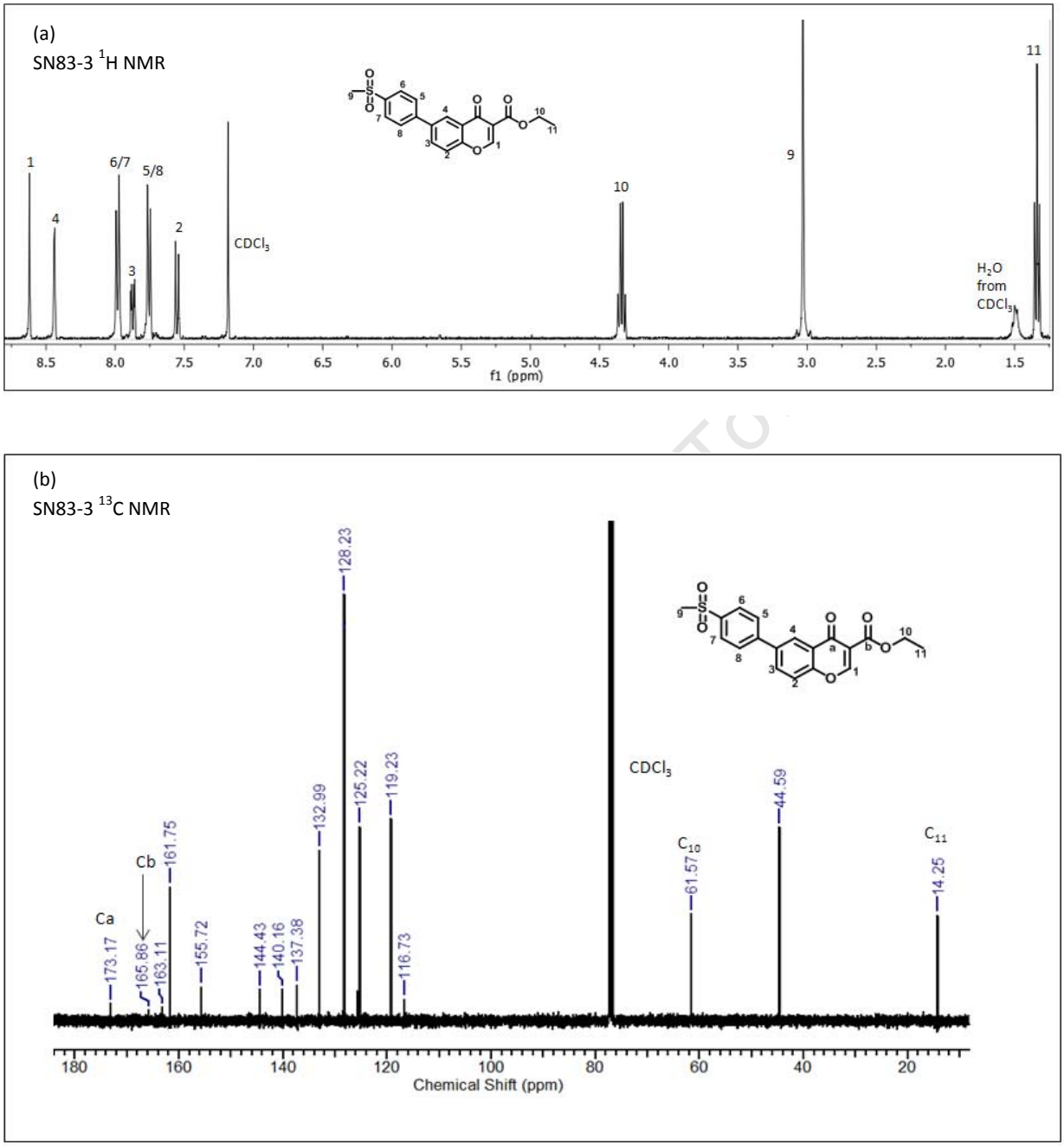

Fig. 3.7: ^{1}H (a) and ^{13}C (b) NMR spectra of **SN83-3** in $CDCl_3$ at 400 MHz and 100 MHz, respectively

3.5 Improvement of Aqueous Solubility by Disruption of the Molecular Planarity

In the design of potential therapeutic agents, it is essential to look at all factors that affect the absorption of the drug. Solubility, molecular size, particle size, degree of ionization, concentration, dosage forms and formulation are just a few that affect the absorption. Thus the aqueous solubility of the synthesized compounds is vital.[27] For small drug-like molecules, solubility depends on their polarity. For example, a compound with a large polar surface area is likely to exhibit greater aqueous solubility and therefore the introduction of polar hydrophilic groups by synthetic methods is traditionally used to improve solubility.[28, 29] A recent review by Ishikawa and colleagues has suggested that aqueous solubility may be improved by increasing the dihedral angle of bicyclic compounds as this will disrupt the molecular planarity, and thus its symmetry, resulting in an improvement of aqueous solubility.[30] Ishikawa and co-workers used the rationale that reducing the melting point of a crystal will improve the solubility. Melting point is dependent on the crystal lattice and crystal packing energies. Therefore, disturbing the crystal packing is another strategy for improving solubility. However, literature suggests that predicting the melting point and crystal packing of solids is extremely difficult.[31, 32]

There are a few examples of improving solubility by chemical modifications, such as removal of the aromaticity, an introduction of substituents on the benzylic position, the twisting of fused aromatic rings or the disruption of molecular symmetry.[30, 27] By attaching aryl substituents onto specific positions of the chromone ring, a rotatable biaryl motif is introduced that could potentially disrupt the planar symmetry, leading to a lowering of the crystal lattice and crystal packing energies. A reduction of these values may lower the melting point and improve its aqueous solubility.

3.5.1 Effect of the Aryl Group Position on the Chromone Ring

All the chromone derivatives synthesized thus far have substituents at position 6 of the chromone ring. Therefore, to determine the effect of the R group position on the chromone ring, derivatives were synthesized with aryl groups at positions 5, 7 and 8 of the heteroaromatic ring. Based on literature findings, attachment of an aryl group at positions 5 and/or 8 of the aromatic ring may increase the dihedral angle and disrupt the planar symmetry, leading to an improvement in solubility.[30] The 4-(methylsulfonyl)phenyl moiety was chosen as the constant R group from *in silico* analyses, as it was predicted to have low aqueous solubility as indicated in the partial least squares (PLS) plot below. The PLS plot gives an indication of a compound's solubility; compounds that appear in the upper right quadrant are predicted to have high solubility those in the lower left quadrant fall in the region of low solubility (Fig. 3.8). Generally, the predicted solubility values were higher than the experimentally determined results.

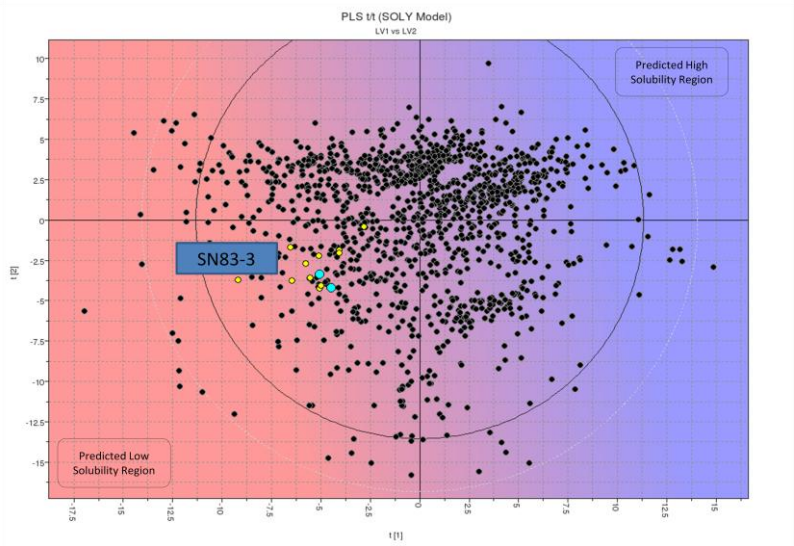

Fig. 3.8: Partial least squares (PLS) plot of predicted solubility, expressed as Log Sol.[33]

Synthesis and Characterization of Biaryl Chromone Derivatives

The synthetic methodology employed was the same as that used in section 3.3, with 3-, 4- and 6-bromo-2-hydroxyacetophenone as the initial starting materials as illustrated in Scheme 3.3. There was a slight modification in the temperature of the Suzuki cross coupling reaction, as it was raised from 95 ^{o}C to 100 ^{o}C. Following the palladium-mediated cross coupling reaction, the chromone ring was formed in a Vilsmeier-Haack reaction and oxidized to produce the acid, which underwent esterification with ethanol.

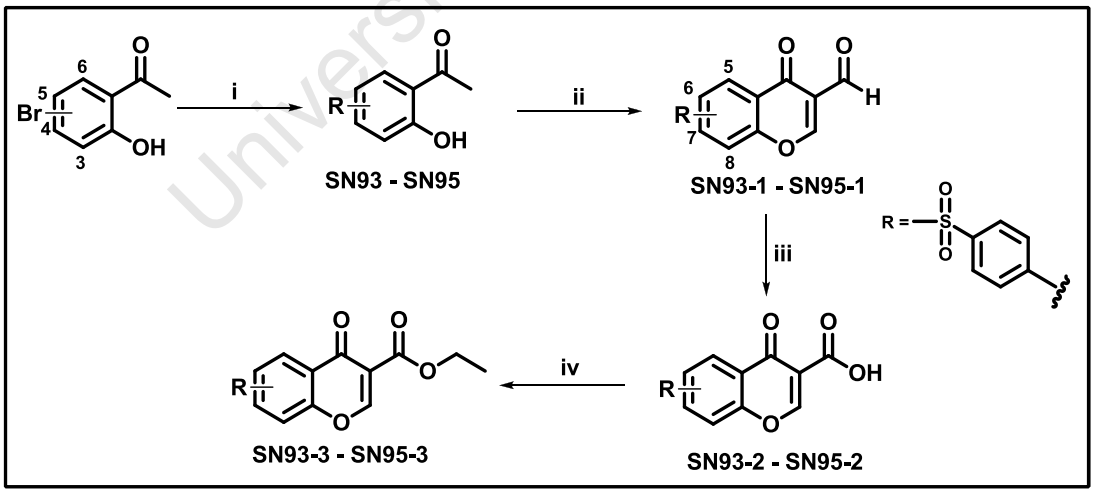

Scheme 3.3: Reagents and conditions: i. R-B(OH)$_2$ (1.2 eq), Pd(PPh$_3$)$_2$Cl$_2$ (0.05 eq), 1M K$_2$CO$_3$ (1.05 eq), DMF, 100 ^{o}C, 12 h; ii. POCl$_3$ (6 eq), DMF, N$_2$, 12 h, H$_2$O, 0 ^{o}C; iii. NaClO$_2$ (6.0 eq), NH$_2$SO$_3$H (8.0 eq), DCM, H$_2$O, RT, 4 - 6 h; iv. SOCl$_2$ (1.5 eq), EtOH, 40 ^{o}C, 18 h

Analytical and spectroscopic data indicated successful synthesis of these chromone derivatives. A summary of their analytical properties are displayed in Table 3.3. Since these compounds were synthesized to potentially improve the solubility of chromones, their kinetic solubility was determined turbidimetrically and will be discussed in section 3.6, along with their antiplasmodial and antimycobacterial activities.

Table 3.3: Summary of the isolated yields, molecular ion peaks and melting points of chromone-ethyl ester derivatives with aryl groups on various positions of the chromone ring

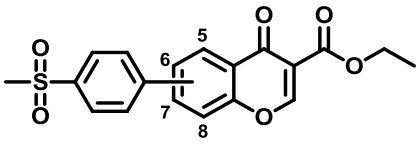

Code	Position	Yield (%)	Melting Point (°C)
SN93-3	5	83	157 – 160
SN83-3	6	49	158 – 162
SN94-3	7	27	179 – 182
SN95-3	8	35	158 – 161

3.6 Physicochemical Properties and Biological Evaluation

Table 3.4 summarizes the physicochemical properties and *in vitro* pharmacological data of the chromone-ethyl esters. The distribution coefficients were calculated at pH 7.4. Caco-2 values are given between -1 (indication of low permeability) and +1 (indication of high permeability). The solubility data was compared to the general assumption that <10 µg/mL indicates low solubility and >60 µg/mL indicates high solubility.[27]

In general, the chromone-ethyl esters were predicted to have moderate to high Caco-2 values and relatively high CLogP values. The compounds were evaluated against the CQS *NF54* strain of *P. falciparum* and displayed poor antiplasmodial activity even at the highest concentration (1000 ng/mL) tested. A comparison was made between **SN70-3**, a chromone-2-carboxylic acid, and **SN38-3**, a chromone-3-carboxylic acid, to determine which position of attachment of the ester group on the chromone ring would yield better activity. From the data, attachment of the ethyl ester group at position 2 appeared to improve antiplasmodial activity, it was also noted that **SN70-3** (solubility: 6 µg/mL) had a greater aqueous solubility than **SN38-3** (solubility: 1 µg/mL). A number of precursors (carboxylic acids) were evaluated for antiplasmodial activity; as with their corresponding esters

these acids did not possess any antiplasmodial activity at the highest concentration tested. Furthermore, the chromone ethyl esters were evaluated for their antimycobacterial activity against the *H37Rv* strain of *Mycobacterium tuberculosis*. No antimycobacterial activity was observed for the chromones as evidenced from their MIC_{99} values which exceeded 160 µM. An improvement of the solubility may improve the biological activity, as most samples were tested as suspensions since precipitation occurred.

From the results in Table 3.4, these chromones exhibited low solubility, indicating that the choice of substituents at position 6 of the chromone ring did not appear to improve solubility when compared to **SN38-3** (solubility: 1 µg/mL), a non-biaryl compound. However, **SN93-3** and **SN95-3** (solubility: 60 µg/mL), with aryl substituents at positions 5 and 8 of the chromone ring, did significantly improve aqueous solubility when compared to the compounds (**SN83-3** and **SN94-3** (solubility: 7 µg/mL)) with aryl substituents at positions 6 and 7 on the chromone ring. The *ortho*-substituted chromones, **SN93-3** and **SN95-3**, displayed the greatest solubility as expected, as the 4-(methylsulfonyl)phenyl group is expected to rotate out of plane as most biaryls systems tend to do.[24] All four compounds with a 4-(methylsulfonyl)phenyl group had high melting points, and thus a conclusion cannot be drawn here on the concept that disruption of planarity may lower the crystal packing energy and thus its melting point, resulting in an improvement of its solubility. Further analysis is needed, such as a crystal structure; unfortunately, several attempts to grow X-ray grade crystals were unsuccessful.

Table 3.4: A summary of the physicochemical properties and biological evaluation against the CQS *NF54* strain of *P. falciparum* and *H37Rv* strain of *Mycobacterium tuberculosis*

Code	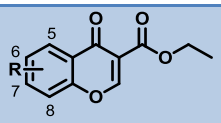 R	Position	[a]Solubility µg/mL	[b]CLogD pH 7.4	[c]CLogP	[d]Caco-2	*NF54*		MIC_{99} µM
							µg/mL	µM	
SN38-3	Br	6	1	2.74	3.05	1.19	10	33.7	>160
SN84-3	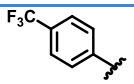	6	2	4.65	4.87	1.11	1	2.76	160
SN85-3	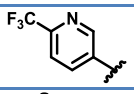	6	7	3.30	3.72	0.86	1	2.75	>160
SN87-3		6	6	3.41	3.62	1.13	1	3.33	>160
SN90-3	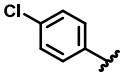	6	2	4.48	4.68	1.33	1	3.04	160
SN91-3	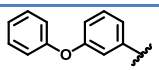	6	2	5.87	5.59	1.27	1	2.59	160
SN92-3	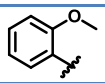	6	3	3.13	3.84	1.20	1	2.69	>160
SN93-3	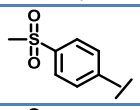	5	60	2.13	2.54	0.83	1	2.69	>160
SN83-3	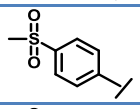	6	7	2.13	2.70	0.77	1	2.69	>160
SN94-3	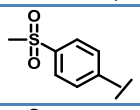	7	7	2.13	2.70	0.31	1	2.69	160
SN95-3	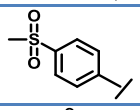	8	60	2.13	2.65	0.38	1	2.69	>160
SN70-3	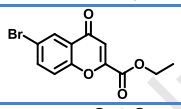	-	6	2.74	3.93	1.20	1	3.37	>160
SN38	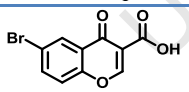	6	54	3.19	-	-		3.72	>160
SN83-2	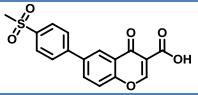	6	69	2.55	-	-		2.90	>160
SN90-2	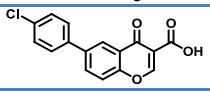	6	-	4.90	-	-		3.33	>160
							CQ 38 nM		**Kanamycin 3.13 µM**

[a] Solubility at pH 7.4, 0.01M phosphate buffered saline containing 1% DMSO, [b] CLogD values were estimated at pH 7.4 using Marvin Sketch, [c] CLogP andCaco-2 values were estimated using Volsurf +

3.7 Conclusion

In the evaluation of chromones as potential antiplasmodial agents with drug-like properties, a small series of compounds was synthesized. Each target molecule was fully characterized using various spectroscopic and analytical techniques, including ^{1}H NMR, ^{13}C NMR and mass spectrometry. The effect of aryl substituents on solubility was also studied. It can be concluded that the attachment of the aryl group at positions 5 and 8 improved solubility (60 µg/mL) as compared to positions 6 and 7 (7 µg/mL). The *in silico* prediction of solubility was generally higher than the experimentally determined results. It was evident from the antiplasmodial and antimycobacterial screening results that these compounds have poor potency.

3.8 References

1. T. J. Egan, R. Hunter, C. H. Kaschula, H. M. Marques, A. Misplon and J. Walden, *J. Med. Chem.*, **2000**, *43*, 283.
2. C. H. Kaschula, T. J. Egan, R. Hunter, N. Basilico, S. Parapini, D. Taramelli, E. Pasini and D. Monti *J. Med. Chem.*, **2002**, *45*, 3531.
3. C. L. Yeates, J. F. Batchelor, E. C. Capon, N. J. Cheesman, M. Fry, A. T. Hudson, M. Pudney, H. Trimming, J. Woolven, J. M. Bueno, J. Chicharro, E. Fernández, J. M. Fiandor, D. Gargallo-Viola, F. Gómez, D. Heras, E. Herreros and M. L. León, *J. Med. Chem.*, **2008**, *51*, 2845.
4. M. W. Mather, K. W. Henry and A. B. Vaidya, *Curr. Drug Targets*, **2007**, *8*, 49.
5. H. J. Painter, J. M. Morrisey, M. W. Mather and A. B. Vaidya, *Nature*, **2007**, *446*, 88.
6. V. Barton, N. Fisher, G. A. Biagini, S. A. Ward and P. M. O' Neill, *Curr. Opin. Chem. Biol.*, **2010**, *14*, 440.
7. R. H. Garrett and C. M. Grisham, *Biochemistry*, Thomson Brooks Cole, California, 3rd Ed., 2005.
8. P. Mitchell, *FEBS Letters*, **1975**, *59*, 137.
9. B. Gurung, L. Yu and C. Yu, *J. Biol. Chem.*, **2008**, *283*, 28087.
10. K. K. Seymour, A. E. T. Yeo, K. H. Rieckmann and R. I. Christopherson, *Ann. Trop. Med. Parasit*., **2006**, *91*, 603.
11. I. K. Srivastava, H. Rottenberg and A. B. Vaidya, *J. Biol. Chem*., **1997**, *272*, 3961.
12. J. Krungkrai, P. Prapunwatana, C. Wichitkul, S. Reungprapavut, S. R. Krungkrai and T. Horii, *Southeast Asian J. Trop. Med. Public* Health, **2003**, *34*, 32.
13. J. L. Cape, M. K. Bowman and D. M. Kramer, *Trends Plant Sci.*, **2006**, *11*, 46.
14. G. Von Jagow and T. Ohnishi, *FEBS Letters*, **1985**, *126*, 311.
15. L. Esser, B. Quinn, Y. Li, M. Zhang, M. Elberry, L. Yu, C. Yu and D. Xia, *J. Mol. Biol.,* **2004**, *341*, 281.
16. R. Cowley, S. Leung, N. Fisher, M. Al-Helal, N. G. Berry, A. S. Lawrenson, R. Sharma, A. E. Shone, S. A. Ward, G. A. Biagini and P. M. O. Neill, *Med. Chem. Commum*., **2012**, *3*, 39.
17. GlaxoSmithKline MALARONE®, [Citied: 31.08.2012] http://www.malarone.com.
18. D. A. Horton, G. T. Bourne and M. L. Smythe, *Chem. Rev.*, **2003**, *103*, 893.
19. The Royal Swedish Academy of Sciences, *Palladium-Catalyzed Cross Couplings in Organic Synthesis*, Scientific Background on the Nobel Prize in Chemistry 2010, 6 October 2010.
20. Nobel Prize 2010. [Online 10.2010], [Cited: 31.08.2012] www.nobelprize.org.
21. J. A. Joule and K. Mills, *Heterocyclic Chemistry*, John Wiley and Sons, Chichester, 5th Ed., 2010.
22. N. Miyaura and A. Suzuki, *Chem. Rev.*, **1995**, *95*, 2457.
23. C. E. Housecroft and A. G. Sharpe, *Inorganic Chemistry,* Pearson Education Limited, England, 2nd Ed., 2005.
24. J. Clayden, N. Greeves, S. Warren and P. Wothers, *Organic Chemistry*, Oxford University Press, Oxford, 1st Ed., 2001.
25. A. Suzuki, *J. Organomet. Chem.*, **1999**, *576*, 147.

26. Y. S. Shim, K. C. Kim, D. Y. Chi, K. H. Lee and H. Cho, *Bioorg. Med. Chem. Lett.*, **2003**, *13*, 2561.
27. E. H. Kerns and L. Di, *Drug-like Properties: Concepts, Structure Design and Methods from ADME to Toxicity Optimization*, Elsevier Academic Press, California, 1st Ed., 2008.
28. C. Hansch, J. E. Quinlan and G. Lawrence, *J. Org. Chem.*, **1968**, *33*, 347.
29. S. C. Valvani, S. Yalkowsky and T. Roseman, *J. Pharm. Sci.*, **1981**, *70*, 502.
30. M. Ishikawa and Y. Hashimoto, *J. Med. Chem.,* **2011**, *54*, 1539.
31. A. Gavezzotti, *Acc. Chem. Res.*, **1994**, *27*, 309.
32. C. A. Lipinski, F. Lombardo, B. W. Dominy, P. J. Feeney, *Adv. Drug Delivery Rev.*, **2001**, *46*, 3.
33. G. Cruciani, P. Crivori, P. A. Carrupt and B. Testa, *J. Mol. Struc. (Theochem)*, **2000**, *503*, 17.

Chapter Four – Summary and Conclusion

4.1 General Summary and Conclusion

Hybrid compounds which contain the chromone substructure and the 4-aminoquinoline nucleus joined by an alkyl or amide linker at either position 2 or 3 of the chromone ring were synthesized. Standard synthetic protocols were used, such as the reductive amination reaction for the synthesis of the alkyl-linked hybrids and the EDC-HOBt coupling reaction for the synthesis of the amide-linked hybrids. Successful synthesis was established using various spectroscopic and analytical techniques, such as ^{1}H NMR, ^{13}C NMR, IR and mass spectrometry. The compounds were evaluated for their antiplasmodial, antitumour and antimycobacterial activities, as well as for their physicochemical properties, specifically turbidimetric aqueous solubility at pH 7.4, CLogP, CLogD and Caco-2.

In the alkyl-linked hybrids, **SN24** (*D10*: IC_{50} = 30.7 nM) displayed the greatest antiplasmodial activity from Series 1. Amongst the amide-linked hybrids at position 3 of the chromone ring (Series 2) compounds **SN44** (*NF54*: IC_{50} = 38.1 nM), **SN48** (*D10*: IC_{50} = 20.9 nM), **SN54** (*D10*: IC_{50} = 46.8 nM; *NF54*: IC_{50} = 57.5 nM) and **SN57** (*D10*: IC_{50} = 39.7 nM; *NF54*: IC_{50} = 63.3 nM) are the most active against the CQS strains of *P. falciparum*. On the other hand, attachment of the amide linker at position 2 of the chromone ring (Series 3) significantly improved the antiplasmodial activity of the hybrids in the CQR *K1* strain of *P. falciparum*, as seen from **SN74** (IC_{50} = 82.9 nM), **SN77** (IC_{50} = 37.6 nM) and **SN78** (IC_{50} = 80.9 nM). The hybrids displayed moderate antitumour activity throughout, with the exception of **SN78** (IC_{50} = 1.78 µM) which demonstrated the most promising result. All compounds tested had low to moderate aqueous solubility; improving their aqueous solubility may lead to enhanced activity as some samples precipitated out of solution during testing. One of the objectives of this project was to evaluate the linker between the pharmacophores. Based on the biological activities of the hybrids, it can be concluded that neither linker resulted in compounds with enhanced potency in the *in vitro* testing.

A further aim of this study was to investigate the effect of the aryl substituents on the chromone ring in terms of solubility and pharmacological activity. Various aryl groups were attached at position 6 of the chromone ring via the Suzuki cross-coupling reaction; these compounds displayed low solubility with results <10 µg/mL. In addition, one aryl group the (4-(methylsulfonyl)phenyl) group, was chosen to investigate the effect of the attachment position by attaching the aryl substituent at positions 5, 6, 7 and 8 of the chromone ring. The *ortho*-substituted chromones, **SN93-3** (60 µg/mL) and **SN95-3** (60 µg/mL), displayed the highest solubility and it is postulated that they increase the dihedral angle between the two phenyl rings thereby disrupting the planar

symmetry. These chromone-ethyl esters exhibited moderate to poor antiplasmodial and antimycobacterial activities.

4.2 Future Work

Further work on the chromone-aminoquinoline hybrids would be to increase the structural diversity in order to create more SAR data based on Series 3, the amide linked hybrids at position 2 of the chromone ring, as they displayed the greatest potency. Another aspect of this project to further investigate would be to determine the antitumour activity of **SN78** in other cancer cell lines.

Chapter Five – Experimental Procedures

5.1 General Remarks

All reagents and solvents were purchased from commercial sources and used as received. DCM was distilled from phosphorous pentoxide prior to use. Reactions were monitored by thin layer chromatography (TLC) using Merck F254 aluminium-backed precoated silica gel plates and were visualized by ultraviolet light at 254 nm. Nuclear Magnetic Resonance (NMR) spectra were recorded on a Varian Unity XR400 MHz (^{1}H at 400 MHz, ^{13}C at 100 MHz), Varian Unity XR300 MHz (^{1}H at 300 MHz, ^{13}C at 75 MHz) or a Bruker Ultrashield 400 Plus spectrometer (^{1}H at 400 MHz, ^{13}C at 100 MHz). Chemical shifts for ^{1}H and ^{13}C NMR shifts were reported using tetramethylsilane (TMS) as the internal standard. The format used for recording ^{13}C NMR data is that accepted by most international journals (including American Chemical Society journals). In this format, chemical shift values are simply listed without specific assignments to carbon atoms. Infrared (IR) absorptions were measured on a Perkin-Elmer Spectrum One FT-IR Spectrometer as KBr pellets. Melting points were determined using a Reichert-Hung Thermovar Hot Stage Microscope and are uncorrected. Mass Spectrometry was recorded on a JEOL GCmatell in Electron Ionisation mode. High Performance Liquid Chromatography (HPLC) was done on a Spectroseries binary gradient pump, P200, using an AS100 autosampler and a UV100 detector. The HPLC column was a Phenomenex 150 x 4.60 mm, 3 micron, Luna 3u C18(2) 100 Å column at ambient temperature. The data was processed on Delta 5.0 software from DataworX, Pty. Ltd. HLPC grade acetonitrile, methanol and Millipore filtered water were used as the eluent.

5.2 Synthesis of Chromone Derivatives

5.2.1 General Synthetic Procedure for Suzuki-coupled Chromone Reactions[1]

A solution of 5-bromo-2-hydroxyacetophenone (1.0 eq), boronic acid (1.2 eq) and $Pd(PPh_3)_2Cl_2$ (0.05 eq) in dry DMF (10 ml) was degassed for 10 minutes, followed by the addition of 1M K_2CO_3 (1.05 eq). The reaction mixture was refluxed at 95 ^{o}C for 12 hours and cooled to room temperature; distilled water (30 mL) was added and extracted with EtOAc (3 x 50 mL). The combined organic layers were washed with brine and dried over anhydrous Na_2SO_4. The residue was purified by flash chromatography on silica gel using Hexane:EtOAc as the eluent to afford the product.

1-(4-Hydroxy-4'-(methylsulfonyl)biphenyl-3-yl)ethanone (SN83)

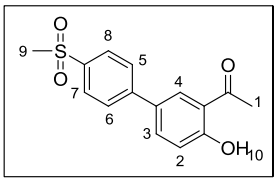

Yellow solid (0.26 g, 37 %); M.p.: 141 – 143 °C; R_f (Hex/EtOAc 8:2) 0.15; δ_H (300 MHz, $CDCl_3$) 2.64 (3H, s, H_1), 3.02 (3H, s, H_9), 7.01 (1H, d, *J* 8.7 Hz, H_2), 7.47 – 7.49 (3H, m, H_3, H_5, H_6), 7.95 (1H, d, *J* 2.3 Hz, H_4) 8.02 (2H, m, H_7, H_8), 12.3 (1H, s, H_{10}); δ_C (100 MHz, $CDCl_3$) 26.6, 44.5, 115.9, 119.4, 119.9, 128.0 (2C), 129.7 (2C), 130.0, 135.1, 139.1, 145.3, 162.8, 204.2; EI - m/z 289.9 $[M]^+$.

1-(4-Hydroxy-4'-(trifluoromethyl)biphenyl-3-yl)ethanone (SN84)

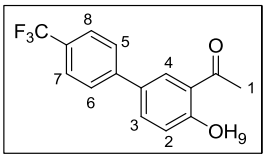

Pale-yellow solid (0.27 g, 41 %); M.p.: 55 – 57 °C; R_f (Hex/EtOAc 9.7:0.3) 0.40; δ_H (300 MHz, $CDCl_3$) 2.72 (3H, s, H_1), 7.10 (1H, d, *J* 8.7 Hz, H_2), 7.64 (1H, dd, *J* 2.1, 8.6 Hz, H_3), 7.69 - 7.74 (4H, m, H_5 - H_8), 7.94 (1H, d, *J* 2.3 Hz, H_4), 12.3 (1H, s, H_9); δ_C (100 MHz, $CDCl_3$) 26.5, 119.8, 122.8, 125.7, 125.8, 125.9, 126.9, 129.1, 129.4, 130.7, 135.1, 142.8, 143.4, 162.4, 202.6; EI - m/z 280.1 $[M]^+$.

1-(2-Hydroxy-5-(6-(trifluoromethyl)pyridin-3-yl)phenyl)ethanone (SN85)

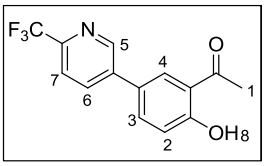

Pale-yellow solid (0.35 g, 54 %); M.p.: 111 – 113 °C; R_f (Hex/EtOAc 9:1) 0.30; δ_H (300 MHz, $CDCl_3$) 2.73 (3H, s, H_1), 7.14 (1H, d, *J* 8.7 Hz, H_2), 7.71 (1H, dd, *J* 2.3, 8.7 Hz H_3), 7.74 (1H, d, *J* 8.2 Hz, H_7), 7.95 (1H, d, *J* 2.3 Hz, H_4), 8.02 (1H, dd, *J* 2.3, 8.1 Hz, H_6), 8.92 (1H, d, *J* 2.2 Hz, H_5), 12.4 (1H, s, H_8); δ_C (100 MHz, $CDCl_3$) 26.5, 119.7, 120.4, 127.2, 129.4, 134.8, 134.9, 135.9, 138.2, 145.5, 147.9, 148.3, 162.9, 205.3; EI - m/z 280.9 $[M]^+$.

1-(4,4'-Dihydroxybiphenyl-3-yl)ethanone (SN86)

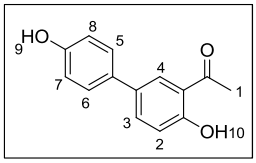

Yellow solid (0.30 g, 56 %); M.p.: 187 – 189 °C; R_f (Hex/EtOAc 7:3) 0.28; δ_H (300 MHz, $CDCl_3$) 2.69 (3H, s, H_1), 5.39 (1H, br s, H_9), 6.90 (2H, d, *J* 8.7 Hz, H_7, H_8), 7.05 (1H, d, *J* 8.6 Hz, H_2), 7.42 (2H, d, *J* 8.7 Hz, H_5, H_6), 7.64 (1H, dd, *J* 2.3, 8.6 Hz, H_3), 7.84 (1H, d, *J* 2.3 Hz, H_4), 12.2 (1H, s, H_{10}); δ_C (100 MHz, $CDCl_3$) 26.3, 115.8, 118.6, 127.8, 128.3, 128.7, 129.5, 129.0, 129.9, 132.4, 134.9, 155.6, 161.3, 203.3; EI - m/z 227.9 $[M]^+$.

1-(2-Hydroxy-5-(thiophen-3-yl)phenyl)ethanone (SN87)

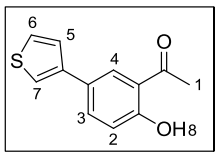

Yellow solid (0.26 g, 50 %); M.p.: 80 – 83 °C; R_f (Hex/EtOAc 7:3) 0.40; δ_H (300 MHz, $CDCl_3$) 2.70 (3H, s, H_1), 7.02 (1H, d, *J* 8.7 Hz, H_2), 7.33 (1H, dd, *J* 2.9, 8.6 Hz, H_5), 7.37 (1H, d, *J* 8.3 Hz, H_6), 7.41 (1H, d, *J* 2.9 Hz, H_7), 7.70 (1H, dd, *J* 2.2, 8.5 Hz, H_3), 7.92 (1H, d, *J* 2.2 Hz, H_4), 12.3 (1H, s, H_8); δ_C (100 MHz, $CDCl_3$) 26.6, 118.8, 119.5, 125.9, 126.5, 127.3, 128.1, 133.9, 134.7, 141.0, 161.5, 204.5; EI - m/z 217.9 $[M]^+$.

1-(4'-Chloro-4-hydroxybiphenyl-3-yl)ethanone (SN90)

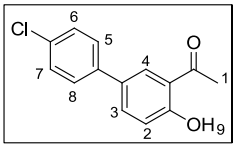

Yellow solid (0.32 g, 56 %); M.p.: 79 – 82 °C; R_f (Hex/EtOAc 9:1) 0.50; δ_H (400 MHz, $CDCl_3$) 2.64 (3H, s, H_1), 7.02 (1H, d, *J* 8.7 Hz, H_2), 7.33 – 7.36 (4H, m, H_5 – H_8), 7.61 (1H, dd, *J* 2.3, 8.6 Hz, H_3), 7.82 (1H, d, *J* 2.3 Hz, H_4), 12.1 (1H, s, H_9), δ_C (100 MHz, $CDCl_3$) 26.7, 119.1, 119.9, 127.9 (2C), 128.9, 129.1 (2C), 131.1, 133.5, 135.1, 138.6, 162.1, 204.4; EI - m/z 245.9 $[M]^+$.

1-(4-Hydroxy-3'-phenoxybiphenyl-3-yl)ethanone (SN91)

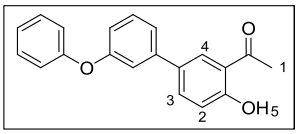

Yellow Oil (0.37 g, 52 %); R_f (Hex/EtOAc 9:1) 0.25; δ_H (400 MHz, $CDCl_3$) 2.65 (3H, s, H_1), 6.91 – 7.42 (10H, m, Ar H, H_2), 7.65 (1H, dd, *J* 2.2, 8.7 Hz, H_3), 7.87 (1H, d, *J* 2.2 Hz, H_4), 12.2 (1H, s, H_5); δ_C (100 MHz, $CDCl_3$) 26.7, 117.2, 117.4, 118.9 (2C), 119.8, 121.5, 122.0, 123.5, 129.0, 129.8 (2C), 130.2, 131.6, 135.2, 141.9, 157.1, 157.9, 162.1, 204.5.

1-(4-Hydroxy-2'-methoxybiphenyl-3-yl)ethanone (SN92)

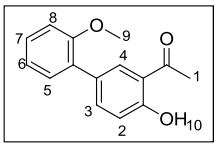

Pale-yellow solid (0.30 g, 57 %); R_f (Hex/EtOAc 9.5:0.5) 0.35; δ_H (400 MHz, $CDCl_3$) 2.65 (3H, s, H_1), 3.83 (3H, s, H_9), 7.03 – 7.07 (3H, m, H_2, H_6, H_8), 7.33 (2H, m, H_5, H_7), 7.67 (1H, dd, *J* 2.2, 8.6 Hz, H_3), 7.90 (1H, d, *J* 2.2 Hz, H_4), 12.3 (1H, s, H_{10}); δ_C (100 MHz, $CDCl_3$) 26.6, 55.6, 111.4, 117.9 (2C), 119.4, 121.0, 128.7, 129.3, 130.4, 131.5, 137.9, 156.5, 161.4, 204.6; EI - m/z 242.0 $[M]^+$.

1-(3-Hydroxy-4'-(methylsulfonyl)biphenyl-2-yl)ethanone (SN93)

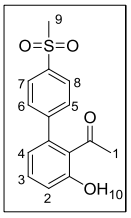

White solid (0.18 g, 53 %); M.p.: 127 – 130 °C; R_f (Hex/EtOAc 5:5) 0.43; δ_H (400 MHz, $CDCl_3$) 2.78 (3H, s, H_1), 3.05 (3H, s, H_9), 6.73 (1H, d, *J* 7.4 Hz, H_2), 7.00 (1H, d, *J* 8.4 Hz, H_4), 7.38 (1H, t, *J* 7.9 Hz, H_3), 7.49 (2H, d, *J* 8.6 Hz, H_5, H_6), 7.96 (2H, d, *J* 8.6 Hz, H_7, H_8), 11.5 (1H, s, H_{10}); δ_C (100 MHz, $CDCl_3$) 22.1, 44.5, 118.7, 120.9, 122.2, 127.8 (2C), 129.9 (2C), 134.2, 140.4, 142.3, 147.7, 161.4, 205.9; EI - m/z 290.0 $[M]^+$.

1-(3-Hydroxy-4'-(methylsulfonyl)biphenyl-4-yl)ethanone (SN94)

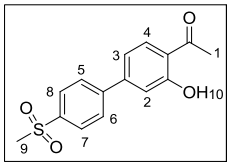

Yellow solid (0.18 g, 41 %); M.p.: 180 – 183 °C; R_f (Hex/EtOAc 6:4) 0.17; δ_H (400 MHz, $CDCl_3$) 2.68 (3H, s, H_1), 3.10 (3H, s, H_9), 7.15 (1H, dd, *J* 1.8, 8.3 Hz, H_3), 7.22 (d, *J* 1.8 Hz, H_2), 7.79 (2H, m, H_5, H_6), 7.85 (1H, d, *J* 8.3 Hz, H_4), 8.03 (2H, m, H_7, H_8), 12.3 (1H, s, H_{10}); δ_C (100 MHz, $CDCl_3$) 23.6, 44.4, 118.7, 119.8, 120.5, 127.2 (2C), 129.8 (2C), 130.7, 135.1, 139.6, 146.1, 163.4, 204.5; EI - m/z 290.0 $[M]^+$.

1-(2-Hydroxy-4'-(methylsulfonyl)biphenyl-3-yl)ethanone (SN95)

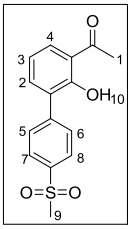

Orange solid (0.22 g, 33 %); M.p.: 135 – 139 ^{o}C; R_f (Hex/EtOAc 6:4) 0.22; δ_H (400 MHz, $CDCl_3$) 2.63 (3H, s, H_1), 3.01 (3H, s, H_9), 6.96 (1H, t, *J* 7.8 Hz, H_3), 7.48 (1H, d, *J* 7.8 Hz, H_2), 7.71 (2H, m, H_5, H_6), 7.76 (1H, d, *J* 8.0 Hz, H_4), 7.92 (2H, m, H_7, H_8), 12.9 (1H, s, H_{10}); δ_C (100 MHz, $CDCl_3$) 22.6, 44.3, 118.7, 119.7, 126.9 (2C), 129.9 (2C), 130.9, 136.8, 138.9, 142.4, 159.4, 162.2, 204.6; EI - m/z 289.9 $[M]^+$.

5.2.2 General Synthetic Procedure of Chromone-3-carbaldehyde Derivatives[2]

$POCl_3$ (9.0 eq) was added over a period of 20 minutes to a stirred solution of the selected hydroxyacetophenone (1.0 eq) and dry DMF (20 mL) under N_2, in a liquid nitrogen bath. The resulting mixture was allowed to stir overnight at room temperature and poured into ice water (25 mL). The resulting precipitate was filtered and washed with distilled water followed by ethanol. Recrystallization from acetone afforded the desired aldehyde.

4-Oxo-4H-chromene-3-carbaldehyde (SN18)

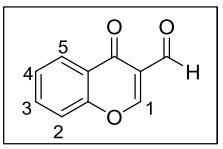

White solid (2.9 g, 61 %); M.p.: 147 – 150 ^{o}C; R_f (EtOAc) 0.25; δ_H (400 MHz, $CDCl_3$) 7.48 (1H, t, *J* 7.2 Hz, H_4), 7.52 (1H, d, *J* 8.8 Hz, H_2), 7.75 (1H, t, *J* 7.8 Hz, H_3), 8.26 (1H, d, *J* 8.5 Hz, H_5), 8.52 (1H, s, H_1), 10.4 (1H, s, CHO); δ_C (100 MHz, $CDCl_3$) 118.6, 120.4, 125.4, 126.2, 126.6, 134.8, 156.3, 160.6, 175.7, 188.7; EI - m/z 174.0 $[M]^+$.

6-Chloro-4-oxo-4H-chromene-3-carbaldehyde (SN19)

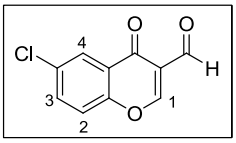

Pale-yellow solid (2.1 g, 89 %); M.p.: 166 – 167 ^{o}C; R_f (EtOAc) 0.29; IR ν_{max} (KBr) /cm^{-1} 1662, 1696 (2 x C=O); δ_H (400 MHz, $CDCl_3$) 7.50 (1H, d, *J* 8.9 Hz, H_2), 7.69 (1H, dd, *J* 2.6, 8.9 Hz, H_3), 8.25 (1H, d, *J* 2.7 Hz H_4), 8.53 (1H, s, H_1), 10.4 (1H, s, CHO); δ_C (100 MHz, $CDCl_3$) 119.1, 120.3, 125.7, 126.4, 132.9, 134.9, 154.5, 160.6, 174.8, 188.1; EI - m/z 207.9 $[M]^+$; HPLC purity: 99 % (t_r = 11.2 min).

6-Bromo-4-oxo-4H-chromene-3-carbaldehyde (SN20)

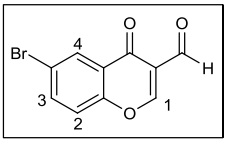

Pale-yellow solid (2.1 g, 90 %); M.p.: 158 – 160 ^{o}C; R_f (EtOAc) 0.35; δ_H (400 MHz, $CDCl_3$) 7.42 (1H, d, *J* 8.9 Hz, H_2), 7.84 (1H, dd, *J* 2.4, 8.9 Hz, H_3), 8.25 (1H, d, *J* 2.3 Hz, H_4), 8.53 (1H, s, H_1), 10.4 (1H, s, CHO); δ_C (100 MHz, $CDCl_3$) 119.3, 120.3, 120.5, 126.7, 128.9, 137.8, 155.0, 160.6, 174.7, 188.0; EI - m/z 251.8 $[M]^+$.

6-Fluoro-4-oxo-4H-chromene-3-carbaldehyde (SN21)

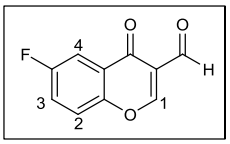

Orange solid (1.6 g, 66 %); M.p.: 146 – 149 °C; R_f (EtOAc) 0.28; δ_H (400 MHz, $CDCl_3$) 7.47 (1H, m, H_2), 7.56 (1H, dd, *J* 2.9, 7.8 Hz, H_3), 7.93 (1H, d, *J* 3.1 Hz, H_4), 8.54 (1H, s, H_1), 10.4 (1H, s, CHO); δ_C (100 MHz, $CDCl_3$) 119.5, 120.8, 122.8, 123.0, 152.4, 159.1, 160.6, 161.5, 175.2, 188.2; EI - m/z 192.1 $[M]^+$.

6-Methoxy-4-oxo-4H-chromene-3-carbaldehyde (SN22)

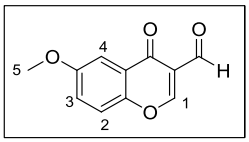

Pale-yellow solid (1.4 g, 61 %); M.p.: 145 – 148 °C; R_f (EtOAc) 0.20; δ_H (400 MHz, $CDCl_3$) 3.92 (3H, s, H_5), 7.31 (1H, d, *J* 9.2 Hz, H_2), 7.46 (1H, dd, *J* 3.1, 9.2 Hz, H_3), 7.64 (1H, d, *J* 3.1 Hz, H_4), 8.52 (1H, s, H_1), 10.4 (1H, s, CHO); δ_C (100 MHz, $CDCl_3$) 56.1, 119.8, 124.4, 125.6, 129.9, 131.2, 147.3, 157.9, 160.2, 175.3, 188.7; LRMS (EI) m/z 203.9 $[M]^+$.

6-Methyl-4-oxo-4H-chromene-3-carbaldehyde (SN23)

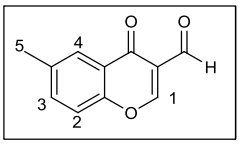

Pale-yellow solid (1.7 g, 73 %); M.p.: 156 – 159 °C; R_f (EtOAc) 0.24; δ_H (400 MHz, $CDCl_3$) 2.47 (3H, s, H_5), 7.41 (1H, d, *J* 8.6 Hz, H_2), 7.54 (1H, dd, *J* 2.3, 8.6 Hz, H_3), 8.06 (1H, d, *J* 2.2 Hz, H_4), 8.50 (1H, s, H_1), 10.4 (1H, s, CHO); δ_C (100 MHz, $CDCl_3$) 20.9, 118.3, 120.3, 125.0, 125.6, 135.9, 136.9, 154.5, 160.5, 176.1, 188.7; EI - m/z 187.9 $[M]^+$.

6-(4-(Methylsulfonyl)phenyl)-4-oxo-4H-chromene-3-carbaldehyde (SN83-1)

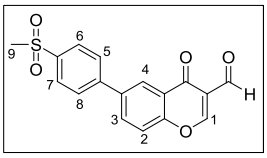

Off-white solid (0.19 g, 81 %); M.p.: 254 – 256 °C; R_f (EtOAc) 0.63; δ_H (400 MHz, $CDCl_3$) 3.04 (3H, s, H_9), 7.60 (1H, d, *J* 8.2 Hz, H_2), 7.86 (2H, d, *J* 7.4 Hz, H_5, H_8), 7.99 (1H, dd, *J* 2.3, 8.2 Hz, H_3), 8.08 (2H, d, *J* 7.5 Hz, H_6, H_7), 8.47 (1H, d, *J* 2.2 Hz, H_4), 8.51 (1H, s, H_1), 10.4 (1H, s, CHO); δ_C (100 MHz, $CDCl_3$) 44.4, 119.4, 124.6, 128.0, 128.1, 129.3, 129.8, 137.7, 140.5, 141.1, 144.1, 148.0, 150.7, 156.2, 160.3, 175.4, 187.9; EI - m/z 327.8 $[M]^+$.

4-Oxo-6-(4-(trifluoromethyl)phenyl)-4H-chromene-3-carbaldehyde (SN84-1)

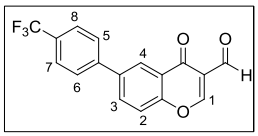

Yellow solid (0.19 g, 51 %); M.p.: 62 – 65 °C; R_f (EtOAc) 0.70; δ_H (400 MHz, $CDCl_3$) 7.65 (1H, d, *J* 8.7 Hz, H_2), 7.79 – 7.73 (4H, m, H_5 – H_8), 7.99 (1H, dd, *J* 2.4, 8.7 Hz, H_3), 8.52 (1H, d, *J* 2.4 Hz, H_4), 8.58 (1H, s, H_1), 10.4 (1H, s, CHO); δ_C (100 MHz, $CDCl_3$) 119.5, 120.5, 124.5, 125.7, 125.9, 126.1 (2C), 126.5, 127.6, 133.5, 138.4, 142.2, 155.4, 156.0, 160.6, 175.8, 188.3; EI - m/z 318.0 $[M]^+$.

4-Oxo-6-(6-(trifluoromethyl)pyridin-3-yl)-4H-chromene-3-carbaldehyde (SN85-1)

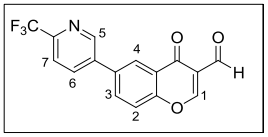

White solid (0.16 g, 49 %); M.p.: 55 – 57 ^{o}C; R_f (EtOAc) 0.32; δ_H (300 MHz, $CDCl_3$) 7.72 (1H, d, *J* 8.7 Hz, H_2), 7.82 (1H, d, *J* 8.2 Hz, H_7), 8.00 (1H, dd, *J* 2.4, 8.7 Hz, H_3), 8.14 (1H, dd, *J* 2.0, 8.0 Hz, H_6), 8.53 (1H, d, *J* 2.4 Hz, H_4), 8.59 (1H, s, H_1), 9.01 (1H, d, *J* 2.1 Hz, H_5), 10.4 (1H, s, CHO); δ_C (100 MHz, $CDCl_3$) 119.8, 120.5, 120.6, 124.8, 125.9, 133.2, 134.8, 135.0, 135.6, 137.1, 148.0, 148.3, 156.3, 160.4, 175.3, 187.8; EI - m/z 318.8 $[M]^+$.

6-(4-Hydroxyphenyl)-4-oxo-4H-chromene-3-carbaldehyde (SN86-1)

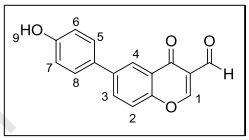

Brown solid (0.08 g, 30 %); M.p.: 229 – 231 ^{o}C; R_f (EtOAc) 0.36; δ_H (300 MHz, $CDCl_3$) 4.85 (1H, br s, H_9), 6.87 (2H, d, *J* 8.7 Hz, H_5, H_8), 7.48 (2H, d, *J* 8.7 Hz, H_6, H_7), 7.56 (1H, d, *J* 8.7 Hz, H_2), 7.85 (1H, dd, *J* 2.3, 8.6 Hz, H_3), 8.37 (1H, d, *J* 2.3 Hz, H_4), 8.49 (1H, s, H_1), 10.4 (1H, s, CHO); δ_C (100 MHz, DMSO-d_6) 116.4, 116.5, 118.3, 123.2, 124.6, 130.8, 130.9, 131.6, 133.8, 135.7, 136.1, 156.3, 157.8, 170.5, 176.3, 189.6; EI - m/z 266.0 $[M]^+$.

4-Oxo-6-(thiophen-3-yl)-4H-chromene-3-carbaldehyde (SN87-1)

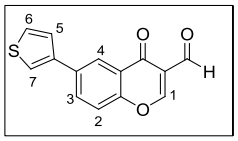

Brown solid (0.21 g, 56 %); M.p.: 156 – 158 ^{o}C; R_f (EtOAc) 0.16; δ_H (300 MHz, $CDCl_3$) 7.45 (2H, m, H_2, H_5), 7.56 (1H, d, *J* 8.7 Hz, H_6), 7.59 (1H, d, *J* 2.3 Hz, H_7), 7.96 (1H, dd, *J* 2.2, 8.7 Hz, H_3), 8.46 (1H, d, *J* 2.2 Hz, H_4), 8.53 (1H, s, H_1), 10.4 (1H, s, CHO); δ_C (100 MHz, $CDCl_3$) 119.1, 120.3, 121.9, 122.9, 125.6, 126.1, 127.1, 132.8, 134.6, 139.9, 155.2, 160.4, 175.9, 188.5; EI - m/z 254.9 $[M]^+$.

6-(4-Chlorophenyl)-4-oxo-4H-chromene-3-carbaldehyde (SN90-1)

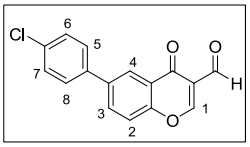

Yellow solid (0.25 g, 45 %); M.p.: 169 – 171 ^{o}C; R_f (EtOAc 7:3) 0.20; δ_H (400 MHz, $CDCl_3$) 7.46 (1H, d, *J* 8.7 Hz, H_2), 7.59 – 7.62 (4H, m, H_5 – H_8), 7.93 (1H, dd, *J* 2.4, 8.7 Hz, H_3), 8.46 (1H, d, *J* 2.4 Hz, H_4), 8.56 (1H, s, H_1), 10.4 (1H, s, CHO); δ_C (100 MHz, $CDCl_3$) 119.3, 120.0, 123.9, 125.6, 128.5 (2C), 129.3 (2C), 133.3, 134.6, 137.2, 138.7, 160.6, 172.3, 175.9, 188.5; EI - m/z 284.0 $[M]^+$.

4-Oxo-6-(3-phenoxyphenyl)-4H-chromene-3-carboxylic acid (SN91-1)

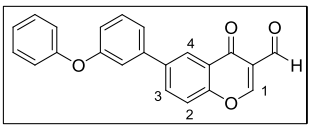

Pale-brown solid (0.19 g, 42 %); R_f (DCM) 0.26; δ_H (400 MHz, $CDCl_3$) 7.05 – 7.08 (3H, m, Ar H), 7.38 – 7.43 (6H, m, Ar H), 7.59 (1H, d, *J* 8.7 Hz, H_2), 7.59 (1H, dd, *J* 2.4, 8.7 Hz, H_3), 8.47 (1H, d, *J* 2.4 Hz, H_4), 8.55 (1H, s, H_1), 10.4 (1H, s, CHO); δ_C (100 MHz, $CDCl_3$) 117.6, 118.5 (2C), 119.8, 119.2, 120.4, 122.1, 123.6, 124.1, 125.5, 129.9 (2C), 130.5, 133.6, 139.3, 140.7, 155.7, 157.0, 158.1, 160.5, 175.9, 185.5; EI - m/z 342.1 $[M]^+$.

6-(2-Methoxyphenyl)-4-oxo-4H-chromene-3-carbaldehyde (SN92-1)

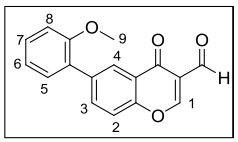

Yellow solid (0.25 g, 73 %); M.p.: 156 – 158 ^{o}C; R_f (EtOAc) 0.16; δ_H (300 MHz, $CDCl_3$) 3.84 (3H, s, H_9), 7.05 (2H, m, H_6, H_8), 7.38 (2H, m, H_5, H_7), 7.55 (1H, d, *J* 8.7 Hz, H_2), 7.96 (1H, dd, *J* 2.2, 8.7 Hz, H_3), 8.42 (1H, d, *J* 2.2 Hz, H_4), 8.55 (1H, s, H_1), 10.4 (1H, s, CHO); δ_C (100 MHz, $CDCl_3$) 55.6, 111.4, 117.9, 120.4, 121.1, 125.1, 126.5, 128.3, 129.7, 130.8, 136.4, 137.5, 155.2, 156.4, 160.4, 176.1, 188.7; EI - m/z 240.9 $[M]^+$.

5-(4-(Methylsulfonyl)phenyl)-4-oxo-4H-chromene-3-carbaldehyde (SN93-1)

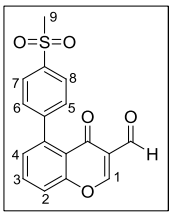

Pink solid (0.17 g, 83 %), M.p.: 213 – 216 ^{o}C; R_f (EtOAc) 0.28; δ_H (400 MHz, $CDCl_3$) 3.11 (3H, s, H_9), 7.23 (2H, d, *J* 8.6 Hz, H_5, H_6), 7.48 (1H, d, *J* 7.4 Hz, H_2), 7.60 (1H, d, *J* 8.5 Hz, H_4), 7.75 (1H, t, *J* 7.9 Hz, H_3), 7.97 (2H, d, *J* 8.6 Hz, H_7, H_8), 8.49 (1H, s, H_1), 10.2 (1H, s, CHO); δ_C (100 MHz, $CDCl_3$) 44.6, 119.3, 121.1, 122.5, 126.8 (2C), 129.5 (2C), 129.7, 133.9, 139.6, 141.8, 146.4, 157.3, 159.9, 175.9, 188.3; EI - m/z 327.9 $[M]^+$.

7-(4-(Methylsulfonyl)phenyl)-4-oxo-4H-chromene-3-carbaldehyde (SN94-1)

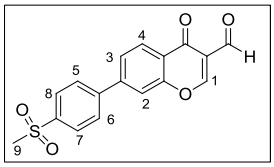

Brown solid (0.18 g, 46 %); M.p.: 239 – 241 ^{o}C; R_f (EtOAc) 0.58; δ_H (400 MHz, $CDCl_3$) 3.06 (3H, s, H_9), 7.69 (2H, m, H_2, H_3), 7.79 (2H, d, *J* 8.2 Hz, H_5, H_6), 8.04 (2H, d, *J* 8.2 Hz, H_7, H_8), 8.35 (1H, d, *J* 8.2 Hz, H_4), 8.52 (1H, s, H_1), 10.4 (1H, s, CHO); δ_C (100 MHz, $CDCl_3$) 44.5, 117.3, 120.7, 125.7, 127.2, 128.4 (2C), 128.5 (2C), 141.1, 143.9, 145.8, 156.6, 160.8, 167.6, 175.5, 188.3; EI - m/z 328.0 $[M]^+$.

8-(4-(Methylsulfonyl)phenyl)-4-oxo-4H-chromene-3-carbaldehyde (SN95-1)

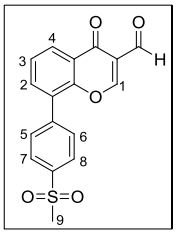

Yellow solid (0.03 g, 25 %); M.p.: 239 – 241 ^{o}C; R_f (EtOAc) 0.19; δ_H (400 MHz, $CDCl_3$) 3.07 (3H, s, H_9), 7.55 (1H, t, *J* 7.8 Hz, H_3), 7.65 – 7.69 (3H, m, H_2, H_5, H_6), 8.08 (2H, d, *J* 8.6 Hz, H_7, H_8), 8.33 (1H, d, *J* 7.9 Hz, H_4), 8.44 (1H, s, H_1), 10.3 (H, s, CHO); δ_C (100 MHz, $CDCl_3$) 44.5, 120.4, 125.9, 126.8, 127.7 (2C), 130.5 (2C), 131.3, 135.7, 137.2, 140.6, 152.9, 160.2, 175.7, 188.2; EI - m/z 327.9 $[M]^+$.

5.2.3 General Synthetic Procedure of Chromone-3-carboxylic acid Derivatives[3]

An aqueous solution of NH_2SO_3H (8.0 eq) was added dropwise to a stirred solution of aldehyde (1.0 eq) in DCM at 0 ^{o}C, followed by the dropwise addition of an aqueous solution of $NaClO_2$ (6.0 eq). The resulting suspension was vigorously stirred for 4 – 6 hours at room temperature. The aqueous layer was extracted with DCM (3 x 50 mL). The organic layers were combined and washed with brine, dried over anhydrous $MgSO_4$ and concentrated. Recrystallization from MeOH afforded the carboxylic acids.

4-Oxo-4H-chromene-3-carboxylic acid (SN11)

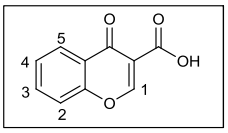

White solid (1.7 g, 78 %); M.p.: 147 – 150 °C; R_f (DCM) 0.25; δ_H (400 MHz, $CDCl_3$) 7.60 (1H, t, *J* 8.1 Hz, H_4), 7.65 (1H, d, *J* 8.1 Hz, H_2), 7.87 (1H, t, *J* 8.2 Hz, H_3), 8.34 (1H, d, *J*, 8.0 Hz, H_5), 9.01 (1H, s, H_1), 13.4 (1H, s, OH); δ_C (100 MHz, $CDCl_3$) 113.6, 119.1, 123.5, 126.6, 127.5, 136.2, 136.9, 157.1, 164.0, 179.6; EI - m/z 190.0 $[M]^+$.

6-Chloro-4-oxo-4H-chromene-3-carboxylic acid (SN29)

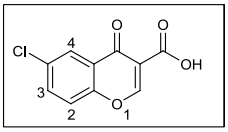

White solid (0.53 g, 77 %); M.p.: 212 – 215 °C; R_f (DCM) 0.29; IR ν_{max} (KBr) /cm^{-1} 1625, 1739 (2 x C=O), 3443 (O-H); δ_H (400 MHz, $CDCl_3$) 7.87 (1H, d, *J* 8.9 Hz, H_2), 7.79 (1H, dd, *J* 2.6, 8.9 Hz, H_3), 8.28 (1H, d, *J* 2.5 Hz, H_4), 8.99 (1H, s, H_1), 13.3 (1H, s, OH); δ_C (100 MHz, $CDCl_3$) 113.6, 120.8, 124.5, 125.9, 133.9, 136.5, 155.3, 163.7, 164.2, 178.6; EI - m/z 223.9 $[M]^+$; HPLC purity: 98 % (t_r = 9.30 min).

6-Bromo-4-oxo-4H-chromene-3-carboxylic acid (SN38)

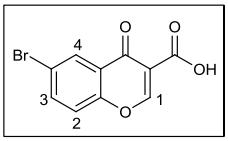

Pale yellow solid (0.46 g, 56 %); M.p.: 175 – 178 °C; R_f (DCM) 0.16; δ_H (400 MHz, $CDCl_3$) 7.55 (1H, d, *J* 8.9 Hz, H_2), 7.75 (1H, dd, *J* 2.4, 8.9 Hz, H_3), 8.46 (1H, d, *J* 2.4 Hz, H_4), 9.01 (1H, s, H_1), 13.1 (1H, s, OH); δ_C (100 MHz, $CDCl_3$) 113.6, 120.9, 121.3, 124.6, 129.1, 139.3, 155.7, 163.7, 164.3, 178.4; EI - m/z 267.9 $[M]^+$.

6-Fluoro-4-oxo-4H-chromene-3-carboxylic acid (SN40)

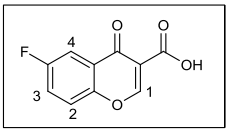

White solid (0.30 g, 85 %); M.p.: 222 – 224 °C; R_f (DCM) 0.24; δ_H (400 MHz, $CDCl_3$) 7.59 (1H, d, *J* 9.2 Hz, H_2), 7.69 (1H, dd, *J* 3.0, 9.2 Hz, H_3), 7.97 (1H, d, *J* 3.0 Hz, H_4), 9.02 (1H, s, H_1), 13.1 (1H, s, OH); δ_C (100 MHz, $CDCl_3$) 110.9, 111.2, 120.7, 120.8, 123.8, 124.1, 159.1, 161.6, 163.6, 178.3; EI - m/z 208.0 $[M]^+$.

6-Methoxy-4-oxo-4H-chromene-3-carboxylic acid (SN41)

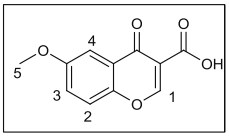

Pale-yellow solid (0.53 g, 81 %); M.p.: 155 – 157 °C; R_f (DCM) 0.25; δ_H (400 MHz, $CDCl_3$) 3.94 (3H, s, H_5), 7.44 (1H, d, *J* 9.2 Hz, H_2), 7.58 (1H, dd, *J* 3.1, 9.2 Hz, H_3), 7.63 (1H, d, *J* 3.1 Hz, H_4), 8.99 (1H, s, H_1), 13.5 (1H, s, OH); δ_C (100 MHz, $CDCl_3$) 55.6, 113.2, 121.3, 125.6, 125.9, 126.3, 149.8, 156.7, 163.5, 164.2, 178.6; EI - m/z 220.0 $[M]^+$.

6-Methyl-4-oxo-4H-chromene-3-carboxylic acid (SN42)

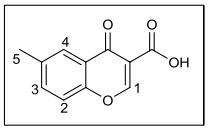

White solid (0.54 g, 77 %); M.p.: 225 – 228 °C; R_f (DCM) 0.25; δ_H (400 MHz, $CDCl_3$) 2.53 (3H, s, H_5), 7.46 (1H, d, *J* 8.6 Hz, H_2), 7.62 (1H, dd, *J* 1.9, 8.6 Hz, H_3), 8.11 (1H, d, *J* 2.0 Hz, H_4), 8.99 (1H, s, H_1), 13.5 (1H, s, OH); δ_C (100 MHz, $CDCl_3$) 21.4, 113.2, 118.8, 123.0, 125.8, 137.6, 138.1, 155.3, 163.9, 164.5, 179.7; EI - m/z 204.0 $[M]^+$.

6-(4-(Methylsulfonyl)phenyl)-4-oxo-4H-chromene-3-carboxylic acid (SN83-2)

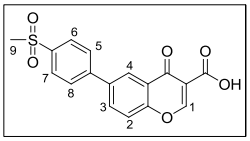

Yellow solid (0.14 g, 79 %); M.p.: 243 – 246 ^{o}C; R_f (DCM/MeOH 9:1) 0.45; δ_H (400 MHz, $CDCl_3$) 3.12 (3H, s, H_9), 7.79 (1H, d, *J* 8.8 Hz, H_2), 7.87 (2H, d, *J* 8.2 Hz, H_5, H_8), 8.07 – 8.10 (3H, m, H_3, H_6, H_7), 8.56 (1H, d, *J* 2.3 Hz, H_4), 9.06 (1H, s, H_1), 13.2 (1H, s, OH); δ_C (100 MHz, $CDCl_3$) 45.7, 110.5, 119.2, 123.4, 127.8 (2C), 129.5, 129.8, 131.4, 135.8, 136.2, 140.1, 145.6, 156.2, 164.1, 166.2, 177.6; LRMS (EI) m/z 344.0 $[M]^+$.

4-Oxo-6-(4-(trifluoromethyl)phenyl)-4H-chromene-3-carboxylic acid (SN84-2)

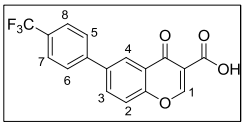

Pale-yellow solid (0.04 g, 46 %); R_f (DCM) 0.30; δ_H (400 MHz, $CDCl_3$) 7.58 (1H, d, *J* 8.6 Hz, H_2), 7.77 – 7.80 (4H, m, H_5 – H_8), 8.10 (1H, d, *J* 8.6 Hz, H_3), 8.53 (1H, s, H_4), 9.04 (1H, s, H_1), 13.2 (1H, s, OH); δ_C (100 MHz, $CDCl_3$) 113.2, 119.7, 123.3, 124.3, 126.1 (2C), 126.2, 127.7 (2C), 130.6, 134.8, 139.1, 141.8, 156.3, 163.8, 164.0, 179.2; EI - m/z 334.0 $[M]^+$.

4-Oxo-6-(6-(trifluoromethyl)pyridin-3-yl)-4H-chromene-3-carboxylic acid (SN85-2)

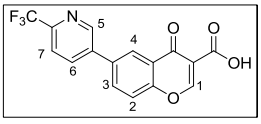

White solid (0.09 g, 56 %); R_f (DCM) 0.18; δ_H (400 MHz, $CDCl_3$) 7.84 (2H, m, H_2, H_7), 8.09 (1H, dd, *J* 2.2, 8.9 Hz, H_3), 8.16 (1H, dd, *J* 2.3, 8.2 Hz, H_6), 8.56 (1H, d, *J* 2.2 Hz, H_4), 9.02 (1H, d, *J* 2.3 Hz, H_5), 9.07 (1H, s, H_1), 13.1 (1H, s, OH); δ_C (100 MHz, $CDCl_3$) 118.8, 120.2, 120.7, 124.0, 125.9 (2C), 134.6, 135.1, 135.8, 136.0, 148.5 (2C), 156.7, 162.5, 164.0, 178.9; EI - m/z 334.9 $[M]^+$.

6-(4-Hydroxyphenyl)-4-oxo-4H-chromene-3-carboxylic acid (SN86-2)

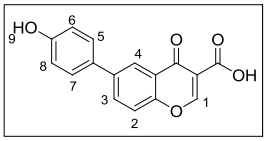

Yellow oil (0.03 g, 8 %), R_f (DCM/MeOH 98:2) 0.52; δ_H (400 MHz, $CDCl_3$) 5.21 (1H, br s, H_9), 6.91 (2H, d, *J* 8.9 Hz, H_6, H_8), 7.56 – 7.60 (3H, m, H_2, H_5, H_7), 8.17 (1H, dd, *J* 2.3, 8.7 Hz, H_3), 8.74 (1H, d, *J* 2.4 Hz, H_4), 9.01 (1H, s, H_1), 13.3 (1H, s, OH); δ_C (100 MHz, DMSO-d_6) 110.8, 116.9 (2C), 119.2, 124.6, 131.3 (2C), 132.4, 133.5, 135.5, 137.8, 155.8, 157.9, 166.8, 168.3, 179.5; EI - m/z 282.0 $[M]^+$.

4-Oxo-6-(thiophen-3-yl)-4H-chromene-3-carboxylic acid (SN87-2)

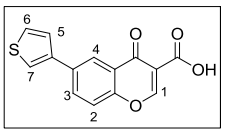

Pale-yellow solid (0.03 g, 78 %); R_f (DCM) 0.20; δ_H (400 MHz, $CDCl_3$) 7.41 (2H, m, H_2, H_5), 7.56 (1H, d, *J* 2.2 Hz, H_7), 7.62 (1H, d, *J* 8.8 Hz H_6), 8.03 (1H, dd, *J* 1.3, 8.7 Hz, H_3), 8.43 (1H, d, *J* 1.6 Hz, H_4), 8.95 (1H, s, H_1), 13.3 (1H, s, OH); δ_C (100 MHz, $CDCl_3$) 119.3, 122.2, 122.8, 123.4, 126.0, 127.4, 132.1, 132.4, 134.1, 137.1, 156.2, 163.7, 168.1, 177.5; EI - m/z 272 $[M]^+$.

6-(4-Chlorophenyl)-4-oxo-4H-chromene-3-carboxylic acid (SN90-2)

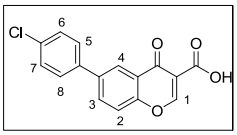

Yellow solid (0.47 g, 34 %); M.p.: 153 – 156 ^{o}C; R_f (DCM) 0.30; δ_H (400 MHz, $CDCl_3$) 7.39 (2H, d, *J* 7.9 Hz, H_5, H_8), 7.50 (2H, d, *J* 7.9 Hz, H_6, H_7), 7.65 (1H, d, *J* 8.7 Hz, H_2), 7.97 (1H, dd, *J* 1.5, 8.7 Hz, H_3), 8.38 (1H, d, *J* 1.6 Hz, H_4), 8.95 (1H, s, H_1), 13.0 (1H, s, OH); δ_C (100 MHz, $CDCl_3$) 113.1, 119.4, 123.2, 123.8, 128.4, 128.5 (2C), 129.4 (2C), 134.6, 134.9, 136.7, 139.4, 156.0, 163.8, 179.3; EI - m/z 298.9 $[M]^+$.

4-Oxo-6-(3-phenoxyphenyl)-4H-chromene-3-carboxylic acid (SN91-2)

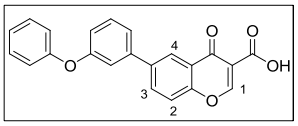

Yellow solid (0.13 g, 65 %); M.p.: 38 – 40 ^{o}C; R_f (DCM) 0.28; δ_H (400 MHz, $CDCl_3$) 7.03 – 7.05 (3H, m, Ar H), 7.36 – 7.45 (6H, m, Ar H), 7.68 (1H, d, *J* 8.8 Hz, H_2), 8.02 (1H, dd, *J* 2.1, 8.8 Hz, H_3), 8.45 (1H, d, *J* 2.1 Hz, H_4), 9.00 (1H, s, H_1), 13.3 (1H, s, OH); δ_C (100 MHz, $CDCl_3$) 113.9, 117.6, 118.7, 119.1 (2C), 120.3, 122.01, 123.2, 123.8, 124.0, 129.9 (2C), 130.6, 134.8, 139.9, 140.2, 156.1, 156.8, 158.2, 163.8, 164.0, 179.3; LRMS (EI) m/z 358.0 $[M]^+$.

6-(2-Methoxyphenyl)-4-oxo-4H-chromene-3-carboxylic acid (SN92-2)

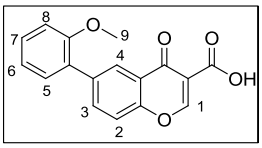

Pale-yellow solid (0.24 g, 92 %); R_f (DCM) 0.35; δ_H (400 MHz, $CDCl_3$) 3.83 (3H, s, H_9), 7.07 (2H, m, H_6, H_8), 7.38 (2H, m, H_5, H_7), 7.66 (1H, d, *J* 8.8 Hz, H_2), 8.06 (1H, dd, *J* 2.2, 8.8 Hz, H_3), 8.44 (1H, d, *J* 2.2 Hz, H_4), 9.02 (1H, s, H_1), 13.1 (1H, s, OH); δ_C (100 MHz, $CDCl_3$) 55.6, 111.4, 118.1, 121.2, 122.7, 126.3, 129.6, 130.1, 130.8, 135.2, 137.2, 137.7, 138.3, 155.6, 156.4, 163.7, 179.5; EI - m/z 296.0 $[M]^+$.

5-(4-(Methylsulfonyl)phenyl)-4-oxo-4H-chromene-3-carboxylic acid (SN93-2)

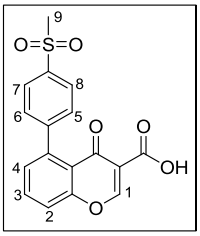

Yellow solid (0.15 g, 64 %); M.p.: 254 – 256 ^{o}C; R_f (DCM) 0.57; δ_H (400 MHz, $CDCl_3$) 3.16 (3H, s, H_9), 7.35 (1H, d, *J* 7.4 Hz, H_2), 7.49 (2H, d, *J* 8.6 Hz, H_5, H_6), 7.73 (1H, d, *J* 8.5 Hz, H_4), 7.73 (1H, t, *J* 7.8 Hz, H_3), 8.01 (2H, d, *J* 8.6 Hz, H_7, H_8), 9.02 (1H, s, H_1), 13.0 (1H, s, OH); δ_C (100 MHz, $CDCl_3$) 43.6, 112.7, 118.4, 119.3, 125.9 (2C), 128.5 (2C), 129.1, 134.0, 138.9, 140.9, 144.7, 156.7, 162.2, 162.7, 178.4; EI - m/z 344.0 $[M]^+$.

7-(4-(Methylsulfonyl)phenyl)-4-oxo-4H-chromene-3-carboxylic acid (SN94-2)

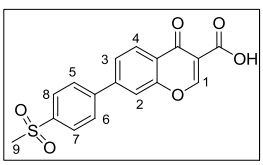

Yellow solid (0.06 g, 37 %); M.p.: 256 – 258 ^{o}C; R_f (DCM) 0.15; δ_H (400 MHz, $CDCl_3$) 3.07 (3H, s, H_9), 7.78 – 7.81 (3H, m, H_3, H_5, H_6), 8.05 (3H, m, H_2, H_7, H_8), 8.41 (1H, d, *J* 8.2 Hz, H_4), 9.00 (1H, s, H_1), 12.7 (1H, s, OH); δ_C (100 MHz, DMSO-d_6) 48.8, 120.1, 122.4, 128.3, 130.9, 131.6, 132.9 (2C), 133.7 (2C), 146.5, 147.7, 150.4, 161.5, 168.8, 180.9, 204.3; EI - m/z 343.9 $[M]^+$.

8-(4-(Methylsulfonyl)phenyl)-4-oxo-4H-chromene-3-carboxylic acid (SN95-2)

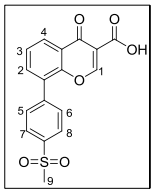

Orange solid (0.098 g, 38 %); M.p.: 162 – 165 ^{o}C; R_f (DCM) 0.34; δ_H (400 MHz, $CDCl_3$) 3.08 (3H, s, H_9); 7.52 (1H, t, *J* 7.8 Hz, H_3), 7.64 – 7.67 (3H, m, H_2, H_5, H_6), 8.03 (2H, m, H_7, H_8), 8.36 (1H, d, *J* 8.0 Hz, H_4), 8.90 (H, s, H_1), 13.0 (1H, s, OH); δ_C (100 MHz, $CDCl_3$) 44.5, 119.1, 123.7, 125.9, 126.8, 127.3, 127.9 (2C), 130.5 (2C), 136.8, 137.4, 145.0, 147.1, 163.5, 175.5, 204.6; EI - m/z 344.1 $[M]^+$.

5.2.4. General Synthetic Procedure of Chromone-2-carboxylic acid Derivatives[4]

A solution of diethyl oxalate (1.1 eq) and the selected hydroxyacetophenone (1.0 eq) was added dropwise under N_2 to a stirred ethanolic solution of NaOEt (generated *in situ* by adding Na metal (3.2 g, 0.1 mol) to absolute EtOH (18 mL)). The yellow reaction mixture was refluxed at 95 ^{o}C for 2 hours. After cooling, the mixture was added to Et_2O (100 mL) and left to stand overnight. The solid was filtered, washed with Et_2O (50 mL), acidified with 2M HCl (100 mL), and the resulting yellow mixture was extracted with Et_2O (3 x 100 mL). The combined organic layers were dried over anhydrous Na_2SO_4 and concentrated *in vacuo* to give a yellow residue. Glacial acetic acid (20 mL) and conc. HCl (20 mL) were added to the residue and refluxed at 95 ^{o}C for 2 hours. After cooling, the resulting precipitate was filtered and washed with acetic acid. Recrystallization from acetic acid afforded the carboxylic acids.

4-Oxo-4H-chromene-2-carboxylic acid (SN68)

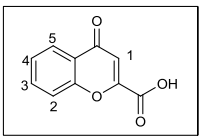

White solid (7.6 g, 72 %); M.p.: 252 – 255 ^{o}C; R_f (EtOAc) 0.51; δ_H (300 MHz, DMSO-d_6)* 6.87 (1H, s, H_1), 7.49 (1H, t, *J* 8.1 Hz, H_4), 7.68 (1H, d, *J* 8.2 Hz, H_2), 7.83 (1H, t, *J* 8.1 Hz, H_3); 8.01 (1H, d, *J* 8.0 Hz, H_5); δ_C (100 MHz, DMSO-d_6) 113.7, 119.0, 123.9, 125.0, 126.2, 135.3, 153.4, 155.6, 161.7, 177.7; EI - m/z 190.0 $[M]^+$.

6-Chloro-4-oxo-4H-chromene-2-carboxylic acid (SN69)

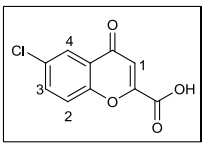

Pale grey solid (0.79 g, 60 %); M.p.: 242 – 245 ^{o}C; R_f (EtOAc) 0.56; IR ν_{max} (KBr) /cm^{-1} 1634, 1735 (2 x C=O), 3425 (O-H); δ_H (300 MHz, DMSO-d_6)* 6.93 (1H, s, H_1), 7.79 (1H, d, *J* 9.1 Hz, H_2), 7.90 (1H, dd, *J* 2.7, 9.0 Hz, H_3), 7.98 (1H, d, *J* 2.8 Hz, H_4); δ_C (100 MHz, DMSO-d_6) 113.7, 121.8, 124.3, 125.2, 130.9, 135.4, 153.9, 154.4, 161.5, 176.9; EI - m/z 223.9 $[M]^+$; HPLC purity: 97 % (t_r = 8.02 min).

* The carboxylic acid proton was not observed, presumably due to the rapid exchange with water present in the deuterated solvent, DMSO-d_6.

6-Bromo-4-oxo-4H-chromene-2-carboxylic acid (SN70)

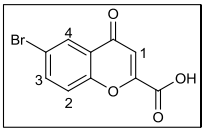

Grey solid (1.12 g, 87 %); M.p.: 263 – 265 °C; R_f (EtOAc) 0.52; δ_H (300 MHz, DMSO-d_6)* 6.94 (1H, s, H_1), 7.72 (1H, d, *J* 8.9 Hz, H_2), 8.01 (1H, dd, *J* 2.5, 8.9 Hz, H_3), 8.12 (1H, d, *J* 2.5 Hz, H_4); δ_C (100 MHz, DMSO-d_6) 113.6, 118.6, 121.7, 125.4, 127.2, 137.9, 153.8, 154.6, 161.3, 176.6; EI - m/z 267.7 $[M]^+$.

6-Fluoro-4-oxo-4H-chromene-2-carboxylic acid (SN71)

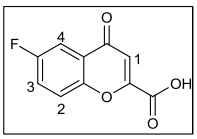

Grey solid (0.37 g, 28 %); M.p.: 243 – 245 °C; R_f (EtOAc) 0.42; δ_H (300 MHz, DMSO-d_6)* 6.92 (1H, s, H_1), 7.74 – 7.79 (3H, m, H_2, H_3, H_4); δ_C (100 MHz, DMSO-d_6) 110.1, 122.3, 123.9, 125.5, 152.4, 154.0, 158.6, 160.9, 161.8, 177.5; EI - m/z 207.8 $[M]^+$.

6-Methoxy-4-oxo-4H-chromene-2-carboxylic acid (SN72)

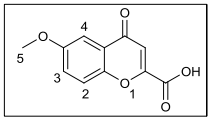

Off-white solid (0.80 g, 62 %); M.p.: 279 – 281 °C; R_f (EtOAc) 0.56; δ_H (300 MHz, DMSO-d_6)* 3.88 (3H, s, H_5), 6.89 (1H, s, H_1), 7.42 (1H, d, *J* 9.2 Hz, H_2), 7.47 (1H, dd, *J* 3.2, 9.2 Hz, H_3), 7.70 (1H, d, *J* 3.1 Hz, H_4); δ_C (100 MHz, DMSO-d_6) 55.9, 104.8, 112.7, 120.6, 124.5, 124.7, 150.3, 153.1, 157.1, 161.6, 177.4; EI - m/z 219.9 $[M]^+$.

5.2.5 Synthesis of Chromone Esters[2]

5.2.5.1 General Synthetic Procedure for Chromone-methyl Esters

Oxalyl chloride (2.5 eq) was added dropwise to a stirred solution of **SN38** (1.0 eq) in dry DCM (20 mL) under N_2. After 90 minutes, the reaction temperature was lowered to 0 °C, followed by the dropwise addition of anhydrous MeOH (3.5 mL). The reaction mixture was warmed to room temperature and stirred overnight. The solvent was removed *in vacuo* and recrystallization from EtOH afforded the product.

Methyl 4-oxo-4H-chromene-3-carboxylate (SN64)

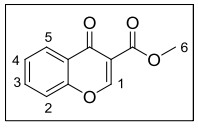

White solid (0.05 g, 10 %); M.p.: 74 – 79 °C; R_f (DCM/MeOH 95:5) 0.81; δ_H (300 MHz, $CDCl_3$) 3.93 (3H, s, H_6), 7.48 (2H, m, H_2, H_4), 7.70 (1H, t, *J* 8.6 Hz, H_3), 8.28 (1H, d, *J* 7.9 Hz, H_5), 8.68 (1H, s, H_1); δ_C (100 MHz, $CDCl_3$) 52.4, 116.2, 118.2, 125.2, 126.3, 126.7, 134.2, 138.9, 155.6, 162.0, 173.4; EI - m/z 203.9 $[M]^+$.

* The carboxylic acid proton was not observed, presumably due to the rapid exchange with water present in the deuterated solvent, DMSO-d_6.

Methyl 6-bromo-4-oxo-4H-chromene-3-carboxylate (SN65)

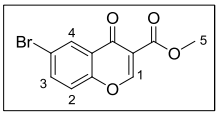

White solid (0.30 g, 48 %); M.p.: 109 – 111 °C; R_f (DCM/MeOH 95:5) 0.60; δ_H (300 MHz, $CDCl_3$) 3.93 (3H, s, H_5), 7.40 (1H, d, *J* 8.9 Hz, H_2), 7.79 (1H, dd, *J* 2.5, 8.9 Hz, H_3), 8.40 (1H, d, *J* 2.4 Hz, H_4), 8.67 (1H, s, H_1); δ_C (100 MHz, $CDCl_3$) 52.5, 116.3, 120.1, 126.5, 129.2, 134.5, 137.3, 154.5, 162.1, 163.6, 172.1; EI - m/z 281.8 $[M]^+$.

5.2.5.2 General Synthetic Procedure for Chromone-ethyl Esters

Thionyl chloride (1.5 eq) was added dropwise to a solution of the desired carboxylic acid in absolute ethanol at 0 °C. The reaction mixture was stirred at 0 °C for 30 minutes, then warmed to 40 °C for 18 hours. A saturated solution of Na_2CO_3 was added and the aqueous mixture was extracted with EtOAc (3 x 30 mL). The combined organic layers were washed with a saturated solution of Na_2CO_3, dried over Na_2SO_4 and the solvent removed to afford the products.

Ethyl 6-bromo-4-oxo-4H-chromene-3-carboxylate (SN38-3)

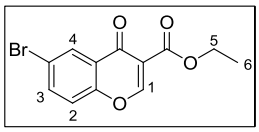

Yellow solid (0.06 g, 38 %); M.p.: 85 – 89 °C; R_f (Hex/EtOAc 5:5) 0.58; δ_H (400 MHz, $CDCl_3$) 1.40 (3H, t, *J* 7.1 Hz, H_6), 4.40 (2H, q, *J* 7.1 Hz, H_5), 7.39 (1H, d, *J* 8.8 Hz, H_2), 7.79 (1H, dd, *J* 2.3, 8.9 Hz, H_3), 8.40 (1H, d, *J* 2.3 Hz, H_4), 8.65 (1H, s, H_1); δ_C (100 MHz, $CDCl_3$) 14.2, 61.6, 116.6, 119.9, 120.1, 126.5, 129.2, 137.2, 154.5, 161.7, 162.9, 172.1; EI - m/z 295.8 $[M]^+$; HPLC purity: 97 % (t_r = 5.32 min).

Ethyl 6-bromo-4-oxo-4H-chromene-2-carboxylate (SN70-3)

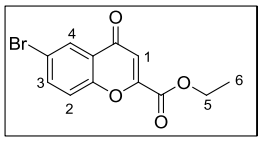

Grey solid (0.11 g, 66 %); M.p.: 132 – 134 °C; R_f (Hex/EtOAc 5:5) 0.80; δ_H (400 MHz, $CDCl_3$) 1.43 (3H, t, *J* 7.1 Hz, H_6), 4.46 (2H, q, *J* 7.1 Hz, H_5), 7.11 (1H, s, H_1), 7.50 (1H, d, *J* 8.8 Hz, H_2), 7.81 (1H, dd, *J* 2.5, 8.9 Hz, H_3), 8.31 (1H, d, *J* 2.5 Hz, H_4); δ_C (100 MHz, $CDCl_3$) 14.1, 63.1, 114.7, 119.5, 120.7, 125.7, 128.4, 137.7, 152.5, 154.8, 160.2, 177.0; EI - m/z 295.9 $[M]^+$; HPLC purity: 99 % (t_r = 5.26 min).

Ethyl 6-(4-(methylsulfonyl)phenyl)-4-oxo-4H-chromene-3-carboxylate (SN83-3)

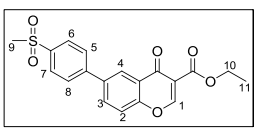

Yellow solid (0.058 g, 49 %); M.p.: 158 – 162 °C; R_f (EtOAc) 0.53; δ_H (400 MHz, $CDCl_3$) 1.34 (3H, t, *J* 7.1 Hz, H_{11}), 3.03 (3H, s, H_9), 4.34 (2H, q, *J* 7.1 Hz, H_{10}), 7.55 (1H, d, *J* 8.7 Hz, H_2), 7.76 (2H, d, *J* 8.3 Hz, H_5, H_8), 7.87 (1H, dd, *J* 2.3, 8.7 Hz, H_3), 7.98 (2H, d, *J* 8.3 Hz, H_6, H_7), 8.44 (1H, d, *J* 2.3 Hz, H_4), 8.62 (1H, s, H_1); δ_C (100 MHz, $CDCl_3$) 14.2, 44.6, 61.5, 116.7, 119.2, 125.2, 128.1 (2C), 128.2 (2C), 132.9, 137.4, 140.2, 144.4, 155.7, 161.7, 163.1, 165.9, 173.2 EI - m/z 371.8 $[M]^+$; HPLC purity: 97 % (t_r = 4.54 min).

Ethyl 4-oxo-6-(4-(trifluoromethyl)phenyl)-4H-chromene-3-carboxylate (SN84-3)

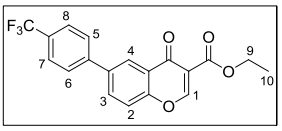

Brown solid (0.037 g, 83 %); M.p.: 109 – 111 °C; R_f (Hex/EtOAc 8:2) 0.65; δ_H (400 MHz, $CDCl_3$) 1.42 (3H, t, *J* 7.1 Hz, H_{10}), 4.41 (2H, q, *J* 7.1 Hz, H_9), 7.61 (1H, d, *J* 8.7 Hz, H_2), 7.75 (4H, s, H_5 – H_8), 7.94 (1H, dd, *J* 2.4, 8.7 Hz, H_3), 8.51 (1H, d, *J* 2.3 Hz, H_4), 8.69 (1H, s, H_1); δ_C (100 MHz, $CDCl_3$) 14.3, 61.5, 116.7, 119.0, 124.9 (2C), 125.5, 126.0, 127.5 (2C), 129.9, 132.9, 137.9, 136.4, 145.1, 156.4, 161.7, 163.9, 179.6 EI - m/z 362.1 $[M]^+$; HPLC purity: 99 % (t_r = 5.68 min).

Ethyl 4-oxo-6-(6-(trifluoromethyl)pyridin-3-yl)-4H-chromene-3-carboxylate (SN85-3)

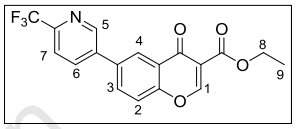

Yellow solid (0.017 g, 24 %); M.p.: 141 – 143 °C; R_f (Hex/EtOAc 8:2) 0.57; δ_H (400 MHz, $CDCl_3$) 1.43 (3H, t, *J* 7.1 Hz, H_9), 4.42 (2H, q, *J* 7.1 Hz, H_8), 7.67 (1H, d, *J* 8.7 Hz, H_2), 7.77 (1H, d, *J* 8.6 Hz, H_7), 7.86 (1H, dd, *J* 2.4, 8.6 Hz, H_6), 7.95 (1H, dd, *J* 2.4, 8.7 Hz, H_3), 8.53 (1H, d, *J* 2.3 Hz, H_4), 8.71 (1H, s, H_1), 8.93 (1H, d, *J* 2.4 Hz, H_5); δ_C (100 MHz, $CDCl_3$) 14.3, 61.2, 116.8, 117.9, 119.6, 120.7, 122.0, 125.4, 126.3, 131.1, 132.8, 135.2, 135.8, 148.4, 155.9, 161.8, 163.0, 177.6; EI - m/z 363.0 $[M]^+$; HPLC purity: 97 % (t_r = 4.79 min).

Ethyl 4-oxo-6-(thiophen-3-yl)-4H-chromene-3-carboxylate (SN87-3)

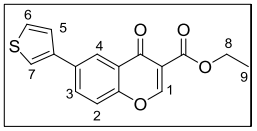

Red solid (0.019 g, 85 %); M.p.: 54 – 56 °C; R_f (Hex/EtOAc 7:3) 0.68; δ_H (400 MHz, $CDCl_3$) 1.39 (3H, t, *J* 7.1 Hz, H_9), 4.39 (2H, q, *J* 7.1 Hz, H_8), 7.43 (2H, m, H_2, H_5), 7.50 (1H, d, *J* 8.7 Hz, H_6), 7.55 (1H, d, *J* 2.3 Hz, H_7), 7.91 (1H, dd, *J* 2.3, 8.7 Hz, H_3), 8.45 (1H, d, *J* 2.3 Hz, H_4), 8.64 (1H, s, H_1); δ_C (100 MHz, $CDCl_3$) 14.3, 61.4, 115.2, 118.7, 120.7, 121.7, 123.5, 123.7, 124.1, 124.9, 126.2, 126.9, 132.3, 161.6, 165.8, 174.1; LRMS (EI) m/z 300.0 $[M]^+$; HPLC purity: 98 % (t_r = 5.33 min).

Ethyl 6-(4-chlorophenyl)-4-oxo-4H-chromene-3-carboxylate (SN90-3)

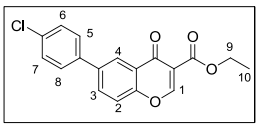

Brown solid (0.17 g, 78 %); M.p.: 128 – 131 °C; R_f (Hex/EtOAc 8:2) 0.48; δ_H (400 MHz, $CDCl_3$) 1.40 (3H, t, *J* 7.1 Hz, H_{10}), 4.40 (2H, q, *J* 7.1 Hz, H_9), 7.43 – 7.45 (4H, m, H_5 – H_8), 7.56 (1H, d, *J* 8.5 Hz, H_2), 7.88 (1H, dd, *J* 2.3, 8.6 Hz, H_3), 8.44 (1H, d, *J* 2.3 Hz, H_4), 8.67 (1H, s, H_1); δ_C (100 MHz, $CDCl_3$) 14.3, 61.5, 116.6, 118.8, 124.4, 125.5, 128.5 (2C), 129.3 (2C), 132.7, 134.4, 137.5, 138.3, 155.2, 161.7, 163.3, 173.4; EI - m/z 328.0 $[M]^+$; HPLC purity: 98 % (t_r = 7.97 min).

Ethyl 4-oxo-6-(3-phenoxyphenyl)-4H-chromene-3-carboxylate (SN91-3)

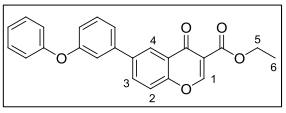

Brown crystalline solid (0.062 g, 48 %); M.p.: 31 – 34 ^{o}C; R_f (Hex/EtOAc 6:4) 0.50; δ_H (400 MHz, $CDCl_3$) 1.41 (3H, t, *J* 7.1 Hz, H_6), 4.41 (2H, q, *J* 7.1 Hz, H_5), 7.08 (3H, m, Ar H), 7.32 – 7.39 (6H, m, Ar H), 7.55 (1H, d, *J* 8.7 Hz, H_2), 7.89 (1H, dd, *J* 2.3, 8.7 Hz, H_3), 8.45 (1H, d, *J* 2.3 Hz, H_4), 8.67 (1H, s, H_1); δ_C (100 MHz, $CDCl_3$) 14.3, 61.5, 117.5, 118.3, 118.7, 119.1 (2C), 122.1, 122.9, 123.6, 124.5, 127.2, 127.6, 129.8 (2C), 130.4, 132.9, 137.2, 138.8, 139.0, 158.1, 161.6, 163.3, 172.7; EI - m/z 385.9 $[M]^+$; HPLC purity: 96 % (t_r = 8.81 min).

Ethyl 6-(2-methoxyphenyl)-4-oxo-4H-chromene-3-carboxylate (SN92-3)

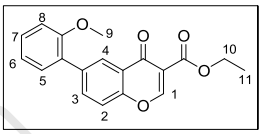

Brown solid (0.114 g, 69 %); M.p.: 42 – 45 ^{o}C; R_f (Hex/EtOAc 5:5) 0.55; δ_H (400 MHz, $CDCl_3$) 1.41 (3H, t, *J* 7.1 Hz, H_{11}), 3.81 (3H, s, H_9), 4.41 (2H, q, *J* 7.1 Hz, H_{10}), 7.03 (2H, m, H_6, H_8), 7.35 (2H, m, H_5, H_7), 7.50 (1H, d, *J* 8.7 Hz, H_2), 7.90 (1H, dd, *J* 2.2, 8.7 Hz, H_3), 8.41 (1H, d, *J* 2.2 Hz, H_4), 8.67 (1H, s, H_1); δ_C (100 MHz, $CDCl_3$) 14.3, 55.6, 61.4, 111.4, 117.6, 117.8, 121.1, 124.9, 126.9, 127.1, 129.5, 130.9, 135.5, 135.8, 154.7, 156.5, 161.6, 162.8, 173.5; EI - m/z 323.9 $[M]^+$; HPLC purity: 99 % (t_r = 5.28 min).

Ethyl 5-(4-(methylsulfonyl)phenyl)-4-oxo-4H-chromene-3-carboxylate (SN93-3)

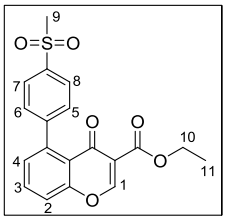

Brown solid (0.09 g, 83 %); M.p.: 157 – 160 ^{o}C; R_f (Hex/EtOAc 3:7) 0.25; δ_H (400 MHz, $CDCl_3$) 1.29 (3H, t, *J* 7.1 Hz, H_{11}), 3.09 (3H, s, H_9), 4.28 (2H, q, *J* 7.1 Hz, H_{10}), 7.15 (1H, d, *J* 7.4 Hz, H_2), 7.41 (2H, d, *J* 8.6 Hz, H_5, H_6), 7.53 (1H, d, *J* 8.5 Hz, H_4), 7.67 (1H, t, *J* 7.8 Hz, H_3), 7.90 (2H, d, *J* 8.6 Hz, H_7, H_8), 8.57 (1H, s, H_1); δ_C (100 MHz, $CDCl_3$) 13.9, 44.4, 61.1, 116.9, 118.6, 122.1, 126.4 (2C), 128.9, 129.2 (2C), 132.9, 138.8, 141.4, 146.6, 156.4, 160.2, 162.3, 172.9; EI - m/z 372.0 $[M]^+$; HPLC purity: 96 % (t_r = 5.26 min).

Ethyl 7-(4-(methylsulfonyl)phenyl)-4-oxo-4H-chromene-3-carboxylate (SN94-3)

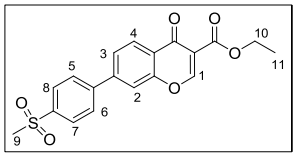

Brown solid (0.09 g; 27 %); M.p.: 179 – 182 ^{o}C; R_f (Hex/EtOAc 4:6) 0.44; δ_H (400 MHz, $CDCl_3$) 1.35 (3H, t, *J* 7.1 Hz, H_{11}), 3.04 (3H, s, H_9), 4.35 (2H, q, *J* 7.1 Hz, H_{10}), 7.63 (2H, m, H_2, H_3), 7.77 (2H, d, *J* 8.1 Hz, H_5, H_6), 8.02 (2H, d, *J* 8.1 Hz, H_7, H_8), 8.32 (1H, d, *J* 8.3 Hz, H_4), 8.63 (1H, s, H_1); δ_C (100 MHz, $CDCl_3$) 14.3, 44.7, 61.4, 117.2, 118.9, 122.4, 126.7 (2C), 129.3, 129.5 (2C), 133.2, 139.1, 141.9, 146.9, 156.7, 160.5, 162.7, 173.2; EI - m/z 372.0 $[M]^+$; HPLC purity: 97 % (t_r = 4.70 min).

Ethyl 8-(4-(methylsulfonyl)phenyl)-4-oxo-4H-chromene-3-carboxylate (SN95-3)

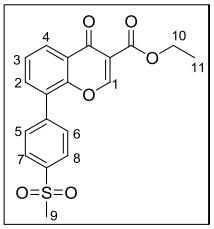

Brown solid (0.01 g, 35 %); M.p.: 158 – 161 °C; R_f (Hex/EtOAc 2:8) 0.51; δ_H (400 MHz, $CDCl_3$) 1.36 (3H, t, *J* 7.1 Hz, H_{11}), 3.09 (3H, s, H_9), 4.35 (2H, q, *J* 7.1 Hz, H_{10}), 7.53 (1H, t, *J* 7.8 Hz, H_3), 7.70 (3H, m, H_2, H_5, H_6), 8.04 (2H, m, H_7, H_8), 8.33 (1H, d, *J* 7.9 Hz, H_4), 8.59 (1H, s, H_1); δ_C (100 MHz, $CDCl_3$) 14.2, 44.5, 61.5, 119.1, 123.7, 124.0, 125.8, 126.3, 127.3, 127.7 (2C), 130.5 (2C), 133.4, 135.1, 140.9, 161.4, 170.6; EI - m/z 372.1 $[M]^+$; HPLC purity: 95 % (t_r = 7.51 min).

5.3 Synthesis of 4-Aminoquinoline Derivative[5]

N^1-(7-Chloroquinolin-4-yl)ethane-1,2-diamine (SN08)

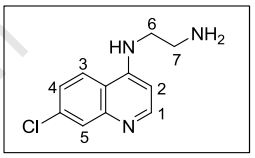

4,7-Dichloroquinoline (2.0 g, 0.01 mol) and ethylene diamine (3.6 g, 0.06 mol, 3.3 mL) were refluxed at 100 °C for 1 hour, and then at 140 °C for a further 4 hours. The dark orange mixture was cooled to room temperature, 1M NaOH (25 mL) was added, and extracted with ethyl acetate (3 x 50 mL). The organic layers were collected, washed with distilled water (2 x 50 mL) and dried over anhydrous $MgSO_4$. The solvent was removed under reduced pressure to yield a pale-yellow solid (1.90 g, 85 %).

M.p.: 128 - 131 °C; R_f (MeOH) 0.15; IR ν_{max} (KBr) /cm^{-1} 1578 (C=N), 3254 (2 x N-H); δ_H (300 MHz, CD_3OD) 2.98 (2H, t, *J* 6.3 Hz, H_7), 3.44 (2H, t, *J* 6.4 Hz, H_6), 6.56 (1H, d, *J* 5.7 Hz, H_2), 7.40 (1H, dd, *J* 2.2, 9.0 Hz, H_4), 7.78 (1H, d, *J* 2.2 Hz, H_5), 8.11 (1H, d, *J* 9.0 Hz, H_3), 8.36 (1H, d, *J* 5.6 Hz, H_1); δ_C (75 MHz, CD_3OD) 40.8, 46.1, 99.7, 118.8, 124.3, 126.1, 127.6, 136.7, 149.7, 152.4, 152.8; EI - m/z 221.6 $[M]^+$; HPLC purity 99 % (t_r = 12.5 min).

5.4. Synthesis of Hybrid Derivatives

5.4.1 General Synthetic procedure of Covalently-linked Hybrids (Series 1)[6]

4-Aminoquinoline (1.0 eq) and aldehyde (1.0 eq) were dissolved in dry DCM (25 mL) and dry MeOH (2.5 mL) under N_2 at room temperature. After 2 hours, $NaBH(OAc)_3$ (3.0 eq) was added and the reaction mixture was stirred overnight. The reaction mixture was added to 2M NaOH (50 mL), and extracted with DCM:MeOH (4:1) (3 x 50 mL). The combined organic layers were dried over anhydrous Na_2SO_4, and concentrated. The residue was purified by flash chromatography on silica gel using DCM:MeOH (9:1) as the eluent to afford the product.

3-((2-(7-Chloroquinolin-4-ylamino)ethylamine)methyl)-4H-chromen-4-one (SN31)

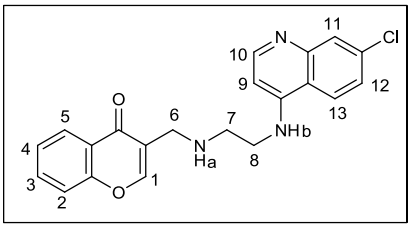

Orange solid (0.26 g, 50 %); M.p.: 81 – 83 ^{o}C ; R_f (MeOH) 0.50; IR ν_{max} (KBr) /cm^{-1} 1581 (C=N), 1653 (C=O), 3413 (strong, 2 x N-H); δ_H (400 MHz, DMSO-d_6) 3.18 (2H, s, H_6), 3.50 (2H, q, *J* 5.5 Hz, H_7), 3.61 (2H, q, *J* 5.8 Hz, H_8), 5.59 (1H, s, H_1), 6.63 (1H, d, *J* 5.5 Hz, H_9), 7.03 (1H, d, *J* 7.2 Hz, H_2), 7.07 (1H, t, *J* 7.5 Hz, H_4), 7.44 (1H, m, NH_a), 7.47 (1H, dd, *J* 2.0, 8.9 Hz, H_{12}), 7.51 (1H, t, *J* 7.3 Hz, H_3), 7.76 (1H, d, *J* 7.6 Hz, H_5), 7.81 (1H, d, *J* 2.2 Hz, H_{11}), 8.29 (1H, d, *J* 9.1 Hz, H_{13}), 8.42 (1H, d, *J* 5.4 Hz, H_{10}), 10.21 (1H, m, NH_b); δ_C (100 MHz, DMSO-d_6) 44.1, 47.9, 52.5, 100.5, 116.8, 117.4, 118.2, 121.6, 123.8, 124.9, 125.2, 127.8, 128.6, 133.5, 134.2, 149.7, 150.7, 152.2, 153.0, 155.7, 178.8; EI - m/z 379.0 $[M]^+$; HPLC purity: 97 % (t_r = 6.36 min).

6-Chloro-3-((2-(7-chloroquinolin-4-ylamino)ethylamino)methyl)-4H-chromen-4-one (SN24)

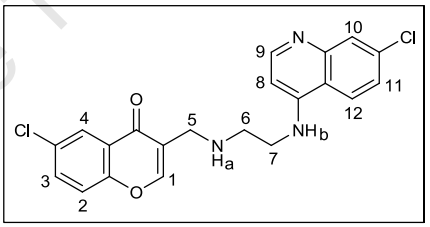

Pink solid (0.37 g, 65 %); M.p.: 96 – 100 ^{o}C; R_f (MeOH) 0.48; IR ν_{max} (KBr) /cm^{-1} 1576 (C=N), 1653 (C=O), 3375 (strong, 2 x N-H); δ_H (400 MHz, DMSO-d_6) 3.20 (2H, s, H_5), 3.47 (2H, q, *J* 5.7 Hz, H_6), 3.58 (2H, q, *J* 5.8 Hz, H_7), 5.58 (1H, s, H_1), 6.57 (1H, d, *J* 5.5 Hz, H_8), 7.02 (1H, d, *J* 8.6 Hz, H_2), 7.40 (1H, m, NH_a), 7.43 (1H, dd, *J* 2.1, 8.9 Hz, H_{11}), 7.46 (1H, dd, *J* 2.4, 8.6 Hz, H_3), 7.64 (1H, d, *J* 2.6 Hz, H_4), 7.79 (1H, d, *J* 2.2 Hz, H_{10}), 8.25 (1H, d, *J* 9.1 Hz, H_{12}), 8.39 (1H, d, *J* 5.4 Hz, H_9), 10.19 (1H, m, NH_b); δ_C (100 MHz, DMSO-d_6) 43.3, 47.0, 54.5, 99.0, 117.4, 120.2, 123.9, 124.6, 124.9, 125.4, 126.2, 127.9, 132.7, 133.4, 149.9, 150.5, 151.8, 153.6, 154.1, 155.5, 176.3; EI - m/z 412.8 $[M]^+$; HPLC purity: 98 % (t_r = 7.96 min).

6-Bromo-3-((2-(7-chloroquinolin-4-ylamino)ethylamino)methyl)-4H-chromen-4-one (SN25)

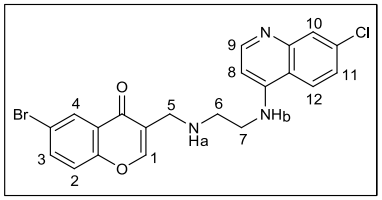

Off-white solid (0.47 g, 75 %); M.p.: 122 – 125 ^{o}C; R_f (MeOH) 0.53; IR ν_{max} (KBr) /cm^{-1} 1580 (C=N), 1656 (C=O), 3224 (strong, 2 x N-H); δ_H (400 MHz, DMSO-d_6) 3.18 (2H, s, H_5), 3.52 (2H, q, *J* 5.7 Hz, H_6), 3.62 (2H, q, *J* 5.9 Hz, H_7), 5.62 (1H, s, H_1), 6.61 (1H, d, *J* 5.5 Hz, H_8), 7.02 (1H, d, *J* 8.7 Hz, H_2), 7.37 (1H, m, NH_a), 7.48 (1H, dd, *J* 2.2, 8.9 Hz, H_{11}), 7.59 (1H, dd, *J* 2.6, 8.6 Hz, H_3), 7.79 (1H, d, *J* 2.2 Hz, H_{10}), 7.81 (1H, d, *J* 2.6 Hz, H_4), 8.27 (1H, d, *J* 9.1 Hz, H_{12}), 8.42 (1H, d, *J* 5.4 Hz, H_9), 10.2 (1H, m, NH_b); δ_C (100 MHz, DMSO-d_6) 43.3, 47.0, 54.6, 102.2, 117.9, 120.7, 122.0, 124.5, 124.7, 125.4, 127.9, 134.0, 136.1, 138.2, 149.4, 150.3, 152.2, 154.5, 155.5, 164.2, 176.8; EI - m/z 458.5 $[M]^+$; HPLC purity: 98 % (t_r = 6.87 min).

3-((2-(7-Chloroquinolin-4-ylamino)ethylamino)methyl)-6-fluoro-4H-chromen-4-one (SN26)

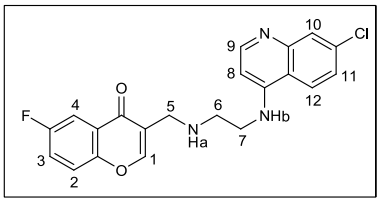

Orange solid (0.25 g, 60 %); M.p.: 117 – 119 ^{o}C; R_f (MeOH) 0.56; IR ν_{max} (KBr) /cm^{-1} 1576 (C=N), 1653 (C=O), 3215 (strong, 2 x N-H); δ_H (400 MHz, DMSO-d_6) 3.20 (2H, s, H_5), 3.47 (2H, q, *J* 5.5 Hz, H_6), 3.59 (2H, q, *J* 5.9 Hz, H_7), 5.55 (1H, s, H_1), 6.58 (1H, d, *J* 5.4 Hz, H_8), 7.03 (1H, d, *J* 8.8 Hz, H_2), 7.23 (1H, dd, *J* 3.3, 8.5 Hz, H_3), 7.38 (1H, d, *J* 3.3 Hz. H_4), 7.40 (1H, m, NH_a), 7.44 (1H, dd, *J* 2.2, 8.9 Hz, H_{11}), 7.76 (1H, d, *J* 2.2 Hz, H_{10}), 8.23 (1H, d, *J* 9.1 Hz, H_{12}), 8.38 (1H, d, *J* 5.3 Hz, H_9), 10.2 (1H, m, NH_b); δ_C (100 MHz, DMSO-d_6) 43.3, 46.9, 54.4, 98.9, 110.5, 117.5, 119.4, 120.4, 124.1, 125.6, 127.5, 133.4, 149.2, 150.1, 151.3, 152.0, 154.1, 155.1, 156.3, 158.3, 177.3 EI - m/z 395.1 $[M]^+$; HPLC purity: 98 % (t_r = 10.1 min).

3-((2-(7-Chloroquinolin-4-ylamino)ethylamino)methyl)-6-methoxy-4H-chromen-4-one (SN27)

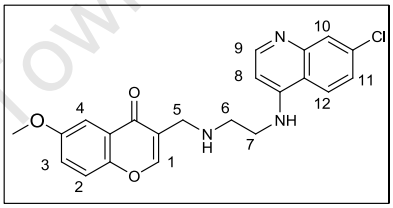

Yellow solid (0.24 g, 41 %); M.p.: 94 – 98 ^{o}C; R_f (MeOH) 0.48; IR ν_{max} (KBr) /cm^{-1} 1580 (C=N), 1658 (C=O), 3211 (strong, 2 x N-H); δ_H (400 MHz, DMSO-d_6) 3.18 (2H, s, H_5), 3.49 (2H, q, *J* 5.8 Hz, H_6), 3.56 (2H, q, *J* 5.8 Hz, H_7), 3.94 (1H, s, OCH_3), 5.47 (1H, s, H_1), 6.62 (1H, d, *J* 5.4 Hz, H_8), 6.88 (1H, d, *J* 9.1 Hz, H_2), 7.04 (1H, dd, *J* 3.2, 9.2 Hz, H_3), 7.21 (1H, d, *J* 3.2 Hz. H_4), 7.43 (1H, m, NH_a), 7.49 (1H, dd, *J* 2.1, 8.7 Hz, H_{11}), 7.80 (1H, d, *J* 2.0 Hz, H_{10}), 8.29 (1H, d, *J* 8.9 Hz, H_{12}), 8.38 (1H, d, *J* 5.4 Hz, H_9), 10.2 (1H, m, NH_b); δ_C (100 MHz, DMSO- d_6) 43.2, 46.6, 54.1, 55.2, 98.8, 107.8, 117.3, 118.3, 119.9, 120.5, 121.5, 123.2, 123.7, 124.0, 127.3, 133.2, 148.8, 149.7, 151.7, 153.7, 154.1, 177.7; EI - m/z 409.1 $[M]^+$; HPLC purity: 98 % (t_r = 7.36 min).

3-((2-(7-Chloroquinolin-4-ylamino)ethylamino)methyl)-6-methyl-4H-chromen-4-one (SN28)

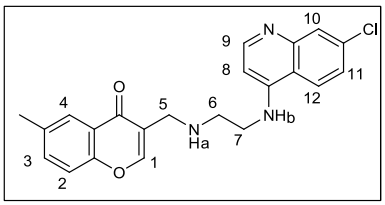

Yellow solid (0.29 g, 52 %); M.p.: 118 – 120 ^{o}C; R_f (MeOH) 0.48; IR ν_{max} (KBr) /cm^{-1} 1582 (C=N), 1651 (C=O), 3452 (strong, 2 x N-H); δ_H (400 MHz, DMSO-d_6) 2.52 (3H, s, CH_3), 3.15 (2H, s, H_5), 3.47 (2H, q, *J* 5.8 Hz, H_6), 3.59 (2H, q, *J* 5.7 Hz, H_7), 5.51 (1H, s, H_1), 6.60 (1H, d, *J* 5.4 Hz, H_8), 6.89 (1H, d, *J* 8.2 Hz, H_2), 7.20 (1H, dd, *J* 2.4, 8.4 Hz, H_3), 7.24 (1H, m, NH_a), 7.45 (1H, dd, *J* 2.2, 8.9 Hz, H_{11}), 7.53 (1H, d, *J* 2.4 Hz, H_4), 7.78 (1H, d, *J* 2.2 Hz, H_{10}), 8.26 (1H, d, *J* 9.0 Hz, H_{12}), 8.39 (1H, d, *J* 5.4 Hz, H_9), 10.1 (1H, m, NH_b); δ_C (75 MHz, DMSO-d_6) 20.2, 43.4, 46.7, 54.3, 101.6, 117.4, 122.9, 124.1, 124.3, 125.1, 127.5, 130.4, 133.9, 134.2, 134.5, 147.0, 149.3, 150.3, 152.2, 153.3, 154.3, 178.3; EI - m/z 393.0 $[M]^+$; HPLC purity: 98 % (t_r = 6.85 min).

5.4.2 General Synthetic Procedure of Amide-linked Hybrids at position 3 on the Chromone Ring (Series 2)[7]

A solution of chromone-3-carboxylic acid (1.0 eq) and HOBt (1.3 eq) in DMF (3 mL) under N_2 at 0 ^oC was made, followed by the addition of a solution of EDC.HCl (1.3 eq) and a drop of Et_3N in DMF (3 ml). Lastly, **SN08** (1.5 eq) and DMAP (0.5 eq) in DMF (3 ml) were added in a dropwise fashion. The reaction mixture was stirred under N_2 at 0 ^oC for 30 minutes, then warmed to room temperature and stirred overnight. Distilled water (30 mL) was added to the reaction mixture and extracted with DCM:MeOH (4:1) (3 x 50 mL). The combined organic layers were dried over anhydrous Na_2SO_4, and the solvent removed to afford the product. The residue was purified by flash chromatography on silica gel using DCM:MeOH (8:2) as the eluent to afford the product.

N-(2-(7-chloroquinolin-4-ylamino)ethyl)-4-oxo-4H-chromene-3-carboxamide (SN44)

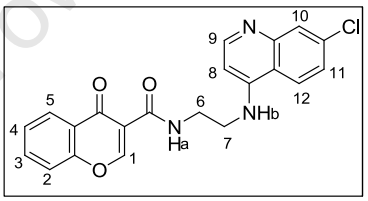

Yellow solid (0.11 g, 49 %); M.p.: 118 – 120 ^oC; R_f (MeOH) 0.53; IR ν_{max} (KBr) /cm^{-1} 1574 (C=N), 1632, 1731 (2 x C=O), 3423 (strong, 2 x N-H); δ_H (400 MHz, DMSO-d_6) 3.55 (2H, q, *J* 5.7 Hz, H_6), 3.63 (2H, q, *J* 5.7 Hz, H_7), 6.66 (1H, d, *J* 5.4 Hz, H_8), 6.81 (1H, s, H_1), 7.28 (1H, t, *J* 7.6 Hz, H_4), 7.35 (1H, m, NH_a), 7.45 (1H, d, *J* 7.9 Hz, H_2), 7.70 (1H, d, *J* 8.9 Hz, H_{11}), 7.80 (1H, s, H_{10}), 7.92 (1H, t, *J* 7.8 Hz, H_3), 8.08 (1H, d, *J* 8.0 Hz, H_5), 8.25 (1H, d, *J* 8.9 Hz, H_{12}), 8.43 (1H, d, *J* 5.4 Hz, H_9), 10.1 (1H, s, NH_b); δ_C (75 MHz, DMSO-d_6) 36.8, 43.2, 99.8, 117.3, 118.1, 119.9, 123.7, 123.9, 127.4, 127.9, 128.4, 133.3, 133.5, 148.9, 149.5, 151.7, 152.2, 156.1, 161.5, 162.1, 170.1; EI - m/z 393.0 $[M]^+$; HPLC purity: 95 % (t_r = 8.52 min).

6-Chloro-N-(2-(7-chloroquinolin-4-ylamino)ethyl)-4-oxo-4H-chromene-3-carboxamide (SN48)

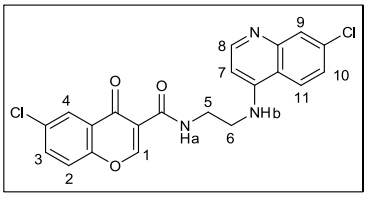

Orange solid (0.19 g, 46 %); M.p.: 241 – 243 ^oC; R_f (MeOH) 0.52; IR ν_{max} (KBr) /cm^{-1} 1582 (C=N), 1632, 1742 (2xC=O), 3418 (strong, 2 x N-H); δ_H (400 MHz, DMSO-d_6) 3.52 (2H, q, *J* 5.4 Hz, H_5), 3.57 (2H, q, *J* 5.4 Hz, H_6), 6.16 (1H, s, H_1), 6.55 (1H, d, *J* 5.4 Hz, H_7), 6.81 (1H, dd, *J* 2.5, 8.9 Hz, H_{10}), 7.23 (1H, d, *J* 8.6 Hz, H_2), 7.33 (1H, m, NH_a), 7.60 (1H, d, *J* 2.5 Hz, H_9), 7.75 (1H, dd, *J* 2.2, 8.6 Hz, H_3), 7.87 (1H, d, *J* 2.2 Hz, H_4), 8.19 (1H, d, *J* 9.0 Hz, H_{11}), 8.41 (1H, d, *J* 5.4 Hz, H_8), 10.1 (1H, m, NH_b); δ_C (75 MHz, DMSO-d_6) 39.2, 44.2, 99.6, 113.8, 117.1, 119.1, 121.3, 124.5, 125.3, 129.0, 129.8, 130.6, 134.9, 136.4, 149.8, 152.6, 154.6, 155.7, 159.4, 162.5, 177.4; ; EI - m/z 428.0 $[M]^+$; HPLC purity: 95 % (t_r = 8.97 min).

6-Bromo-N-(2-(7-chloroquinolin-4-ylamino)ethyl)-4-oxo-4H-chromene-3-carboxamide (SN54)

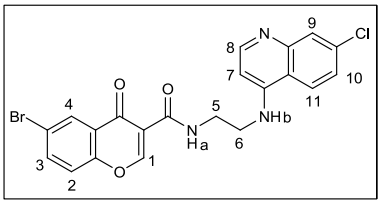

Yellow solid (0.09 g, 36 %); M.p.: 98 – 101 ^{o}C; R_f (MeOH) 0.38; IR ν_{max} (KBr) /cm^{-1} 1580 (C=N), 1625, 1703 (2 x C=O), 3241 (strong, 2 x N-H); δ_H (400 MHz, DMSO-d_6) 3.42 (2H, q, J 5.7 Hz, H_5), 3.64 (2H, q, J 5.8 Hz, H_6), 6.17 (1H, s, H_1), 6.64 (1H, d, J 5.6 Hz, H_7), 6.82 (1H, d, J 8.8 Hz, H_2), 7.33 (1H, dd, J 2.3, 9.0 Hz, H_{10}), 7.40 (1H, dd, J 2.4, 8.8 Hz, H_3), 7.45 (1H, m, NH_a), 7.79 (1H, d, J 2.2 Hz, H_9), 7.98 (1H, d, J 2.4 Hz, H_4), 8.25 (1H, d, J 9.1 Hz, H_{11}), 8.46 (1H, d, J 5.5 Hz, H_8), 10.1 (1H, m, NH_b); δ_C (100 MHz, DMSO-d_6) 38.8, 42.3, 99.7, 117.3, 119.3, 121.6, 123.8, 124.2, 125.8, 129.9, 130.4, 133.5, 135.7, 136.4, 148.4, 150.1, 151.3, 153.1, 156.8, 161.2, 175.4; EI - m/z 472.1 $[M]^+$; HPLC purity: 94 % (t_r = 8.03 min).

N-(2-(7-chloroquinolin-4-ylamino)ethyl)-6-fluoro-4-oxo-4H-chromene-3-carboxamide (SN55)

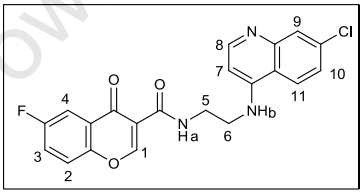

Orange solid (0.25 g, 62 %); M.p.: 118 – 121 ^{o}C; R_f (MeOH) 0.42; IR ν_{max} (KBr) /cm^{-1} 1550 (C=N), 1696, 1733 (2 x C=O), 3240 (strong, 2 x N-H); δ_H (400 MHz, DMSO-d_6) 3.91 (4H, m, H_5, H_6), 6.56 (1H, d, J 5.5 Hz, H_7), 6.89 (1H, s, H_1), 7.38 (2H, m, H_2, H_{10}), 7.72 – 7.78 (4H, m, H_3, H_4, H_9, NH_a), 8.28 (1H, d, J 9.0 Hz, H_{11}), 8.48 (1H, d, J 5.6 Hz, H_8), 9.70 (1H, s, NH_b); δ_C (100 MHz, DMSO-d_6) 39.2, 44.3, 99.5, 113.6, 117.9, 121.1, 121.3, 122.2, 124.8, 125.6, 129.1, 130.2, 134.9, 149.3, 152.5, 152.9, 154.5, 159.8, 161.1, 162.5, 176.5; EI - m/z 410.8 $[M]^+$; HPLC purity: 95 % (t_r = 8.65 min).

N-(2-(7-chloroquinolin-4-ylamino)ethyl)-6-methoxy-4-oxo-4H-chromene-3-carboxamide (SN56)

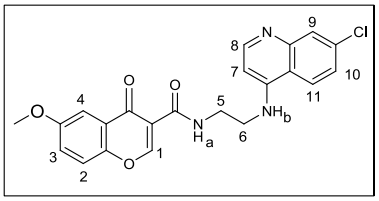

Yellow solid (0.13 g, 46 %); M.p.: 81 – 85 ^{o}C; R_f (MeOH) 0.55; IR ν_{max} (KBr) /cm^{-1} 1533 (C=N), 1687, 1740 (2 x C=O), 3238 (strong, 2 x N-H); δ_H (400 MHz, DMSO-d_6) 3.42 (2H, q, J 5.7 Hz, H_5), 3.51 (2H, q, J 5.8 Hz, H_6), 3.85 (3H, s, OCH_3), 6.61 (1H, d, J 5.4 Hz, H_7), 6.81 (1H, s, H_1), 7.35 – 7.42 (4H, m, H_2, H_3, H_9, NH_a); 7.74 (1H, d, J 9.0 Hz, H_{10}), 7.83 (1H, d, J 3.1 Hz, H_4), 8.28 (1H, d, J 9.0 Hz, H_{11}), 8.46 (1H, d, J 5.5 Hz, H_8), 10.1 (1H, s, NH_b); δ_C (100 MHz, DMSO-d_6) 37.3, 42.4, 55.7, 98.9, 111.4, 117.3, 118.1, 120.7, 120.8, 123.7, 123.9, 124.8, 125.4, 127.4, 133.3, 149.8, 151.7, 152.1, 156.2, 162.7, 163.9, 177.6; EI - m/z 422.8 $[M]^+$; HPLC purity: 96 % (t_r = 8.38 min).

N-(2-(7-chloroquinolin-4-ylamino)ethyl)-6-methyl-4-oxo-4H-chromene-3-carboxamide (SN57)

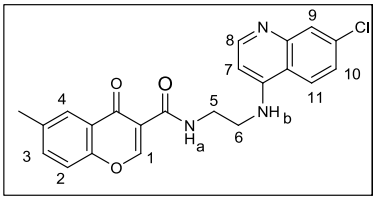

Orange solid (0.16 g, 52 %); M.p.: 82 – 86 °C; R_f (MeOH) 0.50; IR ν_{max} (KBr) /cm^{-1} 1565 (C=N), 1655, 1748 (2 x C=O), 3435 (strong, 2 x N-H); δ_H (400 MHz, DMSO-d_6) 2.28 (3H, s, CH_3), 3.49 (2H, q, *J* 5.8 Hz, H_5), 3.58 (2H, q, *J* 5.8 Hz, H_6), 6.07 (1H, s, H_1), 6.60 (1H, d, *J* 5.3 Hz, H_7), 6.69 (1H, d, *J* 8.1 Hz, H_2), 7.14 (1H, dd, *J* 2.1, 8.3 Hz, H_3), 7.45 (2H, m, H_4, NH_a), 7.77 (1H, dd, *J* 2.4, 9.1 Hz, H_{10}), 7.87 (1H, d, *J* 2.5 Hz, H_9), 8.23 (1H, d, *J* 9.2 Hz, H_{11}), 8.41 (1H, d, *J* 5.3 Hz, H_8), 10.0 (1H, s, NH_b); (100 MHz, DMSO-d_6) 20.1, 41.5, 43.3, 98.7, 117.2, 119.5, 123.9, 124.0, 126.8, 127.9, 128.3, 133.4, 134.6, 135.0, 149.0, 149.9, 151.9, 152.3, 156.1, 159.5, 162.7, 175.1; EI - m/z 407.1 $[M]^+$; HPLC purity: 97 % (t_r = 8.86 min).

5.4.3 General Synthetic Procedure of Amide-linked Hybrids at position 2 on the Chromone Ring (Series 3)[7]

A similar procedure was used as for the synthesis of Series 2 (Section 5.4.2), except that the chromone-2-carboxylic acids were used.

N-(2-(7-chloroquinolin-4-ylamino)ethyl)-4-oxo-4H-chromene-2-carboxamide (SN74)

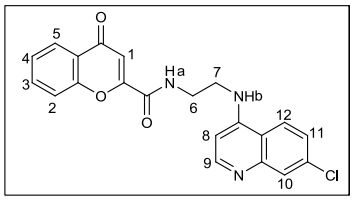

Yellow solid (0.25 g, 46 %); M.p.: 241 – 243 °C; R_f (MeOH) 0.52; IR ν_{max} (KBr) /cm^{-1} 1580 (C=N), 1650, 1741 (2 x C=O), 3435 (strong, 2 x N-H); δ_H (400 MHz, DMSO-d_6) 3.67 (2H, q, *J* 5.9 Hz, H_6), 3.74 (2H, q, *J* 6.0 Hz, H_7), 6.81 (1H, d, *J* 5.5 Hz, H_8), 6.99 (1H, s, H_1), 7.59 (1H, dd, *J* 2.2, 8.9 Hz, H_{11}), 7.68 (2H, m, H_4, NH_a), 7.85 (1H, d, *J* 8.5 Hz, H_2), 7.93 (1H, d, *J* 2.2 Hz, H_{10}), 8.03 (1H, t, *J* 8.7 Hz, H_3), 8.19 (1H, d, *J* 7.9 Hz, H_5), 8.36 (1H, d, *J* 9.0 Hz, H_{12}), 8.57 (1H, d, *J* 5.4 Hz, H_9), 9.49 (1H, m, NH_b); δ_C (100 MHz, DMSO-d_6) 38.4, 41.9, 99.2, 111.1, 118.1, 119.2, 124.2, 124.6, 124.7, 125.5, 126.6, 128.0, 134.0, 135.6, 149.6, 150.6, 152.4, 155.6, 156.1, 160.1, 177.8; EI - m/z 393.1 $[M]^+$; HPLC purity: 95 % (t_r = 8.62 min).

6-Chloro-N-(2-(7-chloroquinolin-4-ylamino)ethyl)-4-oxo-4H-chromene-2-carboxamide (SN75)

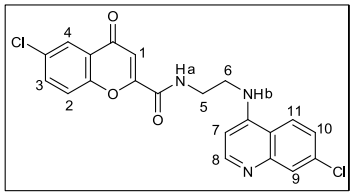

Pale-brown solid (0.41 g, 70 %); M.p.: 173 – 175 °C; R_f (MeOH) 0.56; IR ν_{max} (KBr) /cm^{-1} 1578 (C=N), 1686, 1731 (2 x C=O), 3323 (strong, 2 x N-H); δ_H (400 MHz, DMSO-d_6) 3.37 (2H, q, *J* 5.6 Hz, H_5), 3.49 (2H, q, *J* 5.7 Hz, H_6), 6.75 (1H, d, *J* 5.6 Hz, H_7), 6.87 (1H, s, H_1), 7.40 (1H, dd, *J* 2.3, 8.6 Hz, H_{10}), 7.51 (1H, d, *J* 8.0 Hz, H_2), 7.64 (1H, d, *J* 2.2 Hz, H_9), 7.69 (1H, dd, *J* 2.1, 7.9 Hz, H_3), 7.94 (1H, m, NH_a), 7.98 (1H, d, *J* 2.0 Hz, H_4), 8.40 (1H, d, *J* 8.8 Hz, H_{11}), 8.52 (1H, d, *J* 5.5 Hz, H_8), 9.47 (1H, m, NH_b); δ_C (100 MHz, DMSO-d_6) 37.2, 42.6, 98.4, 110.2, 118.6,

122.5, 123.6, 123.8, 125.3, 126.4, 128.7, 130.2, 134.5, 135.5, 139.4, 146.9, 152.9, 155.4, 158.9, 169.7, 175.8; EI - m/z 427.0 $[M]^+$; HPLC purity: 96 % (t_r = 9.23 min).

6-Bromo-N-(2-(7-chloroquinolin-4-ylamino)ethyl)-4-oxo-4H-chromene-2-carboxamide (SN76)

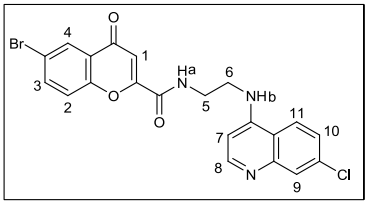

Off-white solid (0.42 g, 72 %); M.p.: 143 – 145 ^oC; R_f (MeOH) 0.42; IR ν_{max} (KBr) /cm^{-1} 1544 (C=N), 1688, 1739 (2 x C=O), 3237 (strong, 2 x N-H); δ_H (300 MHz, DMSO-d_6) 3.39 (2H, q, J 6.0 Hz, H_5), 3.58 (2H, q, J 6.1 Hz, H_6), 6.87 (1H, s, H_1), 7.16 (1H, d, J 5.6 Hz, H_7), 7.38 (1H, d, J 8.9 Hz, H_2), 7.69 (1H, dd, J 2.4, 8.9 Hz, H_{10}), 7.94 (1H, dd, J 2.4, 8.9 Hz, H_3), 7.99 (1H, m, NH_a), 8.06 (1H, d, J 2.5 Hz, H_4), 8.11 (1H, d, J 2.4 Hz, H_9), 8.45 (1H, d, J 8.9 Hz, H_{11}), 8.56 (1H, d, J 5.6 Hz, H_8), 9.52 (1H, s, NH_b); δ_C (100 MHz, DMSO-d_6) 39.5, 44.2, 99.2, 114.4, 117.5, 118.8, 121.6, 123.2, 124.8, 126.1, 129.4, 134.1, 134.9, 141.1, 149.3, 152.7, 154.5, 156.2, 163.8, 166.5, 178.5; EI - m/z 472.8 $[M]^+$; HPLC purity: 95 % (t_r = 8.04 min).

N-(2-(7-chloroquinolin-4-ylamino)ethyl)-6-fluoro-4-oxo-4H-chromene-2-carboxamide (SN77)

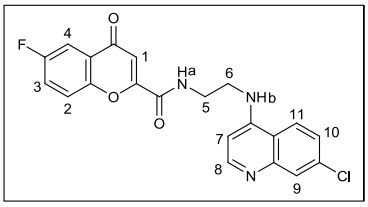

Brown solid (0.38 g, 65 %); M.p.: 240 – 242 ^oC; R_f (MeOH) 0.45; IR ν_{max} (KBr) /cm^{-1} 1552 (C=N), 1690, 1735 (2 x C=O), 3241 (strong, 2 x N-H); δ_H (300 MHz, DMSO-d_6) 3.50 (4H, m, H_5, H_6), 6.66 (1H, d, J 5.4 Hz, H_7), 6.87 (1H, s, H_1), 7.46 (2H, m, H_2, H_{10}), 7.75 – 7.79 (4H, m, H_3, H_4, H_9, NH_a), 8.23 (1H, d, J 8.9 Hz, H_{11}), 8.44 (1H, d, J 5.4 Hz, H_8), 9.31 (1H, m, NH_b); δ_C (100 MHz, DMSO-d_6) 38.5, 42.0, 99.2, 110.2, 117.9, 119.2, 121.9, 123.3, 124.3, 124.6, 127.7, 133.9, 146.4, 149.2, 150.7, 151.9, 156.3, 158.5, 159.9, 160.9, 176.9; LRMS (EI) m/z 410.9 $[M]^+$; HPLC purity: 96 % (t_r = 9.36 min).

N-(2-(7-chloroquinolin-4-ylamino)ethyl)-6-methoxy-4-oxo-4H-chromene-2-carboxamide (SN78)

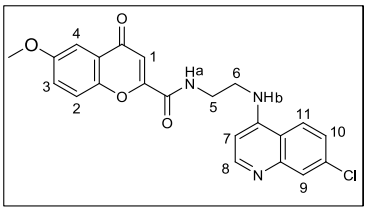

Brown solid (0.41 g, 55 %); M.p.: 113 – 115 ^oC; R_f (MeOH) 0.58; IR ν_{max} (KBr) /cm^{-1} 1535 (C=N), 1686, 1735 (2 x C=O), 3241 (strong, 2 x N-H); δ_H (300 MHz, DMSO-d_6) 3.56 (2H, q, J 5.7 Hz, H_5), 3.62 (2H, q, J 5.7 Hz, H_6), 3.87 (3H, s, OCH_3), 6.67 (1H, d, J 5.2 Hz, H_7), 6.83 (1H, s, H_1), 7.41 (1H, d, J 8.9 Hz, H_2), 7.45 (1H, dd, J 2.2, 9.0 Hz, H_{10}), 7.56 (1H, dd, J 2.7, 8.9 Hz, H_3), 7.65 (1H, m, NH_a), 7.80 (1H, d, J 2.8 Hz, H_4), 8.41 (1H, d, J 2.2 Hz, H_9), 8.23 (1H, d, J 9.0 Hz, H_{11}), 8.44 (1H, d, J 5.2 Hz, H_8), 9.28 (1H, m, NH_b); δ_C (100 MHz, DMSO-d_6) 37.7, 41.4, 55.6, 98.4, 114.6, 117.1, 119.9, 123.0, 123.6, 123.8, 125.4, 126.9, 128.5, 133.2, 146.1, 148.4, 149.8, 151.2, 154.9, 156.6, 159.2, 176.5; LRMS (EI) m/z 422.8 $[M]^+$; HPLC purity: 96 % (t_r = 8.12 min).

5.5 Biological Testing Protocols

Antiplasmodial Testing Protocol

The samples were tested in triplicate against chloroquine-sensitive (*D10* and *NF54*) and -resistant (*K1*) strains of *P. falciparum*. Continuous *in vitro* cultures of asexual erythrocyte stages of *P. falciparum* were maintained using a modified method of Trager *et al*.[8] Quantitative assessment of antiplasmodial activity *in vitro* was determined via the parasite lactate dehydrogenase assay using a modified method described by Makler *et al*.[9] The test samples were prepared as a 20 mg/mL stock solution in 100 % DMSO and sonicated to enhance solubility. Samples were tested as a suspension if not completely dissolved. Stock solutions were stored at -20 ^{o}C. Further dilutions were prepared on the day of the experiment. Chloroquine was used as the reference drug in all experiments. A full dose-response was performed for all compounds to determine the concentration inhibiting 50 % of parasite growth (IC_{50} value). Test samples were tested at a starting concentration of 1000 ng/mL, which was then serially diluted 2-fold in complete medium to give 10 concentrations; with the lowest concentration being 2 ng/mL. The same dilution technique was used for all samples. The highest concentration of solvent to which the parasites were exposed to had no measurable effect on the parasite viability. The IC_{50} values were obtained using a non-linear dose-response curve fitting analysis via Graph Pad Prism v.4.0 software.

Antitumour Testing Protocol

The MTT assay was used to calculate IC_{50} values in *WHCO1* cancer cells. The IC_{50} values were determined using a range of concentrations (0, 0.1, 1, 5, 10, 50, 100 and 200 µM). Cells were plated at 3000 cells per well, in triplicate, in 90 µL of media in 96-well plates and incubated overnight at 37 °C in a humidified atmosphere of 5 % CO_2. Media alone (90 µL) was also plated in triplicate and incubated at 37 ^{o}C under 5 % CO_2. The cells (and media alone) were treated with 10 µL drug diluted in media and DMSO, to give a final DMSO concentration of 0.2 %. The cells were incubated for 48 hours after which 10 µL of 3-(4,5-dimethylthiazol-2-yl)-2,5-diphenyltetrazolium bromide (MTT) solution was added to each well and incubated for 4 hours. MTT reagent consists of yellow tetrazolium salt that is reduced to purple formazan crystals in the mitochondria of living cells. After the 4 hour incubation period, the formazan crystals were solubilized by the addition of 100 µL solubilization solution (10 % w/v SDS, 0.01 M HCl) overnight at 37 ^{o}C, 5 % CO_2. The absorbance, which represents cell viability, was subsequently measured at 595 nm, and corrected. The IC_{50} values were calculated using GraphPad Prism version 4.03. The dose-response curves were generated by non-linear regression analysis (Non-linear regression (Sigmoidal dose-response with variable slope)) to yield an IC_{50} value.

Antimycobacterial Testing Protocol

The MIC was determined using a standard broth microdilution method.[10, 11] A 10 mL culture of *Mycobacterium tuberculosis*, *H37Rv* was grown to an OD_{600} of 0.6 – 0.7. The culture was then diluted 1:500 in liquid 7H9 medium, 50 µL of 7H9 medium was added.[12] The compounds were added in duplicate, at a final concentration of 640 µM (stocks were made up to a concentration of 12.8 mM in DMSO, and diluted to 640 µM in 7H9 medium). A 2-fold serial dilution was prepared. Controls include media only, 5 % DMSO, Rifampicin and Kanamycin. Finally, 50 µL of the 1:500 diluted *M. tuberculosis* culture was added. The microtitre plate was sealed in a ziplock bag and incubated at 37 °C with humidifier to prevent evaporation of liquid. The lowest concentration of drug that inhibits growth of more than 90 or 99 % of the bacterial population is considered to be the MIC_{90} or MIC_{99}. MIC_{99} values are scored visually at 7 days and 14 days post inoculation, and digital images captured and stored.

Turbidimetric Solubility Assay Protocol

Preparation of 0.01M pH 7.4 Phosphate Buffered Saline (PBS) involved dissolving 1 intact PBS buffer tablet (EC Diagnostics AB, Sweden) in sufficient distilled water to make 1000 mL of a solution comprising 0.14M NaCl, 0.003M KCl and 0.01M phosphate buffer. This solution was filtered through a 0.22 µm nylon filter to remove any particulate contaminants and the pH ascertained using a pH meter. The test compounds were prepared by making a 10mM stock solutions by accurately weighing and dissolving each in sufficient DMSO to approximately 1000 µL final volume. From each pre-dilution solution, secondary dilutions of the compounds in both DMSO and 0.01M pH 7.4 PBS were prepared in a 96-well plate, in triplicate. Wells in columns 1–6 contained compound in DMSO while those in columns 7–12 contained samples in PBS at similar nominal concentrations as those in DMSO. The final volume of solvent in each assay plate well was 200 µL, prepared by pipetting 4 µL each of solution from the pre-dilution plate to the corresponding well into both DMSO and PBS (both 196 µL). This ensured that the final concentration of DMSO in the PBS aqueous buffer did not exceed 2 % v/v. The different concentrations in DMSO were prepared to serve as controls to determine potential false turbimetric absorbance readings arising from the compounds in solution absorbing incident radiation at the analysis wavelength. After making the assay plate preparation, the plate was covered and left to equilibrate for 2 hours at ambient room temperature. After incubation, UV-Vis absorbance readings from the plate were measured at 620 nm. Corrected absorbance readings at different concentrations of test compounds were calculated by subtracting absorbance of the blank (i.e. DMSO and 1 % DMSO in PBS) from each subsequent concentration's absorbance.[13]

5.6 References

1. N. Miyaura and A. Suzuki, *J. C. S. Chem. Comm*., **1979**, *590*, 866.
2. N. Ishizuka, K. Matsumura, K. Sakai, M. Fujimoto and S. Mihara, *J. Med. Chem.*, **2002**, *45*, 2041.
3. G. Liu, J. Xu, M. Geng, R. Xu, R. Hui, J. Zhao, Q. Xu, H. Xu, and J. Li, *Bioorg. Med. Chem.*, **2010**, *18*, 2864.
4. H. S. Mahal and K. Venkataraman. *J. Chem. Soc.*, **1934**, 1767.
5. K. Kaur, M. Jain, R. P. Reddy and R. Jain, *Eur. J. Med. Chem.*, **2010**, *45*, 3245.
6. W. Friebolin, B. Jannack, N. Wenzel, J. Furrer, T. Oeser, C. P. Sanchez, M. Lanzer, V. Yardley, K. Becker and E. Davioud-Charvet, *J. Med. Chem.*, **2008**, *51*, 1260.
7. J. K. Lynch, J. C. Freeman, A. S. Judd, R. Iyengar, M. Mulhern, G. Zhao, J. J. Napier, D. Wodka, S. Brodjian, B. D. Dayton, D. Falls, C. Ogiela, R. M. Reilly, T. J. Campbell, J. S. Polakowski, L. Hernandez, K. C. Marsh, R. Shapiro, V. Knourek-Segel, B. Droz, E. Bush, M. Brune, L. C. Preusser, R. M. Fryer, G. A. Reinhart, K. Houseman, G. Diaz, A. Mikhail, J. T. Limberis, H. L. Sham, C. A. Collins, and P. R. Kym, *J. Med. Chem.*, **2006**, *49,* 6569.
8. W. Trager and J. B. Jensen, *Science*, **1976**, *193*, 673.
9. M. T. Trager, J. M. Ries, J. A. Williams, J. E. Bancroft, R. C. Piper, B. L. Gibbins and D. J. Hinrichs, *Am. J. Med. Hyg.*, **1993**, *48*, 739.
10. L. Collins and S. G. Franzblau, *Antimicrob. Agents Chemother.*, **1997**, *41*, 1004.
11. L. A. Collins, M. N. Torrero and S. G. Franzblau, *Antimicrob. Agents Chemother.*, **1998**, *42*, 344.
12. T. R. Ioerger, Y. Feng, K. Ganesula, X. Chen, K. M. Dobos, S. Fortune, W. R. Jacobs, Jr., V. Mizrahi, T. Parish, E. Rubin, C. Sassetti and J. C. Sacchettini, *J. Bacteriol.*, **2010**, *192*, 3645.
13. (a) C. A. Lipinski, F. Lombardo, B. W. Duminy and P. J. Feeney, *Adv. Drug Deliv. Rev.* **2001**, *46*, 3; (b) E. H. Kerns and L. Di, *Drug-like Properties: Concepts, Structure Design and Methods from ADME to Toxicity Optimization*, Elsevier Academic Press, California, 1st Ed., 2008; (c) C. D. Bevan and R. S. Lloyd, *Anal. Chem.* **2000**, *72*, 1781; (d) L. Pan, Q. Ho, K. Tsutsui and L. Takahashi, *J. Pharm. Sci*. **2001**, *4*, 521; (e) J. Alsenz and M. Kansy, *Adv. Drug Deliv. Rev.* **2007**, *59*, 546.